Dissertation
Submitted to the
Combined Faculties for the Natural Sciences and for Mathematics
of the Ruperto-Carola University of Heidelberg, Germany
for the degree of
Doctor of Natural Sciences

Presented by

Jeong Yoon Kim
Born in Seoul, Republic of Korea
Oral examination: September 18, 2020

# ECM-mediated intercellular adhesion prompts cellular position-sensing to pattern the embryo

Referees: Dr. Alexander Aulehla
Prof. Dr. Nicholas S. Foulkes

The work published in this thesis was carried out at the European Molecular Biology Laboratory (EMBL) in Heidelberg, Germany, from July 2016 to June 2020 under the supervision of Dr. Takashi Hiiragi

# Summary

A cell's perception of its position within the tissue critically underlies spatially patterned differentiation and ultimately drives development. However, our understanding of the molecular mechanisms by which individual cells acquire and transmit positional information remains incomplete. By using the mouse model, the present thesis demonstrates how developmentally controlled adhesive interactions enable position-sensing by cells to pattern the preimplantation embryo.

The mouse embryo is initially a cluster of transcriptionally and geometrically equivalent cells. During the 16-32-cell stage, however, spatial differences emerge, closely followed by the first lineage segregation. Outer cells become trophectoderm (TE)-specified while inner cells give rise to the inner cell mass (ICM), which go on to form the extraembryonic tissues and the embryo proper, respectively.

While outer cells are marked by a polarised apical domain on the cell-free surface, inner cells are enveloped by adhesive cell-cell interfaces. By characterising and manipulating the adhesive environment of early embryonic cells, the work presented here illustrates that stage-specific activity of integrins and the extracellular matrix (ECM) at these cell-cell interfaces distinguish the embryonic interior. Immunosurgical isolation of inner cells prior to their lineage commitment removes existing intercellular adhesions and subsequently drives TE specification. In marked contrast, however, provision of exogenous ECM components induces ICM specification instead, and this response is dependent on integrin β1 activity.

Our findings suggest that interactions between integrins and their ECM ligands convey inner positional information for inside-outside patterning of the preimplantation embryo. Furthermore, even in the presence of molecules that mediate direct intercellular adhesion, the ECM is required at the cell-cell interface to prompt position-sensing. While cell-cell and cell-ECM adhesions are commonly considered to be spatially distinct, the present work indicates that ECM components are also present at the cell-cell interface to critically influence patterning. Given the ubiquity of the ECM among metazoans, we predict that future studies would increasingly uncover morphogenetic requirements for intercellular ECM.

# Zuzammenfassung

Die Wahrnehmung der Position einer Zelle innerhalb des Gewebes liegt der räumlich strukturierten Differenzierung kritisch zugrunde und treibt letztendlich die Entwicklung voran. Unser Verständnis der molekularen Mechanismen, mit denen einzelne Zellen Positionsinformationen erfassen und übertragen, bleibt jedoch unvollständig. Anhand des Mausmodells zeigt die vorliegende Arbeit, wie entwicklungsgesteuerte adhäsive Wechselwirkungen die Positionserfassung durch Zellen ermöglichen, um den Präimplantationsembryo zu strukturieren.

Der Mausembryo ist zunächst ein Cluster von transkriptionell und geometrisch äquivalenten Zellen. Während des 16-32-Zell-Stadiums treten jedoch räumliche Unterschiede auf, dicht gefolgt von der ersten Abstammungstrennung. Äußere Zellen werden zum trophectoderm (TE) -spezifiziert, während innere Zellen die innere Zellmasse (ICM) bilden, welche das extraembryonale Gewebe bzw. den eigentlichen Embryo bilden.

Während äußere Zellen durch eine polarisierte apikale Domäne auf der zellfreien Oberfläche markiert sind, werden innere Zellen von adhäsiven Zell-Zell-Grenzflächen umgeben. Durch die Charakterisierung und Manipulation der adhäsiven Umgebung früher embryonaler Zellen zeigt die hier vorgestellte Arbeit, dass die stadienspezifische Aktivität von Integrinen und der extrazellulären Matrix (ECM) an diesen Zell-Zell-Grenzflächen das embryonale Innere unterscheidet. Die immunchirurgische Isolierung innerer Zellen vor ihrer Bindung an die Abstammungslinie entfernt vorhandene interzelluläre Adhäsionen und treibt anschließend die TE-Spezifikation voran. In deutlichem Gegensatz dazu induziert die Bereitstellung exogener ECM-Komponenten stattdessen die ICM-Spezifikation, diese Reaktion hängt von der Integrin-1-Aktivität ab.

Unsere Ergebnisse legen nahe, dass Wechselwirkungen zwischen Integrinen und ihren ECM-Liganden innere Positionsinformationen für die Innen-Außen-Strukturierung des Präimplantationsembryos vermitteln. Selbst in Gegenwart von Molekülen, die eine direkte interzelluläre Adhäsion vermitteln, ist die ECM an der Zell-Zell-Grenzfläche erforderlich, um die Positionserfassung zu veranlassen. Während Zell-Zell- und Zell-ECM-Adhäsionen üblicherweise als räumlich verschieden angesehen werden, zeigt die vorliegende Arbeit, dass ECM-Komponenten auch an der Zell-Zell-Grenzfläche vorhanden sind, um die Strukturierung kritisch zu beeinflussen. Angesichts der Allgegenwart der ECM bei Metazoen sagen wir voraus, dass zukünftige Studien zunehmend morphogenetische Anforderungen an die interzelluläre ECM aufdecken werden.

# Table of Contents

# Abbreviations

| | |
|---|---|
| 2D | two dimensional |
| 3D | three dimensional |
| a.u. | arbitrary units |
| aPKC | atypical protein kinase C |
| BM | basement membrane |
| BSA | bovine serum albumin |
| Cdc42 | cell division control protein 42 |
| Cdh1 | cadherin 1 |
| Cdx2 | caudal type homeobox 2 |
| DAPI | 4,6-diamidino-2-phenylindole |
| DMSO | dimethyl sulfoxide |
| DNA | deoxyribonucleic acid |
| DPBS | Dulbecco's phosphate buffered saline |
| E | embryonic day |
| E-cadherin | epithelial cadherin |
| ECM | extracellular matrix |
| eGFP | enhanced green fluorescent protein |
| EPI | epiblast |
| ESC | embryonic stem cell |
| FGF | fibroblast growth factor |
| GATA4 | GATA-binding protein 4 |
| gDNA | genomic DNA |
| GTPase | guanosine triphosphatase |
| H-KSOM | KSOM with HEPES |
| hCG | human chorionic gonadotropin |
| HEPES | 4-(2-hydroxyethyl)-1-piperazineeethanesulfonic acid |
| ICM | inner cell mass |
| Itga6 | integrin α6 |

| | |
|---|---|
| Itgb1 | integrin β1 |
| IU | international unit |
| KO | knockout |
| KSOM | potassium simplex optimization medium |
| M | molar |
| min | minutes |
| Myh9 | myosin IIA |
| Oct4 | Octamer-binding transcription factor 4 |
| Par | partitioning defective |
| PCR | polymerase chain reaction |
| pERM | phosphorylated Ezrin Radixin Moesin |
| PFA | paraformaldehyde |
| PMSG | pregnant mare serum gonadotropin |
| PrE | primitive endoderm |
| RGD | arginine, glycine, aspartate |
| RNA | ribonucleic acid |
| RT | room temperature |
| Sox2 | SRY box 2 |
| TE | trophectoderm |
| TEAD4 | TEA domain family member 4 |
| U | units |
| v/v | volume per volume |
| w/v | weight per volume |
| WT | wildtype |
| YAP | yes-associated protein |
| ZP | zona pellucida |

# Introduction

The development of multicellular organisms entails dynamic proliferation and organisation among cells as diverse arrays of gene expression signatures, spatial patterns, and morphologies arise. Coordinating the emergence of such diversity requires that cells perceive and interpret information from their immediate microenvironment as well as global cues across the embryo. In particular, the question of how a cell commits to a specific fate relative its neighbours is a fundamental one, which the present thesis aims to address using the early mouse embryo as a model system.

## Positional information in fate regulation and pattern formation

### *Classical models of pattern formation*

At the organismal level, a body plan follows spatial coordinates along a set of axes to guide morphogenesis during development. In addition to cell differentiation, processes such as proliferation, movement and growth vary between anterior-posterior, dorsal-ventral, and left-right regions of an embryo. Moreover, each of these axes are determined at chronologically distinct periods as the geometry of the embryo evolves. Therefore, a system to provide and process spatial cues is constantly at work over increasing scales during development.

The notion of 'positional information' in morphogenesis was first brought to prominence by Lewis Wolpert to explain how genetic information leads to spatial patterns of cell differentiation (Wolpert, 1969). In his words, positional information is the specification of physical position, while polarity is the direction in which positional formation is measured. Positional information may be provided in several ways. These include quantitative variation in the concentration of a chemical substance, and wave-like propagation of pacemaker activity as proposed by Goodwin and Cohen (Goodwin and Cohen, 1969) (Figure 1A). In response, the genetic makeup and developmental history of a cell determine its 'interpretation' of the given positional information, as well as subsequent 'conversion' of this information into a particular behaviour. Ultimately, Wolpert stipulated that patterns emerge at the tissue level from spatial gradients.

Prior to Wolpert's gradient model, Alan Turing introduced the concept of 'morphogens' as diffusible chemical substances that react with each other to determine the anatomical structure of an organism in his reaction-diffusion (RD) model (Turing, 1952).

Turing's chief interest was to explain the emergence of instability and subsequent complexity from an originally homogenous system through the activity of chemical reactions. He reasoned that even a symmetrical system exhibits stochastic fluctuations in its component reactions. Once amplified, these fluctuations promote a state of instability, leading to a new equilibrium by breaking symmetry, and thus prompts pattern formation (Figure 1B). The RD model is distinct from Wolpert's gradient model in that the former's chemical 'peaks' are not unique to a specified position but emerge locally through self-organisation. In contrast, the gradient model assumes a prior asymmetry in the tissue to drive complex patterning. Nevertheless, the relationship between these two models is not one of mutual exclusion. The RD model could impart symmetry-breaking and robustness through self-organisation, while the resulting spatial asymmetries drive pattern formation according to the gradient model (Green and Sharpe, 2015; Kondo and Miura, 2010; Wolpert, 1969).

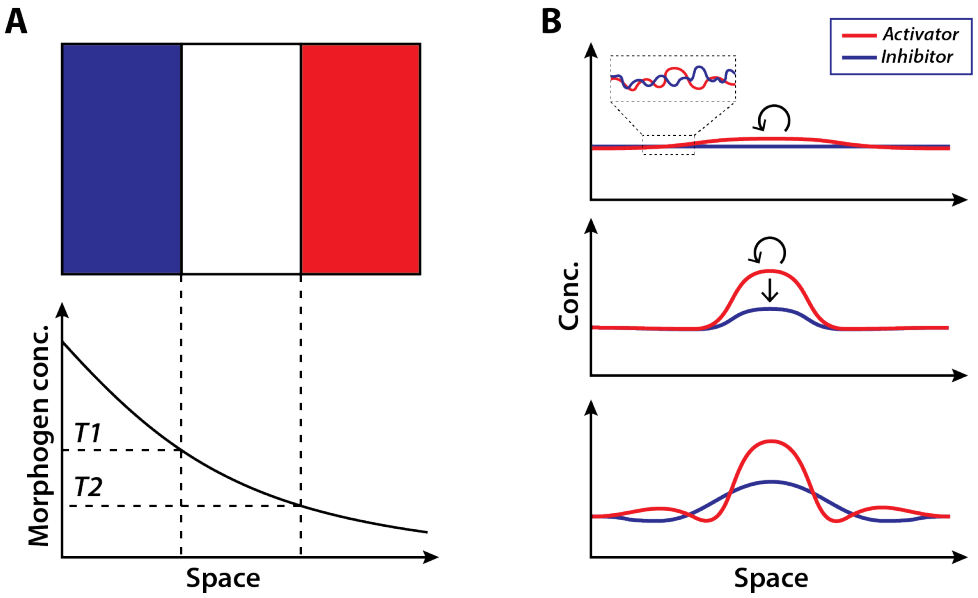


**Figure 1. Schematic representation of the classical models of patterning.**

**A.** In Wolpert's gradient model, a polarised boundary generates a directional gradient that encodes positional information. Just as a French flag retains its tricolour regardless of size, a relative gradient is preserved despite changes in the size of the "positional field" to maintain patterning. Concentration thresholds (*T1, T2*) of morphogens determine fate along the field of cells.
**B.** In essence, Turing's reaction-diffusion model proposes that two diffusible substances interacting with each other can generate patterns. Molecular fluctuations and auto-activation drive symmetry-breaking. In this case, an activating morphogen (red) induces expression of an inhibitor (blue). The more rapidly diffusing inhibitor creates a zone of inhibition around the activator peak. However, new activator peaks can from beyond this inhibition zone as reaction-diffusion propagates, resulting in pattern formation. Schematic adapted from Green and Sharpe, 2015.

***Distinct spatial cues are integrated to govern pattern formation***

Although little was known of the molecular basis of patterning at the time of Turing and Wolpert's writing, the current literature describes a myriad of different positional cues. In plants, for example, several aspects of patterning are regulated by the phytohormone auxin. Sites of auxin biosynthesis are localised to specific parts of a plant, and active transport of the hormone sets up concentration gradients that organise the plant body. Auxin produced in the shoot apex drives stem elongation while inhibiting development of lateral buds, thus establishing 'apical dominance' to promote vertical growth of the plant (Barbier et al., 2017). In addition, auxin drives asymmetric growth in response to directional light by preferentially accumulating in 'shaded' regions of the plant. This enables a positive phototrophic response whereby the plant bends and grows towards the light source (Figure 2A) (Holland et al., 2009). As such, localised availability and regulation of auxin provide positional information necessary to distinguish different regions of the plant and pattern its growth in response to the external environment.

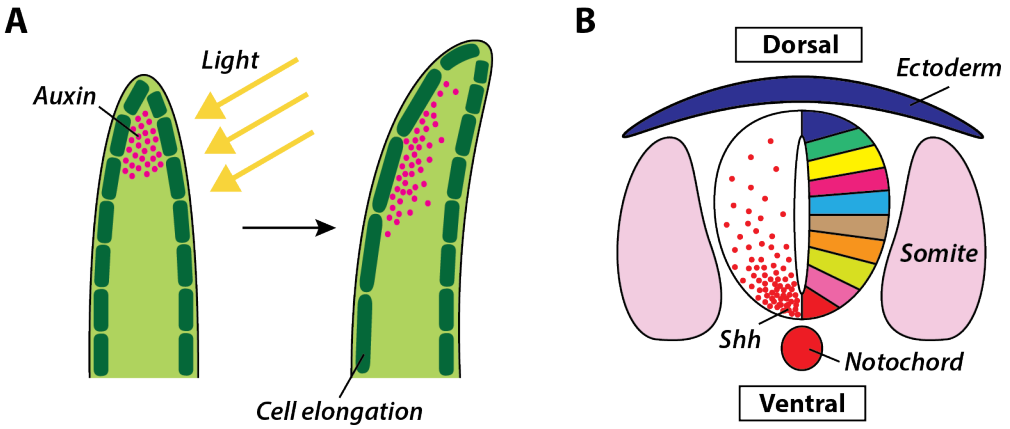


**Figure 2. Spatial cues direct growth and patterning.**

**A.** Asymmetric exposure to light leads to preferential auxin accumulation in shaded regions of the plant to drive phototropic growth through selective cell elongation. Localised production and polar transport of auxin coordinates plant body development.
**B.** Ventral-to-dorsal gradient of Sonic hedgehog (Shh) directs cell differentiation in the vertebrate neural tube. Additional positional information is provided by site-specific interactions with surrounding tissues to guide development along the length of the neural tube.

Similarly, pattern formation in a variety of animal systems is regulated by positional information encoded in morphogen gradients. One prominent example of morphogen activity is Sonic hedgehog (Shh) signalling in the neural tube. Following neurulation in vertebrate embryos, Shh secreted from the notochord and the ventral portion of the neural tube spreads in the dorsal direction (Figure 2B) (Martí et al., 1995; Roelink et al., 1995). Through a series of transcription factors controlled by graded Shh availability, cells of the neural tube attain distinct positional identity, resulting in spatially segregated specification of neuronal subtypes along the dorsoventral axis (Fig 2B) (Briscoe et al., 1999; Ericson et al., 1997; Yamada et al., 1993).

This classical model, however, has been extended by observations made through *in toto* live-imaging of neural development in zebrafish (Xiong et al., 2013). Although graded Shh certainly guides the general direction of fate specification, authors report considerable spatial noise in the response of neural tube cells to the morphogen gradient. Fate specification occurs in an overlapping and intermingled 'salt-and-pepper' manner, and sharply delineated progenitor domains are established only after cell sorting. Therefore, the outcome of graded morphogen signalling as a function of position is not smooth, and cell-cell interactions provide additional positional information to refine pattern formation. The response to different sources of positional information can be again tuned by multiple parameters, including duration of signalling and physical changes in the environment brought by cell movement and tissue growth (Dessaud et al., 2007; Harfe et al., 2004; Sagner and Briscoe, 2017). For example, the neural tube is flanked by pairs of somites that are themselves rhythmically produced by a clock and wave mechanism based on molecular oscillators (Aulehla et al., 2008), and inter-tissue interactions critically affect bilateral symmetry of the neural tube (Guillon et al., 2020). In this way, spatiotemporal changes in the biochemical and physical environment of a cell, as well as changes to competence of the cell itself, present a slew of context-dependent factors that influence position-sensing and subsequent patterning during development.

***Spatial asymmetry underlies position-specific cell differentiation***

An inherent feature of pattern formation is an underlying asymmetry that facilitates differential regulation of cell behaviour within a given space. Therefore, as Turing alluded to, patterning requires that symmetry first be broken within the system, either through external cues or by intrinsic processes (Li and Bowerman, 2010; Turing, 1952). Subsequent

propagation of the initial asymmetry begets a host of downstream asymmetries that provide distinct spatial cues and progressively pattern the embryo.

In many invertebrates, parental factors are asymmetrically deposited to establish distinct embryonic regions prior to the first cell division. In *Caenorhabditis elegans*, the site of sperm entry determines the posterior pole of the embryo. A microtubule organising centre (MTOC) deposited by the sperm initiates actomyosin-dependent cortical flows that result in polarised anterior-posterior distribution of Par proteins in the zygote (Kemphues et al., 1988) (Munro et al., 2004; Nance et al., 2003). Par protein polarisation leads to asymmetric localisation of several molecules that influence cell fate, including ribonucleoproteins known as P-granules (Cheeks et al., 2004; Kemphues, 2000). At every division up until the 16-cell stage, these P-granules are segregated to only one daughter cell, which becomes the germline precursor (Hird et al., 1996; Strome and Wood, 1982). Therefore, the asymmetry induced by sperm entry, via amplification through other embryonic components, sets up the body plan and establishes the germline.

Likewise, mRNA molecules transcribed from maternal effect genes in *Drosophila melanogaster* are asymmetrically transported along the anterior-posterior axis during oogenesis (Nusslein-Volhard et al., 1987; Riechmann and Ephrussi, 2001; Roth and Lynch, 2009). Upon fertilisation and translation of these mRNAs, corresponding protein gradients are set up, which ensures spatially distinct regulation of downstream segmentation and homeotic genes to pattern the whole embryo (Clyde et al., 2003; Gavis and Lehmann, 1994; Rongo et al., 1995).

In adult tissues, a variety of stem cell niches highlight the relationship between position-dependent cellular interactions and cell differentiation states (Li and Xie, 2005). Schofield was the first to propose that a population of stem cells occupies a specific anatomical 'niche' (Schofield, 1978). A niche provides a physical anchor as well as specialised support cells that produce extrinsic signals to regulate stem cell self-renewal and differentiation.

In the hermaphroditic gonad of *C. elegans*, the germline niche is governed by the distal tip cell (DTC) where germline stem cells (GSCs) are in direct contact with the somatic DTC (Crittenden et al., 2006; Kimble and White, 1981). Interaction between the DTC and GSCs activates a Notch-like signalling cascade that promotes self-renewal and represses differentiation (Austin and Kimble, 1987). Conversely, as progeny move further away from the DTC, they transition from a mitotic to meiotic phase to form differentiated germ cells

(Cinquin et al., 2010). Therefore, increasingly differentiated cells are found at more proximal locations within the niche. In mammals, well-known niches include the intestinal crypt and the trabecular bone surface that guard intestinal and haematopoietic stem cells, respectively (Lander et al., 2012). Position-specific signals received and interpreted by cells in these structured microenvironments regulate differentiation state, proliferation and migration to ultimately preserve tissue integrity.

## Early mammalian development

### *Early mammalian embryos exhibit regulative patterning*

In contrast to worms and flies, there is little convincing evidence to suggest that parental factors have an instructive role in establishing spatial asymmetry during mammalian development (Alarcon and Marikawa, 2005; Dietrich and Hiiragi, 2007; Hiiragi and Solter, 2004; Louvet-Vallée et al., 2005). In fact, early development of mouse, rabbit and sheep are regulative, as these systems can adapt to perturbations in size to preserve embryonic patterning. In these model systems, halved and quartered embryos generated by removal of blastomeres after the first or second cleavage division can result in the birth of viable progeny (N. W. Moore, Adams, & Rowson, 1968; Tarkowski, 1959; Willadsen, 1981). Therefore, rather than relying on prepatterned asymmetries, cells of the mammalian embryo dynamically sense their relative position to ensure robust patterning.

### *Three distinct cell lineages are established in the preimplantation mouse embryo*

Mouse preimplantation development spans the first four days following fertilisation as the embryo traverses through the oviduct before implanting in the uterine epithelium. Towards the end of this stage, the embryo becomes a blastocyst consisting of a fluid-filled cavity surrounded by cells of three distinct lineages: trophectoderm (TE), epiblast (EPI) and primitive endoderm (PrE) (Figure 3A).

The divergence of TE and inner cell mass (ICM) during the 16-32 cell stage marks the very first lineage segregation event in mouse development (Marikawa and Alarcon, 2009). The *Cdx2*-expressing TE cells form an outer epithelial layer that will facilitate embryo-uterus interactions during implantation, and eventually give rise to the bulk of extraembryonic

tissues including the placenta (Collins and Fleming, 1995; Strumpf et al., 2005). Meanwhile, increased SOX2 levels in the embryonic interior mark the ICM, and nascent blastocoel fluid begins to accumulate between cells through transport of ions (Kawagishi et al., 2004; Manejwala et al., 1989; Wicklow et al., 2014; Wiley, 1984).

As the blastocyst matures, a mutually exclusive 'salt-and-pepper' pattern of EPI and PrE-specific markers emerges within the ICM. Soon thereafter, PrE cells are sorted to the ICM surface lining the cavity, while the EPI remain sandwiched between the PrE and the overlying TE (Chazaud et al., 2006; Plusa et al., 2008). Sorted PrE cells mature into a polarised epithelial monolayer, similar to the TE, and its derivatives eventually contribute to the yolk sac (Saiz et al., 2013).

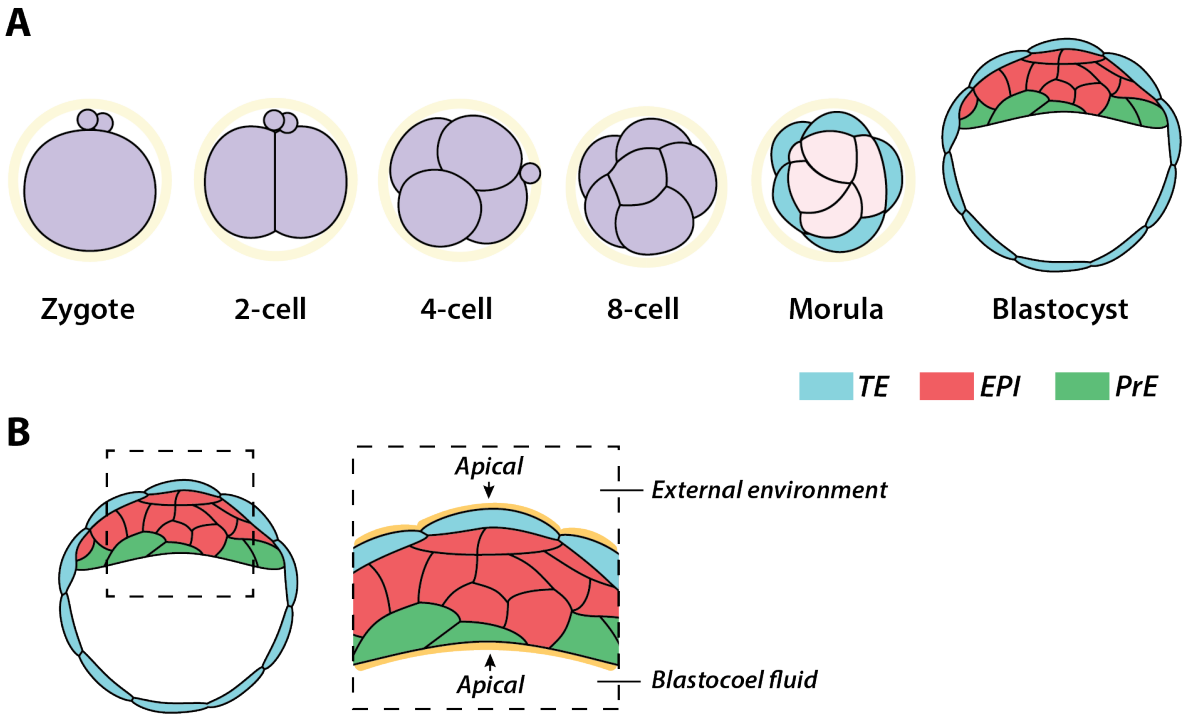


**Figure 3. Schematic representation of mouse preimplantation development.**

**A.** During preimplantation development, the mouse embryo undergoes cleavage divisions, and extracellular fluid accumulation results in an expanded cavity that characterises blastocysts. The outer trophectoderm (TE) is the first lineage to be specified in the morula (16-32-cell stage), and the epiblast (EPI) and primitive endoderm (PrE) emerge from the inner cell mass (ICM) in the embryonic interior. EPI and PrE cells arise in an intermingled 'salt-and-pepper' pattern, but these become spatially sorted as the blastocyst matures.

**B.** The direction of polarity is reversed between the TE and PrE. The apical side faces the external environment in the TE, while it faces inwards towards the blastocoel cavity in the PrE.

Despite shared epithelial features, the TE and PrE exhibit inverted polarity with respect to each other (Figure 3B). The apical surface of PrE cells faces the blastocoel cavity while their basal side is in contact with adjacent EPI cells. In contrast, it is the basal surface of TE cells that faces the cavity while the apical domain is exposed to the external environment. Given that most epithelial tissues in the body, such as the gut and lungs, exhibit apical polarisation towards the internal lumen, the orientation of TE polarity is a curious anomaly (Roignot et al., 2013). Although efforts to compare TE and PrE polarities have been sparse, the differences may bear significant implications for the fate and function of each lineage.

Encapsulated between basal surfaces of the TE and PrE, the EPI remains apolar during preimplantation development. The surface of each EPI cell is bound by contact with adjacent neighbours, thus lacks direct exposure to the blastocoel cavity or the external environment. These enclosed cells give rise to the embryo proper and serve as a source of pluripotent embryonic stem cells (ESCs) when isolated and cultured *in vitro* (Evans and Kaufman, 1981; Martin, 1981).

The TE, PrE and EPI are marked by clear morphological and positional differences as they emerge in the preimplantation embryo. By the 64-cell blastocyst stage, cells of these three lineages are distinguishable by their gene expression profile (Guo et al., 2010; Ohnishi et al., 2014). Since the mouse zygote lacks prepatterned asymmetry, however, these differentiation events must be preceded by symmetry-breaking within the early embryo.

### *Compaction and polarisation break symmetry in the 8-cell stage embryo*

Prior to symmetry-breaking in the mouse embryo, the first three cleavage divisions generate morphologically and functionally equivalent cells whose fate is neither predictable nor restricted to a particular lineage (Kelly, 1977; Tarkowski & Wróblewska, 1967). Analysis of mRNA levels for lineage markers indeed confirm that no distinguishing features are apparent between blastomeres in 2-, 4-, and early 8-cell stage embryos (Guo et al., 2010). Intracellular differences then emerge as a result of two major morphogenetic events: compaction and polarisation (Ducibella and Anderson, 1975; Ducibella et al., 1977; Lehtonen, 1980). Blastomeres enlarge contact with adjacent cells through compaction and assemble a polarised apical domain on their cell-free cortex (Figure 4A). As a result, the outer surface of the embryo becomes distinct from its inner regions. This asymmetry provides crucial positional information for subsequent patterning of the embryo.

*Compaction*

During compaction, adjacent cells flatten against each other and their membranes become tightly apposed, decreasing the proportion of free surface exposed to the external environment. Intercellular adhesion between blastomeres is strengthened by calcium-dependent interactions mediated by E-cadherin, encoded by *Cdh1* (Ducibella and Anderson, 1975). Embryos that lack E-cadherin, as well as those cultured in calcium-free medium, fail to compact (Ducibella and Anderson, 1975; Larue et al., 1994; Shirayoshi et al., 1983; Stephenson et al., 2010). This in turn impairs formation of a junctional permeability seal and prevents blastocoel fluid accumulation. Embryos that are unable to compact thus fail into mature into blastocysts.

Actomyosin-mediated cortical contractility is another an important driver of compaction (Maître et al., 2015). Measurements of interfacial tension revealed that cortical tension at the cell-medium interface increases during compaction. Conversely, tension decreases at cell-cell interfaces, coupled to local reduction in the levels of actin and myosin. Furthermore, pharmacological inhibition of actin polymerisation and myosin activity with cytochalasin D and blebbistatin, respectively, disrupts compaction (Fleming et al., 1986; Maître et al., 2015). Closer inspection through live-imaging at high temporal resolution revealed that blastomeres of the 8-cell stage display periodic travelling waves of cortical actomyosin contractions, and that the propagation of these waves is dampened at sites of intercellular contact and the apical domain (Figure 4B-D) (Maître et al., 2016). Therefore, compaction generates intracellular mechanical asymmetry through differential actomyosin activity and cell adhesion (Anani et al., 2014; Maître et al., 2016; Samarage et al., 2017).

*Polarisation*

Around the time of compaction, cells polarise along the radial axis of the 8-cell embryo by forming an apical domain on their outer surface (Ziomek and Johnson, 1980). Reminiscent of differentiated epithelial cell systems with distinct apical and basolateral regions, the embryonic apical domain is characterised by a concentration of microvilli and localisation of Par6, atypical protein kinase C (aPKC), and phosphorylated ERM (Ezrin, Radixin, Moesin) proteins (Fleming et al., 1986; Plusa, 2005; Rodriguez-Boulan & Macara, 2014; (Dard et al., 2001; 2009a; Pauken and Capco, 2000; Vinot et al., 2005). Although the molecular mechanism of this polarisation is not precisely understood, the Rho GTPase family member Cdc42 is known to be critically required (Etienne-Manneville, 2004; Korotkevich et

al., 2017). Functional analyses in budding yeast and epithelial cell cultures show that Cdc42 can recruit proteins that crosslink and bundle actin filaments, interact with other apically localised proteins, and regulate vesicular trafficking by interacting with the Rab family of GTPases (Aceto et al., 2006; Adamo et al., 2001; Wedlich-Soldner et al., 2003). There is also evidence that cell adhesion stimulates Cdc42, leading to spatial regulation of its activity (Kim et al., 2000). While these processes are yet to be studied in mouse development, Cdc42-deficient embryos fail to polarise and consequently degenerate during the preimplantation period (Korotkevich et al., 2017).

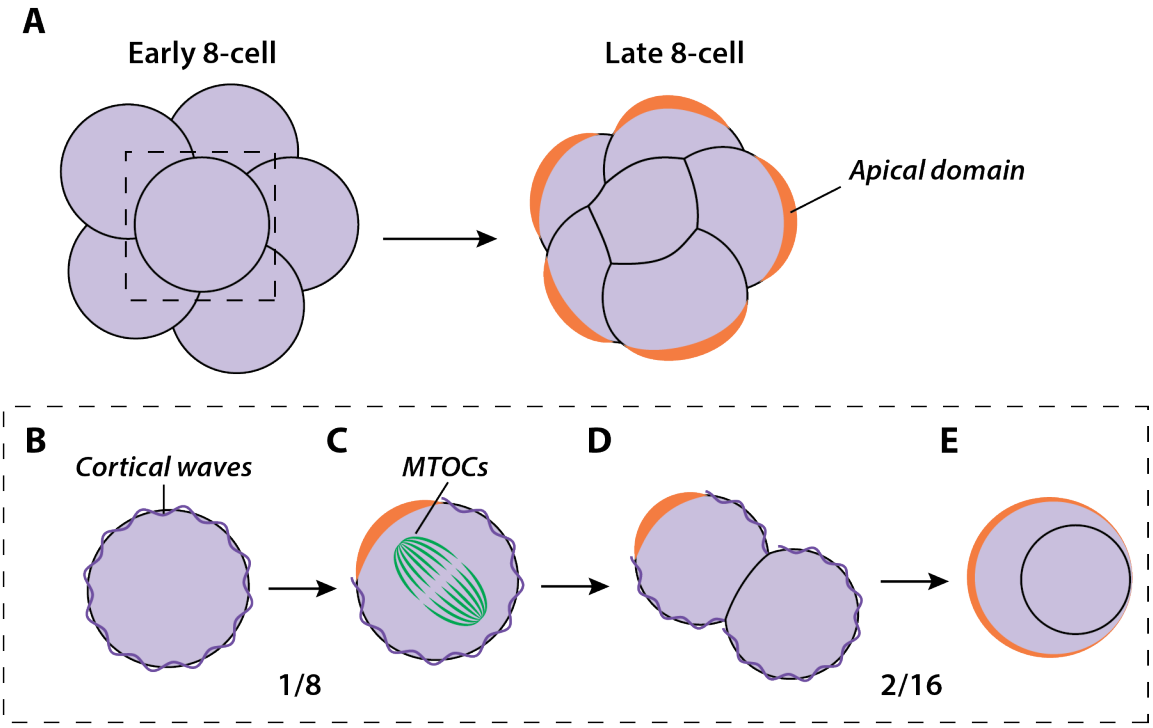


**Figure 4. Symmetry-breaking occurs during the 8-cell stage.**

**A.** During this stage, both mechanical and biochemical asymmetry emerges as the mouse embryo undergoes compaction and polarisation. The late 8-cell stage exhibits increased cell-cell adhesion, and the outer surface of each blastomere is marked by an apical domain that contains microvilli and proteins including pERM, aPKC, and Pard6b. Notably, symmetry-breaking and subsequent patterning can be recapitulated by individual blastomeres isolated from the early 8-cell stage (B-E).
**B.** Early 8-cell blastomeres exhibit waves of cortical actomyosin activity.
**C.** The apical domain recruits microtubule organising centres (MTOCs) and directs spindle orientation for asymmetric cell division.
**D.** Since the cortical contractility is suppressed by the apical domain, asymmetric inheritance of polarity between daughter cells results in mechanical differences that drive differential cell sorting as represented in **E.**

Apical domain assembly is observed in dissociated 8-cell stage blastomeres, suggesting that polarisation is cell-autonomous (Figure 4C) (Korotkevich et al., 2017; Lorthongpanich et al., 2012). Nevertheless, the incidence of isolated polarisation is considerably lower compared to conditions where a contact interface is shared with a neighbouring cell (Korotkevich et al., 2017). In the latter, the apical domain tends to assemble on the cortical region furthest from the adhesive interface. This contact cue therefore potentiates polarisation and also guides its orientation. Notably, given that the effects of cell-cell adhesion can be reproduced by contact with biologically inert beads and potentially display a force threshold, the role of this 'contact' may not be limited to biomolecular cues but also extend to mechanical interactions (Korotkevich 2017; Bun et al., 2014).

***Interplay between cortical contractility and polarity directs cell positioning***

Compaction and polarisation break symmetry by establishing mechanical and biochemical differences between inner and outer regions of the 8-cell embryo. While both processes are sensitive to intercellular adhesion, there is also evidence for more direct interplay between cortical contractility and the apical domain in the preimplantation embryo. During the late 8-cell stage, surface contractility is reduced at the embryo periphery, suggesting local suppression of actomyosin by the apical domain (Figure 4C-D) (Maître et al., 2016). Later, as the blastomere prepares to divide, the apical domain recruits MTOCs to align the spindle along the radial axis of the embryo (Fig 4C-E) (Korotkevich et al., 2017). This drives a strong bias towards asymmetric cell division where the apical domain is inherited by one daughter cell but not the other (Anani et al., 2014; Johnson and Ziomek, 1981; Korotkevich et al., 2017; Maro et al., 1991). As a result, upon 8- to 16-cell stage transition, the embryo is composed of cells that differ in their polarity as well as actomyosin-mediated tension. Experiments with 2/16 doublets and physical modelling have demonstrated that this differential tension is sufficient to drive cell sorting behaviour where apolar cells are internalised by polarised cells (Anani et al., 2014; Maître et al., 2016; Samarage et al., 2017). This interplay between cortical tension and polarity therefore instructs the initial inner-outer configuration within the embryo.

### *Models to explain TE/ICM specification*

The breaking of embryonic symmetry and subsequent inner-outer sorting of cells is imperative to TE/ICM specification. Historically, two models were proposed to explain the mechanism of TE/ICM specification: the Inside-Outside model and the Polarity model. The Inside-Outside model stipulates that cell position within the 16-32 cell stage embryo determines fate, with outer cells becoming TE and inner cells ICM. Researchers noted that, although a given blastomere isolated from an early embryo at the 2-, 4-, or 8-cell stage is capable of recapitulating preimplantation patterning, the incidence of blastocyst formation decreases with dissociation at later stages (Tarkowski and Wróblewska, 1967). The rest instead forms "trophoblastic vesicles" where a single layer of TE-specified cells surrounds a cavity devoid of an ICM. The explanation for these observations was that the later the dissociation, fewer cells are present at the time of cavitation, which imposes geometric constraints against complete envelopment of a cell by its neighbours. The Inside-Outside model proposes that inner and outer cells receive distinct microenvironmental cues to govern fate, and therefore positional differences underlie TE/ICM specification.

On the other hand, the Polarity model states that the TE and ICM are specified upon asymmetric division during the 8- to 16-cell stage (Johnson and Ziomek, 1981). Using blastomeres from dissociated 8-cell embryos, authors of this model found that the majority of 1/8 to 2/16 cell divisions result in asymmetric inheritance of the apical domain. Concurrently, they observed in whole embryos that polarised cells remain on the peripheral surface enclosing apolar cells. These led to the proposal that positional differences are a corollary to asymmetric division, and the presence and absence of polarity determines TE and ICM specification, respectively.

### *The apical domain marks the outer cells of the embryo*

Decades of research continued to build on these two models to elucidate the mechanism of TE/ICM specification. One prominent difference between the TE and ICM is the activity of the Hippo signalling pathway (Cockburn et al., 2013; Hirate et al., 2013; Nishioka et al., 2009; Wicklow et al., 2014). The Hippo pathway, first identified in flies with overgrowth phenotypes, integrates a host of upstream signals to regulate cell fate and tissue growth. In addition to growth factors and nutrients, the pathway is also sensitive to cell adhesion and mechanical forces in the surrounding microenvironment. Given such breadth, this highly conserved pathway is well suited to transmit positional information. In inner cells

of the morula, junction associated protein Amot is localised to adherens junctions and activates the Hippo pathway, leading to phosphorylation and cytoplasmic retention of YAP (Yes-associated protein) (Figure 5A) (Hirate and Sasaki, 2014). In outer cells, Amot localises to the apical domain, and YAP translocates to the nucleus where it activates Tead4 (Anani et al., 2014). Tead4 in turn induces the expression of TE-specific genes such as *Cdx2* and *Gata3*. For this reason, differential localisation of YAP is often used in the literature as a proxy marker for TE/ICM fate.

Importantly, however, Hippo signalling is not strictly dependent on cell position. In fact, differential YAP localisation is also observed between cells occupying similar positions within the embryo. In 16-cell embryos, geometric constraints often allow only one or two cells to be completely internalised, thus apolar cells are often found on the outer surface. Some of these apolar cells have high levels of phosphorylated YAP (pYAP) despite their outer position. Therefore, asymmetric Hippo signalling better mirrors asymmetric inheritance of the apical domain rather than cell position (Figure 5B). Cells that have an apical domain display high levels of nuclear YAP while the phosphorylated form prevails in the cytoplasm of apolar cells (Anani et al., 2014).

Critically, even if a cell does not inherit an apical domain, it can polarise *de novo* if positioned outward. Such cells subsequently decrease cytoplasmic YAP and upregulate *Cdx2,* just as those that had directly inherited the apical domain from the parental 8-cell stage blastomere. As a result, the outer surface of the preimplantation embryo remains consistently polarised from the 8-cell stage onwards. This indicates that cell positioning is not predetermined. Rather, blastomeres are able to dynamically sense their position, such that outer cells are marked by polarity regardless of their division history from the 8-cell stage onwards (Dard et al., 2009b; Korotkevich et al., 2017; Watanabe et al., 2014).

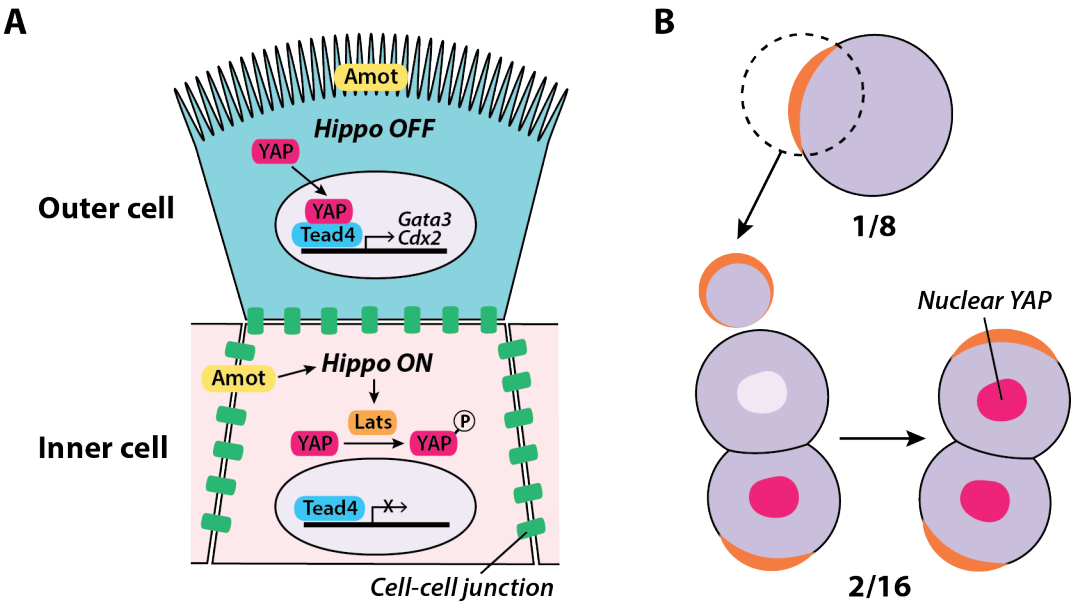


**Figure 5. Hippo signalling differentially active in polar and apolar cells.**

**A.** In inner cells junctionally localised Amot activates Hippo signalling, and YAP is phosphorylated by the kinase Lats. Phosphorylated YAP remains cytoplasmic. In polarised outer cells, Amot is apically localised and Hippo signalling is inactive. YAP translocates to the nucleus and binds with Tead4 to drive expression of TE-specific genes.
**B.** An apical domain can be pinched off from a polarised 8-cell stage blastomere and grafted onto an apolar 16-cell stage blastomere. This apical domain graft is sufficient to inactivate Hippo signalling, as indicated by nuclear translocation of YAP (Korotkevich et al., 2017).

### *The apical domain is necessary and sufficient for TE fate*

The polarised outer cells in the preimplantation embryo form the TE. Knockdown of Pard6b, a component of the PAR-aPKC complex that regulates apicobasal polarity, results in YAP phosphorylation and downregulation of *Cdx2* in outer cells (Alarcon, 2010). More severely, the TE layer fails to form at all in embryos that lack *Cdc42*, a Rho GTPases family member critically involved in polarisation (Korotkevich et al., 2017). To unequivocally examine sufficiency of the apical domain in promoting TE specification, Korotkevich and colleagues employed a reduced experimental system using isolated 8-cell stage blastomeres (1/8) and doublets equivalent to the 16-cell stage (2/16) (Figure 5B). The apical domain pinched off from a polarised 8-cell stage blastomere was transplanted onto an apolar cell of a 2/16 doublet. This transplantation induced sequestration of Amot to the grafted apical region and nuclear accumulation of YAP, reminiscent of events that occur in outer cells of the embryo as they become TE-specified. In this way, it was elegantly demonstrated that the apical domain is both necessary and sufficient to direct TE specification.

### *Inner positional cues remain elusive*

As described above, embryonic polarity prescribes the spatial bearings that ensure outer cells are TE-specified. Furthermore, the signalling events that bridge polarisation and upregulation of *Cdx2* in the morula are relatively well understood. In contrast, however, much less is known about the signals that inform inner cells of their position and direct ICM specification.

Studies of ICM specification are hindered by several factors. Asynchrony of divisions, dynamic cell sorting, and transcriptional heterogeneity within the embryo lead to variable timing of inner cell emergence and ICM specification (Anani et al., 2014; Dietrich & Hiiragi, 2007; Fleming, 1987; Guo et al., 2010). Moreover, inner cells are fewer in number compared to outer cells in the morula, and upregulation of ICM markers is generally delayed compared to TE counterparts. Consequently, the microenvironmental cues pertinent for ICM specification thus far remain ambiguous.

### *'Contact' is required for patterned TE/ICM specification*

Generally, the microenvironment of apolar inner cells is characterised by enrichment of intercellular contacts. To examine the influence of intercellular contact on TE/ICM specification, Lorthongpanich and colleagues separated blastomeres of the 2-cell stage embryo and continued separating daughter cells after each round of division during preimplantation development (Lorthongpanich et al., 2012). All positional cues were thus removed from each cell. Although the resulting gene expression profile showed an overall 'TE-like' signature, these cells were neither TE nor ICM -specified, suggesting that positional information provided through cell contact is required for establishment of lineage-specific gene expression.

## Adhesive interactions in pattern formation

### *Cell-cell interactions govern cell sorting: the differential adhesion hypothesis*

While early discussions on positional information were mainly concerned with global cues for pattern formation, a growing body of work was detailing the importance of adhesive interactions in multicellular organisation. It was reported more than a century ago that cells dissociated from siliceous sponges self-assemble into syncytial masses to give rise to new sponges (Wilson, 1907). Similar observations were made in amphibian and avian embryos, highlighting a remarkable 'self-organising' ability of cell mixtures to approximate mature tissue structures (Moscona and Moscona, 1952; Townes and Holtfreter, 1955).
These eventually led to Steinburg's differential adhesion hypothesis, which stipulates that cells bind to cells of similar adhesion strength or surface tension to produce a thermodynamically stable structure, thus contributing to morphogenesis through cell sorting (Figure 6A) (Steinberg, 1963; Townes and Holtfreter, 1955). The differential adhesion hypothesis thus offered a physical explanation for patterning, even before adhesive molecules were discovered. In the decades that followed, adhesive contacts became molecularly defined and broadly categorised into two types: cell-cell adhesion and cell-extracellular matrix (ECM) adhesion (Figure 6B).

### *Cell-cell adhesion mediated by E-cadherin plays key roles in early development*

Cell-cell adhesion is generally mediated by the cadherin family of proteins. The founding member E (epithelial) -cadherin was first described by Masatoshi Takeichi as a calcium-dependent adhesion molecule that holds epithelial cells together (Figure 6C) (Takeichi, 1977; Yoshida and Takeichi, 1982). Observing morphological changes in cells upon calcium modulation, Takeichi went on to correctly predict that cadherins not only let cells stick to one another, but also collectively regulate morphogenesis during development.

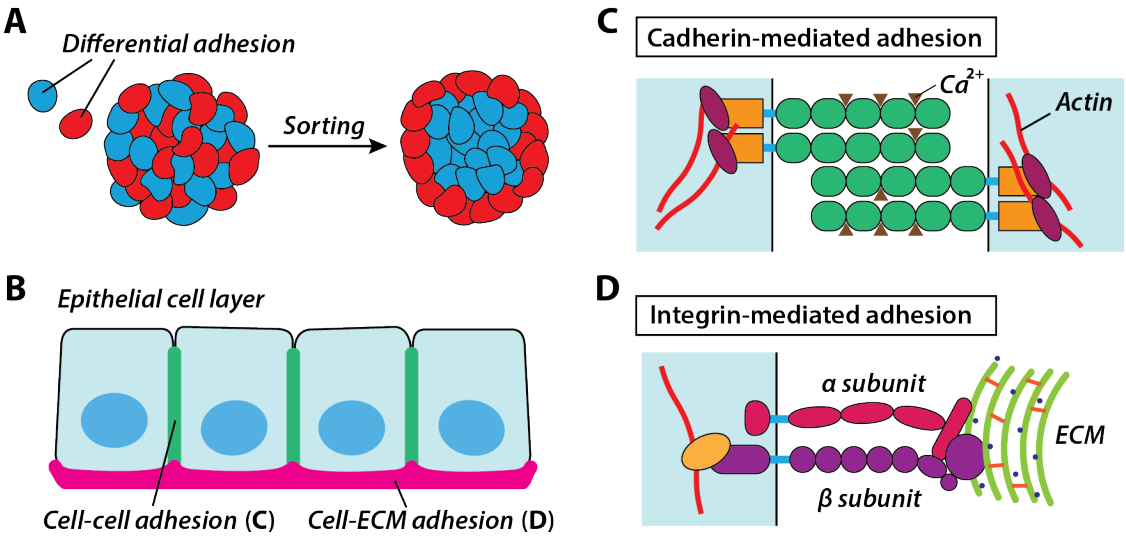


**Figure 6. Adhesive interactions underlie pattern formation.**

**A.** The differential adhesion hypothesis stipulates that cells sort according to relative surface tension, which is determined by their adhesive strength, to achieve a state of minimal interfacial free energy.

**B.** A typical epithelial cell engages in two types of adhesive interactions with its microenvironment: cell-cell adhesion with adjacent cells (green), and cell-ECM adhesion with the underlying basement membrane (magenta).

**C.** Cadherins are mediators of cell-cell adhesion. Calcium ions to stabilise the extracellular domains of cadherins to facilitate homophilic *trans* interactions that underlie cell-cell adhesion. On the cytoplasmic side, cadherins are linked to the actin cytoskeleton via various adaptor proteins.

**D.** Integrin heterodimers, consisting of an α and β subunit, are major ECM receptors that mediate cell-ECM adhesion. A diversity of integrin heterodimers allows recognition of different types of ECM proteins and drives a broad repertoire of bidirectional signalling events.

In gastrulating zebrafish embryos, E-cadherin is required for epiboly and convergent extension. Deficiency in E-cadherin disrupts the spreading and coordinated movement of cells required for dorsoventral patterning, leading to embryonic lethality (Shimizu et al., 2005). In mouse embryos lacking E-cadherin-mediated adhesion, compaction and epithelialisation of the TE layer is severely disrupted (Ducibella and Anderson, 1975; Larue et al., 1994). Cells often exhibit broad distribution of apical proteins around the entire membrane as adhesions weaken. Since inside-outside patterning is lost, these mutant embryos do not survive beyond the preimplantation stage. Cadherin-mediated adhesion is thus critical for guiding pattern formation, and ultimately required for survival.

### *The ECM is a major regulator of cell behaviour*

The second type of adhesive interactions found in multicellular tissues occurs between cells and the ECM, commonly via integrin receptors (Figure 6D). Historically, the recognition of connective fibres in tissues actually preceded cell theory. It was not until the mid 1800s that tissues were found to be made out of cells, and as collagen became characterised early in the last century the term 'extracellular' matrix appeared (Clark and Schaad, 1936; Schmitt et al., 1942). Other major protein components of the ECM – including fibronectin and laminin - were subsequently discovered alongside various glycosaminoglycans (Meyer and Palmer, 1934; Meyer et al., 1956; Ruoslahti and Vaheri, 1975; Timpl et al., 1979).

The evolutionarily conserved ECM is found in all phyla of metazoans as a key mediator of multicellularity (Ozbek et al., 2010; Whittaker et al., 2006). Each protein component comprises a family of multiple isoforms, and their constituent polypeptide chains assemble into oligomeric or polymeric complexes. The myriad of ways in which ECM components are combined and crosslinked produce matrices unique in their chemical, structural, and mechanical properties. Among its numerous roles, the ECM provides physical scaffolding for cellular interactions, carries soluble components to regulate signalling, and relays topographical information about the microenvironment (Ohashi et al., 1999; Rahman et al., 2005; Yayon et al., 1991). Accordingly, ECM structures are actively engaged in crosstalk with cells. Multiple pathways and proteases are involved in their turnover and remodelling as they regulate a host of processes spanning cell movement, survival, polarisation, division and differentiation during morphogenesis (Palecek et al., 1997; Willingham et al., 1977; Yamada et al., 1976).

### *The requirement for ECM during development*

During oogenesis in *Drosophila*, the initially spherical egg breaks symmetry by elongating along the anterior-posterior axis to become ellipsoid in shape (Roth and Lynch, 2009). The developing egg is enclosed in a follicle epithelium, which migrates in a circumferential direction orthogonal to the anterior-posterior axis (Went, 1978). Since the follicle epithelium is a geometrically continuous structure, this collective migration results in global rotation of the whole tissue over its underlying ECM substrate (Haigo and Bilder, 2011). As a result, sparsely distributed collagen IV chains in this matrix become organised into dense circumferentially oriented fibrils (Cetera et al., 2014). This polarised ECM

subsequently forms to a 'molecular corset' that constrains egg growth in the dorsoventral direction and drives elongation along the anterior-posterior axis. In this way, cells modulate ECM structure, which in turn mechanically regulates egg shape and thereby facilitates asymmetric deposition of maternal factors as described earlier.

In vertebrates, neural crest cells delaminate from the midline and migrate extensively within the vertebrate embryo, giving rise to various cell types including neurons, glia, melanocytes and craniofacial cartilage (Duband et al., 1995). Spatiotemporally controlled interactions with the ECM microenvironment critically underlie their highly patterned migratory behaviour and spatially coordinated differentiation (Duband and Thiery, 1987; Erickson and Weston, 1983; Pietri et al., 2004). Regionally specific combinations of ECM components function as permissive, non-permissive, or inhibitory cues to migration, and even influence its timing and rate (Henderson and Copp, 1997; Lallier et al., 1992; Strachan and Condic, 2008). For example, cranial neural crest cells migrate faster than trunk neural crest cells on laminin, but not on fibronectin (Strachan and Condic, 2003). Furthermore, conditional knockout of the laminin α5 chain results in expansion of neural crest migratory streams and is linked to the craniofacial abnormalities in mice (Coles et al., 2006).

Similarly, heart morphogenesis in the zebrafish requires ECM-dependent migration of myocardial precursors from the left and right sides of the embryo towards the midline (Stainier et al., 1993; Trinh and Stainier, 2004). Upon arrival at the midline, they mature into polarised epithelia and fuse with endocardial cells to form the heart tube. Mutation in the gene encoding fibronectin disrupts both polarisation and migration of myocardial precursors, resulting in cardia bifida, the formation of two separate hearts in the lateral regions of the embryo (Trinh and Stainier, 2004).

***Integrin receptors sense the ECM***

Indispensable for the function of the ECM is the cell's ability to perceive its components and thus deduce the chemical and mechanical milieu. This 'sensing' is mainly achieved through binding of integrin receptors to their cognate ECM ligands. Integrins were first identified by Tamkun and colleagues as transmembrane glycoproteins mediating adhesion between fibronectin and the cytoskeleton of chicken fibroblasts (Tamkun et al., 1986). Discovery of integrins across various species including mammals, birds, and insects followed soon thereafter (Hynes, 1987; 2004). Integrins are a family of heterodimeric ECM receptors, each consisting of an α and β subunit (Figure 6D) (Haas and Plow, 1996). There

are 19 α subunits and 8 β subunits known to date, which combine to form at least 25 different heterodimers in mammals. Specific ECM components are often recognised by multiple integrin heterodimers, and conversely, a particular integrin heterodimer may bind to several different ECM components.

Besides mediating cell-ECM adhesion, integrins serve as bidirectional signal transducers (Bazzoni et al., 1998; Hughes et al., 1996; O'Toole et al., 1991; Takagi et al., 2002). Upon integrin ligation, extracellular signals can be relayed to the cytoplasm to regulate a variety of cellular events, and vice versa. In general, the extracellular domain of the α subunit confers ECM ligand specificity, while the cytoplasmic domain of the β subunit regulates intracellular signalling activity (Xiong et al., 2002). Furthermore, affinity modulation through integrin conformational changes, clustering on the plasma membrane, as well as endosomal trafficking dynamics, add to the complexity of integrin-mediated cell-ECM interactions (Arjonen et al., 2012; Bazzoni et al., 1998; Li et al., 2003; Miyamoto et al., 1995; Tadokoro et al., 2003; Yauch et al., 1997).

On the cytoplasmic side, integrins interact with cytoskeletal adaptors such as talin and vinculin that bind to actin (Calderwood et al., 1999; Humphries et al., 2007; Kanchanawong et al., 2010; Pfaff et al., 1998). In this way, the cells become mechanically linked to the surrounding matrix, and forces can be sensed and exerted bidirectionally. Furthermore, although integrins do not have catalytic activity of their own, they can engage a range of enzymes including focal adhesion kinase, integrin-linked kinases, and Rho GTPases (Clark et al., 1998; Hannigan et al., 1996; Huveneers and Danen, 2009). The mechanosensitive signalling platforms assembled as such are indispensable for spatiotemporally controlled cell behaviour throughout development.

***Integrins and laminin are expressed early during preimplantation development***

An assortment of cell-ECM interactions features in the preimplantation mouse embryo. Among the major ECM components, laminin is the earliest to be expressed, followed by nidogen, collagen IV and fibronectin (Figure 7) (Cooper and MacQueen, 1983; Dziadek and Timpl, 1985; Futaki et al., 2019; Georges-Labouesse et al., 1996; Klaffky et al., 2006; Leivo et al., 1980; Wu et al., 1983). Laminin is a cross-shaped, heterotrimeric disulfide-bonded complex of α, β, and γ polypeptide chains. The amino-terminals of the three chains mediate intermolecular interactions that lead to network assembly in the extracellular space. At least 16 different laminin heterotrimers are reported in mammals, and

the main isoforms implicated in preimplantation development are laminin-111 and laminin-511, consisting of chains α1β1γ1 and α5β1γ1, respectively (Klaffky et al., 2006; Tzu and Marinkovich, 2008).

The earliest detection of a full heterotrimer of laminin is reported at the 16 cell stage (Leivo et al., 1980). The trimer is initially found in the cytoplasm and extracellular space in a granular distribution pattern, and its expression progressively increases thereafter. By the blastocyst stage, laminin is found in the basement membrane underlying the TE layer, as well as within the ICM. However, the actual transcription of the laminin β1and γ1 mRNAs are reported to occur as early as the 2-cell stage, while the expression of laminin α1 lags behind by appearing at the 16-32 cell stage (Cooper and MacQueen, 1983). Notably, the reported onset of laminin α1 expression and trimerisation temporally coincides with the emergence of the first 'inner' cells within the embryo that become ICM-specified.

Therefore, laminin may be a major component of the embryonic 'inner' microenvironment that provides positional cues to direct ICM fate. Although the functional role of laminin in TE/ICM specification is not yet known, embryos lacking zygotic copies of laminin chains β1 or γ1 do not survive beyond embryonic day (E) 5.5 (Miner et al., 2004; Smyth et al., 1999) . In these mutant embryos the basement membrane is absent, and spatial organisation between the TE, EPI, and PrE is severely disrupted, indicating impaired transduction of positional information.

In fact, studies in other epithelial systems have demonstrated that laminins are certainly involved in directing polarisation as well as differentiation. Antisera against laminin inhibits polarisation and differentiation of kidney tubule epithelium in *in vitro* cultures of induced metanephric mesenchyme and whole kidney explants (Klein et al., 1988; Sorokin et al., 1990). Likewise, loss of laminin in the retina disrupts apicobasal polarity of glial cells that support retinal neurons, resulting in retinal dysplasia (Pinzón-Duarte et al., 2010).

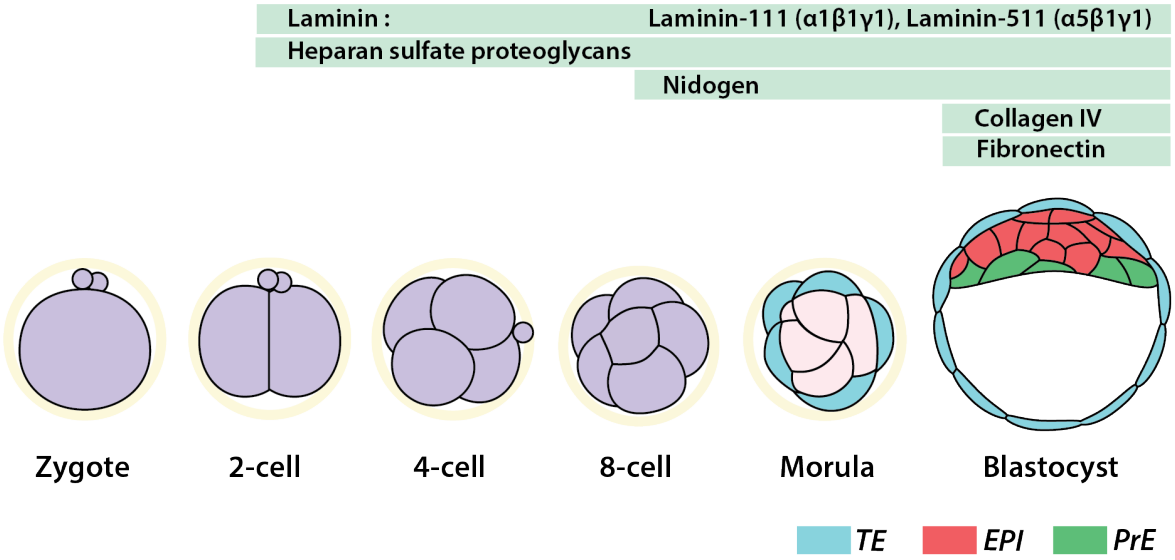


**Figure 7. Expression of ECM components during preimplantation development.**

A variety of ECM components are expressed in a spatiotemporally controlled manner as the embryo develops. Laminin chains are the first major protein components of the ECM to be expressed. While laminin chain expression is detected as early as the 2-cell stage, the formation of a full αβγ heterotrimer is reported to occur around the morula (16-32 cell) stage.

The major integrins known to bind to laminin are integrin heterodimers α3β1 and α6β1 (Belkin and Stepp, 2000; Cooper et al., 1991; Sorokin et al., 1990). Similar to reports on laminin deficient mouse embryos, those lacking the integrin β1 subunit display a disorganised mass of cells in the inner region of the embryo and do not survive beyond E5.5 (Figure 8A, B) (Fässler and Meyer, 1995; Stephens et al., 1995). Furthermore, laminin receptor integrin α6β1 is one of the primary integrins to be expressed by ICM-derived ESCs, and cell adhesion assays show that ESCs strongly adhere to laminin substrates (Aumailley et al., 1990) (Cattavarayane et al., 2015). Accordingly, blocking the integrin β1 subunit inhibits ESC adhesion and impairs pluripotency.

In 3D, suspension of ESCs gives rise to smooth spherical embryoid bodies (EBs) that mimic EPI and PrE differentiation and sorting *in vitro*. Wildtype EBs consist of a polarised outer layer of PrE cells enclosing a core of EPI cells. In comparison, EBs derived from *Itgb1*-/- ESCs that lack integrin β1 exhibit an uneven surface interrupted by clusters of outgrowths (Figure 8C) (Li et al., 2002). These are also smaller in size, and surface polarity is disrupted as PrE cells fail to sort to the periphery (Li et al., 2002). In addition, the basement membrane lining the PrE-EPI boundary is underdeveloped (Aumailley et al., 2000; Moore et al., 2014). These observations altogether suggest that ECM-integrin interactions are

important determinants of cell differentiation state, spatial sorting, polarisation, as well as basement membrane maturation. Therefore, their involvement in patterning *in vivo*, particularly as the first lineages are laid down in the mouse embryo, warrants close examination.

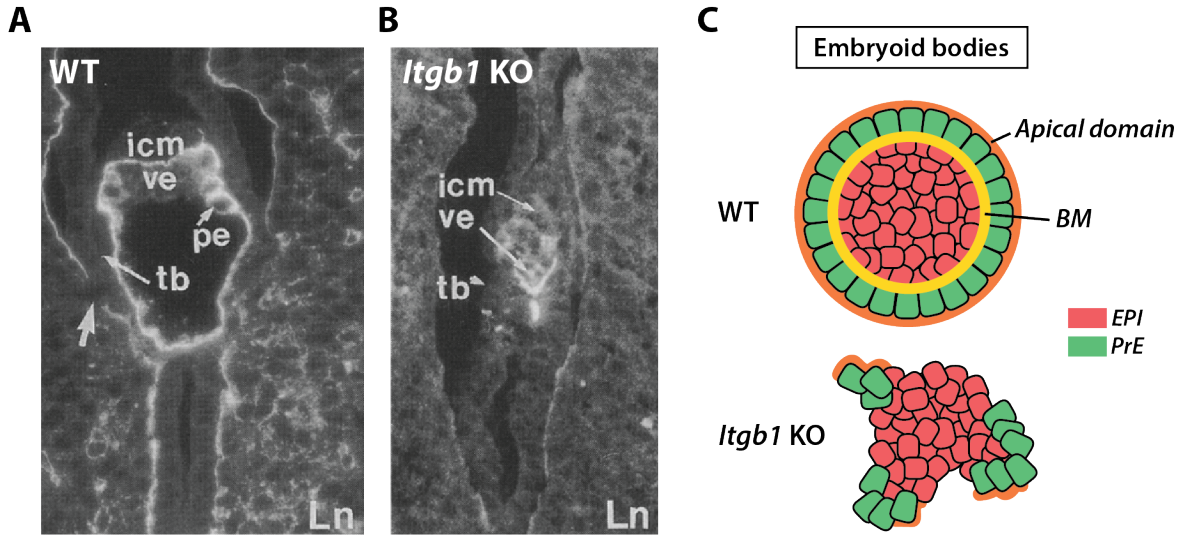


**Figure 8. Integrin β1 is required for embryonic survival and patterning.**

**A.** Immunofluorescence staining against laminin-111 shows a wildtype E4.5 embryo implanted in the uterine tissue. Befitting this stage of development, the embryo exhibits patterned arrangement of ICM, visceral endoderm (ve), parietal endoderm (pe), and trophoblast (te) cells.
**B.** In contrast to **A.**, embryo deficient in zygotic *Itgb1* exhibit reduced size and disorganised arrangement of cells. Images in **A.** and **B.** are taken from Stephens et al., 1995.
**C.** Embryoid bodies lacking integrin β1 fail to form organised spheroids. Small clusters of PrE cells are observed at the periphery instead of forming a continuous, polarised layer. Both apical polarisation and basement membrane deposition is severely disrupted compared to wildtype (WT) EBs.

# Aims & Experimental Design

Much progress has been made over the last decades to identify factors that pattern the early mouse embryo. However, our understanding of the functional relationship between each of these components is incomplete. While spatially distinct engagement of polarity and cortical contractility are important positional cues leading to TE/ICM specification, their direct relationship have not been examined in full. Furthermore, although earlier studies provide valuable insight into TE specification of outer cells, the interior the embryo has been relatively overlooked. High-resolution transcriptional maps gained from single cell studies allow distinction of lineages, yet fail to capture the functional relevance of cell-cell interactions during initial fate specification. More than half a century has passed since Tarkowski and Wroblewska proposed the Inside-Outside model, but the molecular constituents of the positional information underlying TE/ICM specification remain to be elucidated.

Therefore, the overarching goal of this study is to understand how position-sensing is robustly achieved to affect cell fate specification and ultimately pattern the preimplantation mouse embryo. We hypothesise that asymmetric cell-cell interactions and the ECM provide positional information that distinguish between inner and outer regions of the embryo. Moreover, we predict that modulation of the adhesive environment by provision of exogenous ECM components can alter preimplantation patterning, particularly ICM specification. To explore these possibilities, reduced systems, immunosurgery, and Matrigel culture are utilised as described below.

The preimplantation mouse embryo has remarkable regulative capacity, which makes it an experimentally amenable system that can adapt to perturbations such as removal of cells. Single blastomeres isolated from the 2-, 4-, 8-cell embryo can recapitulate all the hallmarks of preimplantation development, including patterned specification of the three lineages (TE, ICM, PrE) and formation of a blastocoel cavity. Likewise, inner cells isolated from 16-32-cell embryos develop into 'mini-blastocysts' that retain features of full blastocysts. In fact, individual blastomeres up until the 16-32 cell stage are totipotent, having the potential to give rise to every cell type found in the adult mouse as well as the extraembryonic tissues that support its *in utero* development (Suwińska, Czołowska, Ożdżeński, & Tarkowski, 2008; Tarkowski, Suwińska, Czołowska, & Ożdżeński, 2010). Such regulative capacity emphasises how major morphogenetic processes persist regardless of the number of cells present, driven by a temporal clock whose mechanism is unknown (R. Smith & McLaren, 1977). Moreover, given that complex interactions entwine factors spanning cell polarity, shape, adhesion, and

contractility in whole embryos, such 'reduced' systems and isolated cells enable more deliberate examination of individual parameters that contribute to patterning.

Doublets formed by division of 1/4 or 1/8-blastomeres are particularly useful in the present study for examining the relationship between cortical contractility and the formation of the apical domain (Figure 9A). One the other hand, isolation of inner cells through immunosurgery allows perturbation of inner-outer positional identities. Immunosurgery involves sequential incubation of embryos in antibody and complement, resulting in the selective lysis of outer cells while inner cells remain intact (Figure 9B) (Handyside & Barton, 1977; Solter & Knowles, 1975). The isolated cluster of inner cells, which would have remained apolar and upregulated SOX2 within the whole embryo, adapt to immunosurgery by undergoing *de novo* polarisation on their outer surface (Stephenson et al., 2010; Wigger et al., 2017). These newly polarised cells upregulate CDX2 while SOX2 is limited to the interior of the cluster as division continues.

To mimic and modulate cues potentially provided by the ECM, Matrigel culture is used. Matrigel is an ECM-rich secretion from Engelbreth-Holm-Swarm mouse sarcoma cells known to be rich in laminin, fibronectin, and collagens (Orkin 1977). In conjunction with a range of available transgenic mouse lines and imaging tools, experimental manipulations discussed above enable careful examination of the adhesive interactions that provide positional information to pattern the preimplantation embryo.

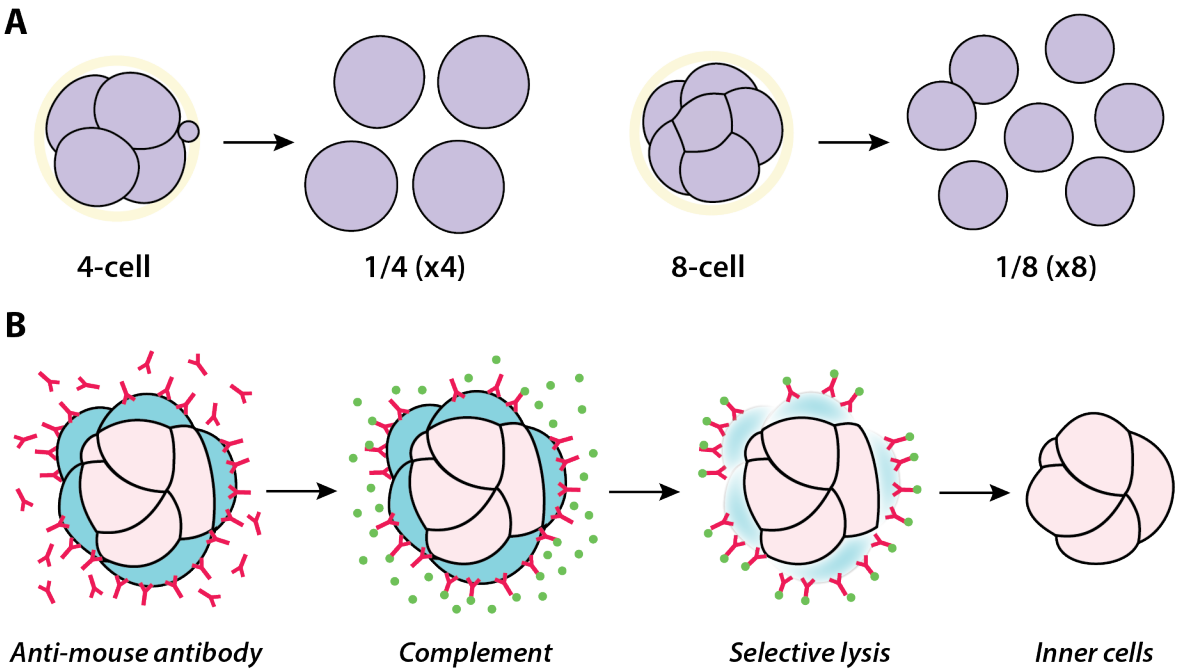


**Figure 9. Experimental strategy: reduced systems & immunosurgery.**

**A.** Given the regulative capacity of early blastomeres, individual cells dissociated from 4-and 8-cell stage embryos can be used to manipulate and recapitulate preimplantation patterning at a reduced, more experimentally amenable scale.
**B.** Immunosurgery isolates inner cells through selective complement-mediated lysis of outer cells. Reduced systems in **A.** and the inner cell cluster isolated from the morula in **B.** can go on to from 'mini-blastocysts' that recapitulate the patterning and lineage specification seen in whole blastocysts.

# Materials & Methods

## Animal work

All animal work was performed in the Laboratory Animals Resources (LAR) facility at the European Molecular Biology Laboratory with permission from the institute's veterinarian overseeing the operation. The LAR facility operates according to guidelines and recommendations set by the Federation for Laboratory Animal Science Associations. Mice were maintained in pathogen-free conditions under 12-hour light-dark cycles.

### *Mouse lines*

Wildtype (WT) embryos were obtained by crossing F1 (C57Bl/6xC3H) females and males. Furthermore, the following transgenic mouse lines were used in this study: *Myh9* $^{tm5Rsad\ (floxed)}$ (Jacobelli et al., 2010), *Itgb1*$^{tm1Efu\ (floxed)}$ (Raghavan et al., 2000), Zp3-Cre (de Vries et al., 2000).

To generate maternal zygotic *Myh9* knockout embryos, *Myh9*$^{floxed/floxed}$ Zp3-Cre$^{tg/+}$ females were crossed with *Myh9*$^{+/-}$ males. To obtain zygotic *Itgb1* knockout embryos, *Itgb1*$^{+/-}$ females were crossed with *Itgb1*$^{+/-}$ males.

### *Superovulation*

Superovulation was induced in females prior to mating to increase the number of preimplantation embryos obtained per mouse. Intraperitoneal injection of 5IU of PMSG (Intervet, Intergonan) and hCG (Intervet, Ovogest 1500) were carried out, with a 48-50 hour interval between the two injections. Each female mouse was put in a cage with a male immediately following hCG injection for mating.

### *Dissection of reproductive organs*

Timing of sacrifice post-hCG injection depends on the developmental stage relevant for the experiment. Given 11AM hormone injections for superovulation, 4- and 8-cell stage embryos were recovered in the afternoon of E1.5 and in the morning of E2.5, respectively. To obtain 16-32 cell stage embryos, recovery was performed in the afternoon or E2.5. Blastocysts were obtained on E3.5. Female mice were sacrificed by cervical dislocation. Following lateral incision at the ventral midline, the peritoneum is cut and the gut is moved

out of the way to locate the uterine horns. The first cut is made between the oviduct and the ovary, and the second cut is made between the oviduct and long the length of the uterus, depending of the expected stage of development of the embryos. For example, at least 1cm of the upper part of the uterus is collected oviduct to obtain E2.5 embryos. Oviducts dissected out of the mice are transported submerged in KSOM (potassium Simplex Optimized Medium; (Lawitts and Biggers, 1991)) containing HEPES (H-KSOM; LifeGlobal, LGGH-050) in 1.5ml Eppendorf tubes.

## Embryo work

Embryos for all experiments are handled with a mouth pipette: an aspirator mouthpiece connected to a flame-pulled glass capillary (Blaubrand intraMARK 100µl, 7087144) by rubber tubing. To shape glass capillaries, the glass is heated over a Bunsen burner until soft, then quickly pulled at both ends to produce a tube with an internal diameter of approximately 200µm. The two halves are broken apart and the tips are fire-polished to prevent damaging the embryos.

All live embryos were handled under a stereomicroscope (Zeiss, Discovery.v8) equipped with a heating plate (Tokai hit, MATS-UST2). All live embryos were cultured inside an incubator (Thermo Fisher Scientific, Heracell 240i) with a 37°C humidified atmosphere of 5% CO2 and 95% air.

### *Flushing to obtain preimplantation embryos*

The oviduct and its attached segment of the uterus is laid out on a 35-mm petri dish under a stereomicroscope. A flushing needle, attached to a 1ml syringe filled with H-KSOM, is slid into the opening of the oviduct (infundibulum). The oviduct is flushed with 100-200µl of medium, and the embryos exit the reproductive tract through the opening on the uterus side. Embryos are collected by mouth pipetting and transferred through several microdroplets of H-KSOM for washing. Collected embryos are subsequently cultured in 10µl microdroplets of KSOM in 35mm sterile plastic culture dishes (Falcon, 353001) with a mineral oil (Sigma, M8410) overlay. The oil overlay stabilises the medium and minimises

evaporation and changes in pH and temperature. Micromanipulations outside the incubator were carried out in H-KSOM.

***Dissociation of embryos to isolate single blastomeres***

Zona pellucida were removed from embryos with 3-4 min pronase (0.5% w/v Proteinase K, Sigma P8811, in H-KSOM supplemented with 0.5% PVP-40) treatment at 37°C. Subsequently, embryos were washed and incubated in $Ca^{2+}$ and $Mg^{2+}$ -free KSOM (Biggers et al., 2000) for 10 minutes at 37°C to weaken cell-cell adhesions. Effect of $Ca^{2+}$ and $Mg^{2+}$ -free KSOM is evident by decompaction of the embryo. Blastomeres are then separated by mouth-pipetting with a glass capillary that has an opening smaller than the diameter of the embryo. Dissociation of 4-cell and 8-cell stage embryos yield "1/4" and "1/8" reduced systems, respectively.

***Blebbistatin treatment of embryos and blastomeres***

Powdered blebbistatin was reconstituted in DMSO (Sigman, D2650) at 25mM. Embryos and isolated blastomeres were treated with blebbistatin (Tocris, 1852) at a final concentration of 25μM. For assessment of myosin inhibition on polarisation, samples were treated for 12 hours from the 4-to 8-cell stage. For assessment of myosin inhibition on TE/ICM specification, samples were treated for 3-12 hours from E2.75-3.25.

***Immunosurgery***

Zona pellucida were removed from embryos with 3-4 min pronase treatment at 37°C (as described above). Subsequently, embryos were incubated in serum containing anti-mouse antibody (Cedarlane, CL2301, Lot no. 049M4847V) diluted 1:3 with KSOM for 30 min at 37°C. Following three brief washes in H-KSOM, embryos were incubated in guinea pig complement (Sigma, 1639, Lot no. SLBX9353) diluted 1:3 with KSOM for 30 min at 37°C. Lysed outer cells were removed by mouth-pipetting with a narrow glass capillary to isolate the inner cells.

***Embedding cells in Matrigel and hydrogel***

Matrigel mix consists of Matrigel (Corning, 356230) diluted in DPBS to desired concentration. Hydrogel mix consists of 1.5% PEG-A (non-degradable hydrogel) and Factor XIII (1U/ml) in H-KSOM. All components of the hydrogel mix, except the H-KSOM, were gifts from Matthias Lutolf (EPFL, Lausanne) (Gjorevski and Lutolf, 2017). Both mixes were prepared fresh for each experiment, mixed thoroughly through pipetting, and kept on ice during immunosurgery. Upon completion of immunosurgery, isolated inner cells were promptly resuspended in the mixes, and 15μL droplets were made on 35mm petri dishes (Falcon, 351008). To ensure that cell clusters from different embryos do not stick together, a closed glass capillary was used to space them apart. These petri dishes were inverted to prevent cells sticking to the bottom of the dish, and incubated at 37°C for 30 minutes for the mix to form a gel. After gel formation, 4ml of prewarmed KSOM was gently pipetted into each dish to cover the gel.

***Immunostaining***

Embryos were fixed in 4% PFA (Sigma, P6148) at room temperature for 15 min, washed 3 times (5 min each) in wash buffer (DPBS-T containing 2% BSA), permeabilized at room temperature for 30 min in permeabilization buffer (0.5% Triton-X in DPBS; Sigma T8787), washed (3 x 5 min), followed by incubation in blocking buffer (PBS-T containing 5% BSA) either overnight at 4°C or for 2 h at room temperature. Blocked samples were incubated with primary antibodies (Table 1) overnight at 4°C, washed (3 x 5 min), and incubated in fluorophore-conjugated secondary antibodies and dyes (Table 2) for 2 hours at room temperature. Stained samples were washed (3 x 5 min), incubated in DAPI solution (Life Technologies, D3571; diluted 1:1000 in DPBS) for 10 min at room temperature. These samples were then transferred into droplets of DPBS overlaid with mineral oil on a 35mm glass bottom dish (MatTek, P356-1.5-20-C) for imaging.

**Table 1. Primary antibodies**

| Epitope | Host | Catalogue # | Company | Dilution |
|---|---|---|---|---|
| aPKC (PKCζ) | Rabbit | sc-216 | Santa Cruz Biotechnology | 1:200 |
| CDX2 | Mouse | MU392A-UC | Biogenex | 1:200 |
| E-cadherin | Rat | U3254 | Sigma Aldrich | 1:100 |
| GATA4 | Goat | AF2606 | R&D Systems | 1:200 |
| Integrin $\alpha$6 | Rat | 555734 | BD Pharmingen | 1:100 |
| Integrin β1 | Rat | MAB1997 | Millipore | 1:100 |
| Laminin 1 | Rabbit | NB300-14422 | Novus Biologicals | 1:100 |
| Laminin $\alpha$1 | Rat | | Gift from Sorokin Group | N/A |
| Laminin $\alpha$5 | Rat | | Gift from Sorokin Group | N/A |
| Laminin $\beta$1 | Rat | | Gift from Sorokin Group | N/A |
| Laminin $\gamma$1 | Rat | | Gift from Sorokin Group | N/A |
| Megalin | Mouse | sc-515750 | Santa Cruz Biotechnology | 1:100 |
| Pard6b | Rabbit | sc-67393 | Santa Cruz Biotechnology | 1:200 |
| Phopho-YAP | Rabbit | 4911S | Cell Signaling Technology | 1:100 |
| Phospho-ERM | Rabbit | 3726 | Cell Signaling Technology | 1:200 |
| Sox-2 (D9B8N) | Rabbit | 23064 | Cell Signaling Technology | 1:200 |

**Table 2. Secondary antibodies and dyes**

| Fluorophore | Target | Host | Catalogue # | Company | Dilution |
|---|---|---|---|---|---|
| Alexa Fluor 488 | Goat IgG | Donkey | A11055 | Life Technologies | 1:200 |
| Alexa Fluor 488 Plus | Rabbit IgG | Donkey | A32790 | ThermoFisher | 1:200 |
| Cy5 | Mouse IgG | Donkey | 715-175-150 | Jackson ImmunoResearch | 1:200 |
| Cy5 | Rat IgG | Donkey | 712-175-153 | Jackson ImmunoResearch | 1:200 |
| DAPI | (DNA) | - | D3571 | Life Technologies | 1:1000 |
| Rhodamine phalloidin | (Actin) | - | R415 | Invitrogen | 1:200 |

## Molecular work

### *Extraction of genomic DNA from mouse tails and genotyping*

Tails were digested at 55°C with gentle shaking overnight in 400µl genotyping buffer (50mM Tris-HCI (Sigma, T2663), 100mM EDTA (Fluka, 03690), 100mM NaCl, 1% sodium dodecyl sulphate (Serva, 39575.02), Proteinase K (0.5mg/ml; Sigma P2308)). The supernatant was mixed with equal volume of isopropanol to precipitate gDNA. Following centrifugation, the gDNA pellet was washed with 80% ethanol and resuspended in 100µl $H_2O$. Extracted gDNA were used to determine the genotype of each mouse by PCR with either *Taq* (Thermo Scientific, EP0402) or *ExTaq* (Takara, RR001C) polymerase. Primers relevant to the mouse strains used are listed in Table 3.

### *Single embryo genotyping*

Transgenic mutant embryos were genotyped retrospectively after imaging. Individual embryos were mouth pipetted into 200µL PCR tubes containing 10µL of lysis buffer consisting of 200µg/ml Proteinase K in *Taq* polymerase buffer (Thermo Scientific, B38). Lysis reaction took place for 1 hour at 55°C, followed by 10 minutes at 96°C. Resulting genomic DNA was mixed with relevant primers (Table 3) for determination of genotype via PCR.

**Table 3. Sequence of genotyping primers**

| **Mouse line/locus** | Primer 1 | Primer 2 | Primer 3 |
|---|---|---|---|
| Itgb1 deleted | TGAATATGGGCTT GGCAGTTA | CCACAACTTTCCC AGTTAGCTCTC | |
| Itgb1 tm1Efu | CGGCTCAAAGCAG AGTGTCAGTC | CCACAACTTTCCC AGTTAGCTCTC | |
| Myh9 deleted | TTGCAGCCCTTCTT GACCTA | GCCACATCTCAGC CTAGGAT | CGGGAAGGAAGG AGACACTT |
| Myh9 tm5Rsad | ATGGGCAGGTTCT TATAAGG | GGGACACAGTGGA ATCCCTT | |
| ZP3 Cre | TGCTGTTTCACTGG TTGTGCGGCG | TGCCTTCTCTACAC CTGCGGTGCT | |

***Gel electrophoresis***

PCR products mixed with loading dye (Life Technologies, R0611) were separated by electrophoresis in 1-1.5% (w/v) agarose (Lonza 50004) gel supplemented with 0.03µl/ml DNA staining dye (Serva, 39804.01) in TAE buffer. DNA fragments were visualised under ultraviolet light on a video-based gel document system (Intas, GEL Stick "Touch"), and fragment lengths were measured against standardised DNA ladders (Life Technologies, SM0323, SM0313).

***Microscopy and image analyses***

Stained embryos were imaged on the Zeiss LSM780 and LSM880 confocal microscopes. For both systems, a 40X water-immersion C-Apochromat 1.2 NA objective lens was used. Imaging was carried out with the Zen (Zeiss) software interface. Resulting raw images were processed using ImageJ. Further quantification of fluorescence intensities and nuclei/cell counting was performed on either ImageJ or Imaris as described below.

***Quantification of fluorescence intensity of lineage markers***

For measure of lineage specification, Imaris was used. Imaris Surpass allowed 3D visualisation of the image data. Under the object toolbar of Imaris, the 'Add Spots' function was used to detect each nucleus on the DAPI channel. Estimated spot (nucleus) diameter was set to 6 µm, and manual corrections were made for each image as necessary to detect all nuclei. Mean fluorescence intensity of SOX2, CDX2 or GATA4 were measured for each detected nucleus. Spot detection of each nucleus was also used as a cell counter.

***Quantification of fluorescence intensity of apico-basal markers***

Fluorescence signal intensity of cortical pERM and integrin β1 was used as a measure of apical and basal polarity, respectively. Images of samples co-stained for both proteins were analysed on ImageJ. To reduce noise, the Gaussian filter was applied to smooth the image. For each z-stack, a mid-slice was selected, and a line (width = 5 pixels) was traced along the perimeter of the smoothed image. A plot profile along the line was obtained for the pERM and integrin β1 channels. Individual data points were exported from ImageJ for statistical analysis.

### *Quantification of apical domain positioning in 2/8-doublets*

Quantification of apical domain positioning was performed on ImageJ using its angle function. For each z-stack, a mid-slice was selected, and a line was drawn bisecting the doublet perpendicular to the cell-cell interface. A second line was drawn connecting the geometric centre of the cell and the centre of the apical domain. The angle at the intersection of these two lines was measured.

### *Statistical analysis*

Statistical analyses and graph generation was performed using the ggplot2 package in R and Microsoft Excel. Comparison of the distribution of fate marker intensities was performed by the Mann-Whitney U test. Differences in cell count, cell-cell contact diameter, and angle of apical domain assembly was assessed using the student's *t*-test. Statistical dependence between diameter of cell-cell contact and apical domain positioning was assessed by Pearson correlation.

# Results

### *ICM specification takes place in fully enclosed cells*

Following symmetry-breaking in the 8-cell stage embryo, inner-outer configuration emerges during the 16-32-cell stage. Inner cells, which are entirely enclosed by adjacent cell surfaces, arise asynchronously and become ICM-specified. The transcription factor SOX2 is the first ICM-specific marker to be expressed (Wicklow et al., 2014). Even as CDX2-high and -low cells become distinguishable between outer and inner regions of the early morula, the embryo remains SOX2 negative or express barely detectable levels of the protein (Figure 10A). Likewise, upon asymmetric division of 1/8-blastomeres, TE marker asymmetry precedes differential SOX2 expression between daughter cells during the late 16-cell stage (Figure 10B). In such doublets, appreciable SOX2 expression is detected in fully enclosed cells (Figure 10C). While the apical domain marks the outer surface and initiates TE-specification upon the 8- to 16-cell transition, ICM specification appears comparatively delayed until a cell is geometrically closed off from the external environment. These observations suggest that a fully internalised microenvironment facilitates ICM specification.

### *Laminin and integrin are enriched at the cell-cell interface of morulae*

To understand how occupying an inner position within the embryo leads to ICM specification, we examined the molecular composition of the cell-cell interface during preimplantation stages. Consistent with earlier studies, low levels of E-cadherin are distributed on the surface of each blastomere until the 8-cell stage. As the embryo undergoes compaction, however, the protein increasingly accumulates at the cell-cell interface and remains enriched between all cells for the remainder of preimplantation development (Figure 11A) (Larue et al., 1994; Shirayoshi et al., 1983).

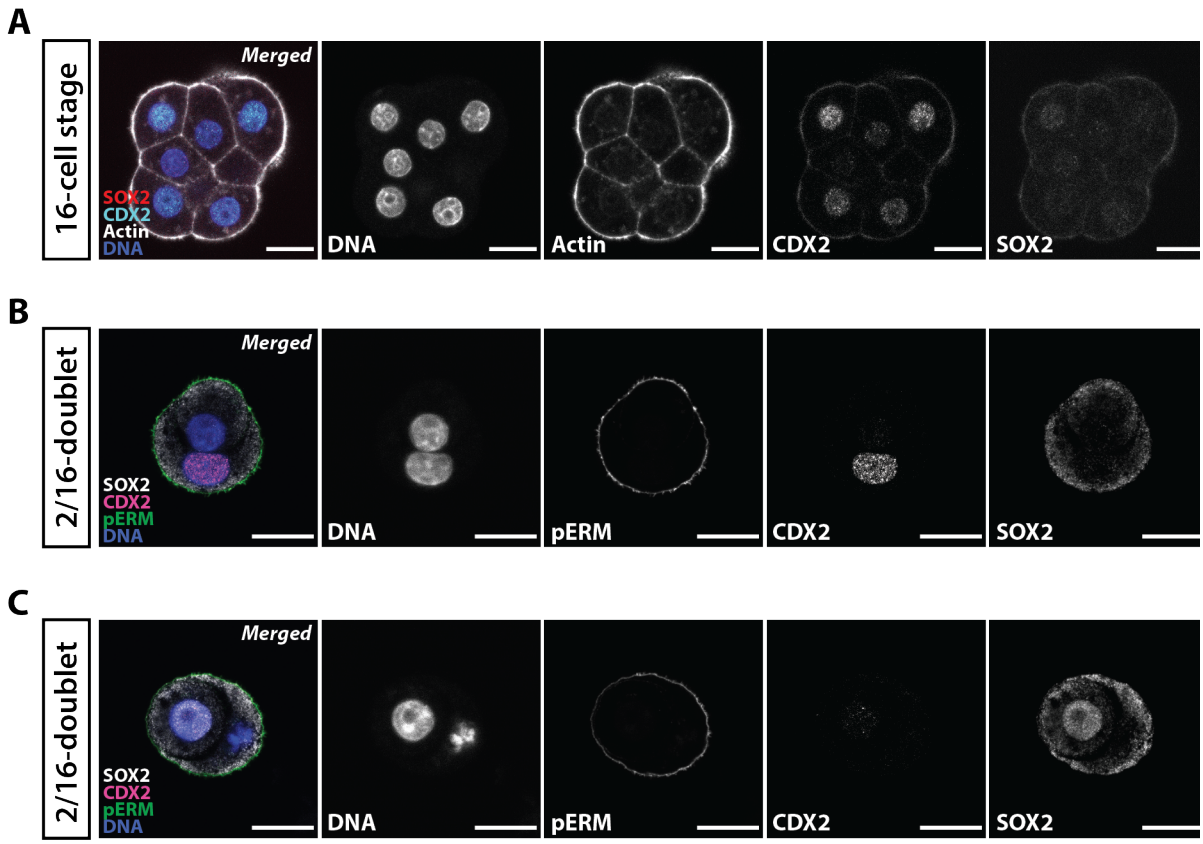


**Figure 10. SOX2 is upregulated in geometrically fully enclosed cells**

**A.** While the earliest ICM marker SOX2 is barely detectable in the early morula, nuclei in outer regions of the embryo express higher levels TE marker CDX2 compared to those located interiorly. Asymmetry in CDX2 expression is observed earlier than SOX2 upregulation, suggesting that the TE specified earlier than the ICM. N = 3, 16 embryos.
**B.** A blastomere isolated from the 8-cell stage embryo divides asymmetrically and gives rise to a doublet of cells equivalent to the 16-cell stage ('2/16'). Mechanical asymmetry between cells results in inside-outside sorting. In these doublets, the polarised outer cell expresses higher levels of CDX2 than the inner cell. The apical domain is marked by phosphorylated ezrin, radixin, moesin (pERM) proteins. Similar to the whole embryo in **A.**, SOX2 is barely detectable.
**C.** In a 2/16-doublet where the inner cell is fully enclosed by the outer cell, SOX2 upregulation is observed in the nucleus of the internalised cell. Scale bars, 20 μm.

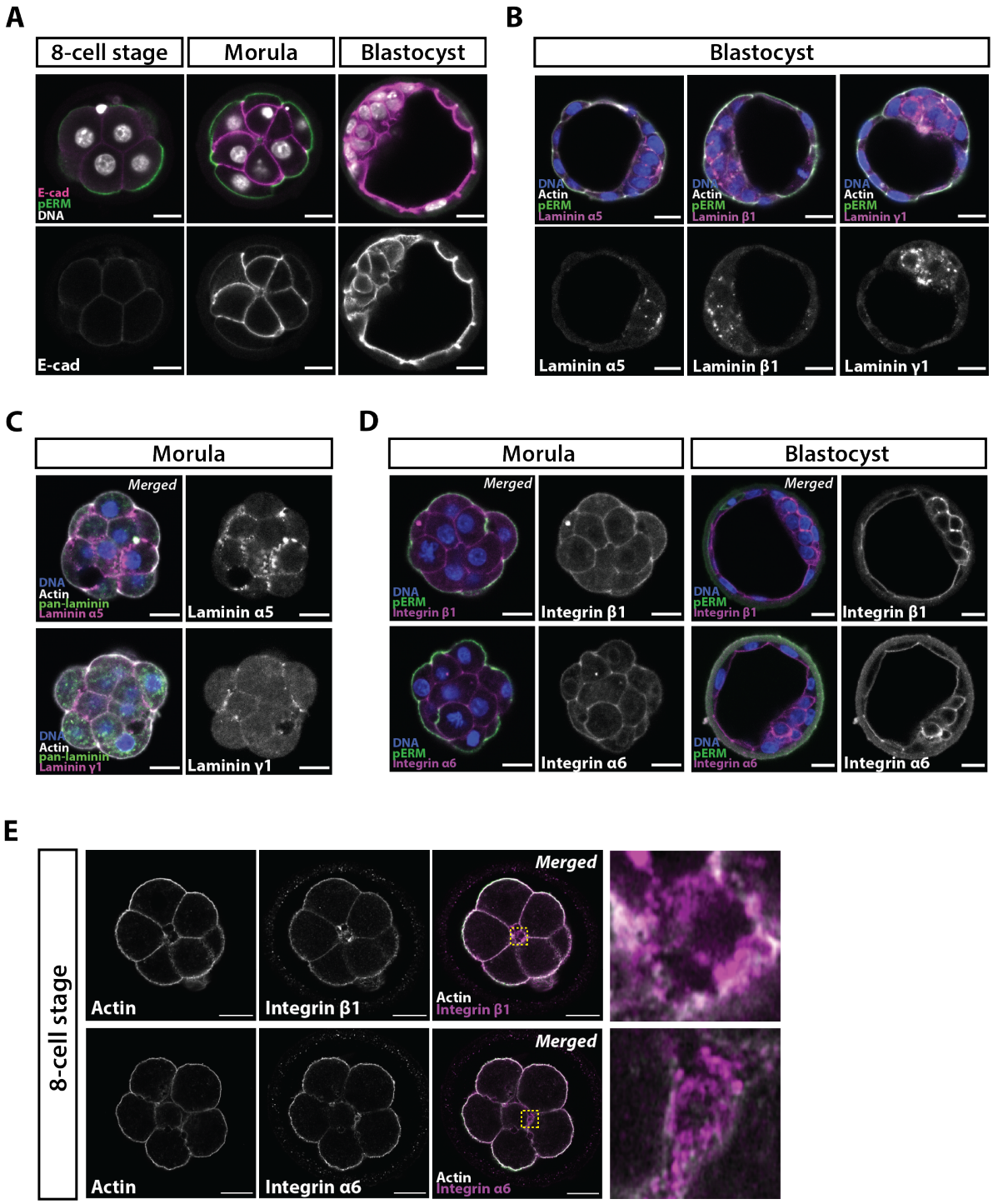


**Figure 11. E-cadherin, laminin and integrin α6β1 are present at the cell-cell interface.**

**A.** The cell-cell adhesion protein E-cadherin is initially expressed at low levels around the cell cortex until the early 8-cell stage. From the 8-cell stage onwards, however, it is upregulated at the cell-cell interface and remains mutually exclusive with the apical domain that lines the exterior surface of embryo. The apical domain is marked by pERM proteins.

**B.** Laminin chains α5, β1, γ1 are enriched within the ICM region of the blastocyst. These chains are components of the laminin-511 heterotrimer.

**C.** Laminin chains α5 and γ1are enriched at the cell-cell interface of 16-32-cell stage embryos.

**D.** Integrin subunits α6 and β1 are enriched at the cell cortex of 16-32-cell stage embryos. By the blastocyst stage, these line the basal side of the TE and are enriched at the cell-cell interface in the ICM region. The integrin α6β1 heterodimer is a well-known receptor of laminin.
**E.** Imaging of 8-16 cell embryos at high spatial resolution reveals integrin α6 and β1 localisation at the embryo periphery as well as at the cell-cell interface. Integrin subunits α6 and β1 are also found in pockets of extracellular space between blastomeres, suggesting their trafficking to the cell-cell interface. Scale bars, 20 μm.

In addition to cadherin molecules, the narrow extracellular space between adjacent cells is lined by the ECM. The literature indicates that laminin is the first major ECM component to be synthesised during mouse development, specifically, laminin chains α1, α5, β1, and γ1 (Klaffky et al., 2006). Immunostaining for each chain showed enrichment of laminin α5, β1, and γ1 in the ICM of blastocysts as expected (Figure 11B). Testing for a working laminin α1 antibody is currently underway. Further examination of 16-32 cell stage embryos revealed enrichment of laminin α5 and β1 at cell-cell junctions, coinciding with inner cell emergence (Figure 11C). Signals from pan-laminin antibody, however, was variable between embryos and exhibited diffuse localisation. While the fidelity of each antibody may differ, our observations confirm the presence of laminin-511 (α5β1γ1) at the cell-cell interface of morulae.

The integrin family of heterodimeric transmembrane proteins is the major receptor for ECM proteins. Among the known variety of integrin heterodimers, the β1 subunit is the most ubiquitously expressed (Humphries et al., 2006; Villa-Diaz et al., 2016). Immunostaining shows that integrin β1 accumulation spatiotemporally resembles that of laminin. It is enriched between blastomeres of the 16-32 cell stage embryo, as well as around the cortex of ICM cells in the blastocyst (top panels, Figure 11D).

Earlier studies have identified integrin α6β1 as a laminin-specific receptor, and given the deposition of laminin heterotrimers in the embryo, integrin α6 subunit was considered the most likely candidate to heterodimerise with the detected β1 subunit (Aumailley et al., 1990). Indeed, the pattern of integrin α6 localisation closely resembles that of β1 in both morulae and blastocysts, suggesting integrin α6β1 heterodimer formation during preimplantation development (bottom panels, Figure 11D). Integrin α6β1 clearly lines the surface of inner cells and the basal side of TE cells, but its signal intensity is weak at the ICM-cavity interface. These blastocysts had not developed enough to exhibit a sorted PrE layer, but

observations are consistent with late maturation of the PrE epithelium and reversed axes of polarity between TE and PrE lineages.

In order to examine how integrin α6β1 becomes enriched at cell-cell interfaces and around the ICM, localisation of both subunits was imaged at high spatial resolution with the Airyscan detector on the Zeiss LSM880 confocal microscope. Images revealed that during the 8-16 cell stage, both the α6 and β1 subunits are weakly enriched at the apical surface of the embryo. However, accumulation of α6 and β1subunits are also seen in pockets of extracellular space between cells, suggesting that integrin may be trafficked from the embryo periphery to cell-cell interfaces prior to ICM specification (Figure 11E) (Caswell et al., 2009).

The enrichment of laminin and its cognate receptor integrin α6β1 at the cell-cell interface is delayed compared to E-cadherin upregulation. However, the timing of their accumulation coincides with the emergence of inner cells within the embryo. Therefore, we hypothesised that laminin, by signalling through integrin α6β1, may be a functional component of the inner microenvironment that relays positional information and instructs ICM specification.

***Itgb1 plays a key role in patterning the embryonic interior***

In order the assess how laminin-integrin interaction generally affects preimplantation development, embryos lacking *Itgb1*, which encodes the integrin β1 subunit, were examined. Previous characterisation of *Itgb1* knockout (KO) embryos reported embryonic lethality shortly after implantation at around E5.5 (Stephens et al., 1995). The authors noted that maturation into blastocysts appeared normal and that defects emerged around the time of implantation. Despite the presence of laminin-positive cells, degeneration of the inner embryonic region and failure of cells to sort to fate-appropriate positions were observed in these mutants. However, due to technical limitations at the time, these preimplantation *Itgb1* KO embryos were not thoroughly characterised, and the origins of their post-implantation defects remained unknown.

Zygotic *Itgb1* KO embryos were generated by crossing *Itgb1*-/+ parents, and recovered during the 16-32-cell stage to assess TE/ICM patterning. Cell number and fluorescence intensity of CDX2 and SOX2 were measured through imaging, and each embryo was genotyped individually to retrospectively identify knockout mutants. In the absence of zygotic integrin β1, cell adhesion and compaction appeared normal, and TE/ICM

specification persisted in a spatially segregated manner (Figure 12A). However, the overall levels of CDX2 and SOX2 were significantly reduced (Figure 12A-B). Low expression of fate markers may indicate that upstream positional cues are weak in inducing TE/ICM specification among *Itgb1* KO cells. Given that *Itgb1* KO embryos consisted of fewer cells than age-matched wildtype (WT) counterparts, though this difference was statistically non-significant, the reduced CDX2 and SOX2 intensities may also be due to a developmental delay (Figure 12C). Alternatively, the phenotype of these mutants may be attenuated by maternally contributed integrin β1 or compensation by dystroglycan, a major non-integrin laminin receptor (Williamson et al., 1997). While the data can be interpreted in a few different ways, the phenotype of the mutants suggest that zygotic expression of integrin β1 is not strictly required for overall TE/ICM segregation in whole embryos.

When *Itgb1* KO embryos were examined at E4.0, embryos appeared as mature blastocysts with fully expanded fluid-filled cavities as previously reported. Detailed analysis at cellular resolution, however, revealed aberrant spatial arrangement of ICM derivatives PrE and EPI (Figure 12D). In mature WT blastocysts, the PrE consisted of a single layer of GATA4-postive cells facing the blastocoel cavity and lining the OCT4-high EPI cells. In contrast, *Itgb1* KO embryos displayed a multi-layered PrE, where GATA4-positive cells appeared clustered. As a result, the ICM resembled a rounded ball of cells while WT blastocysts exhibited an ICM flattened and spread out against the overlying TE. In addition, mutants consisted of significantly fewer cells, again suggesting developmental delay (Figure 12E). These findings demonstrate that despite seemingly mild effect of integrin β1 deficiency during the preimplantation stage, reduced cell number and spatial disorganisation among inner cells precedes the embryonic lethality reported post-implantation.

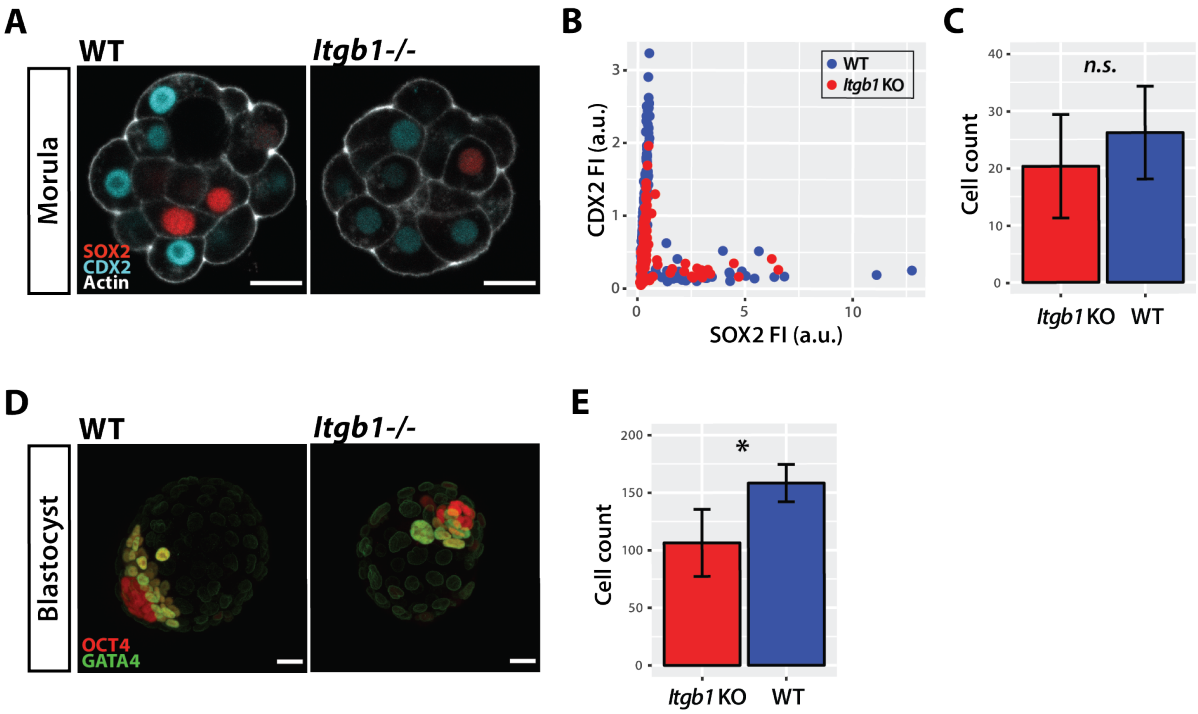


**Figure 12.** ***Itgb1*-deficient embryos exhibit mild patterning defects prior to implantation.**

**A.** Patterned TE/ICM specification is preserved in WT and *Itgb1* knockout (KO) embryos at the 16-32-cell stage, as these exhibit CDX2-positive outer cells and SOX2-positive inner cells.

**B.** Analysis of CDX2/SOX2 fluorescence intensities of individual nuclei reveal significantly reduced levels of both transcription factors in *Itgb1* KO morulae. These *Itgb1* KO morulae also consist of fewer cells, albeit non-significantly, compared to age-matched WT controls.

SOX2 intensity: *p*-value = 0.008; CDX2 intensity: *p*-value = $1.462e^{-11}$, Mann-Whitney U test. Cell count: *p*-value = 0.24, independent student's *t*-test. N=1, 13 embryos.

**C.** Representative maximum projections of the ICM in WT and *Itbg1* KO blastocysts at E4.0 are shown. Although EPI/PrE cells are segregated within the ICM of *Itbg1* KO blastocysts, the PrE (GATA4) is clustered instead of resolving into a single layered epithelium surrounding the EPI (OCT4). Scale bars, 20 μm.

**D.** *Itbg1* KO blastocysts at E4.0 consist of significantly fewer cells compared to age-matched WT blastocysts. Cell count: *p*-value = 0.012, independent student's *t*-test. N=1, 14 embryos.

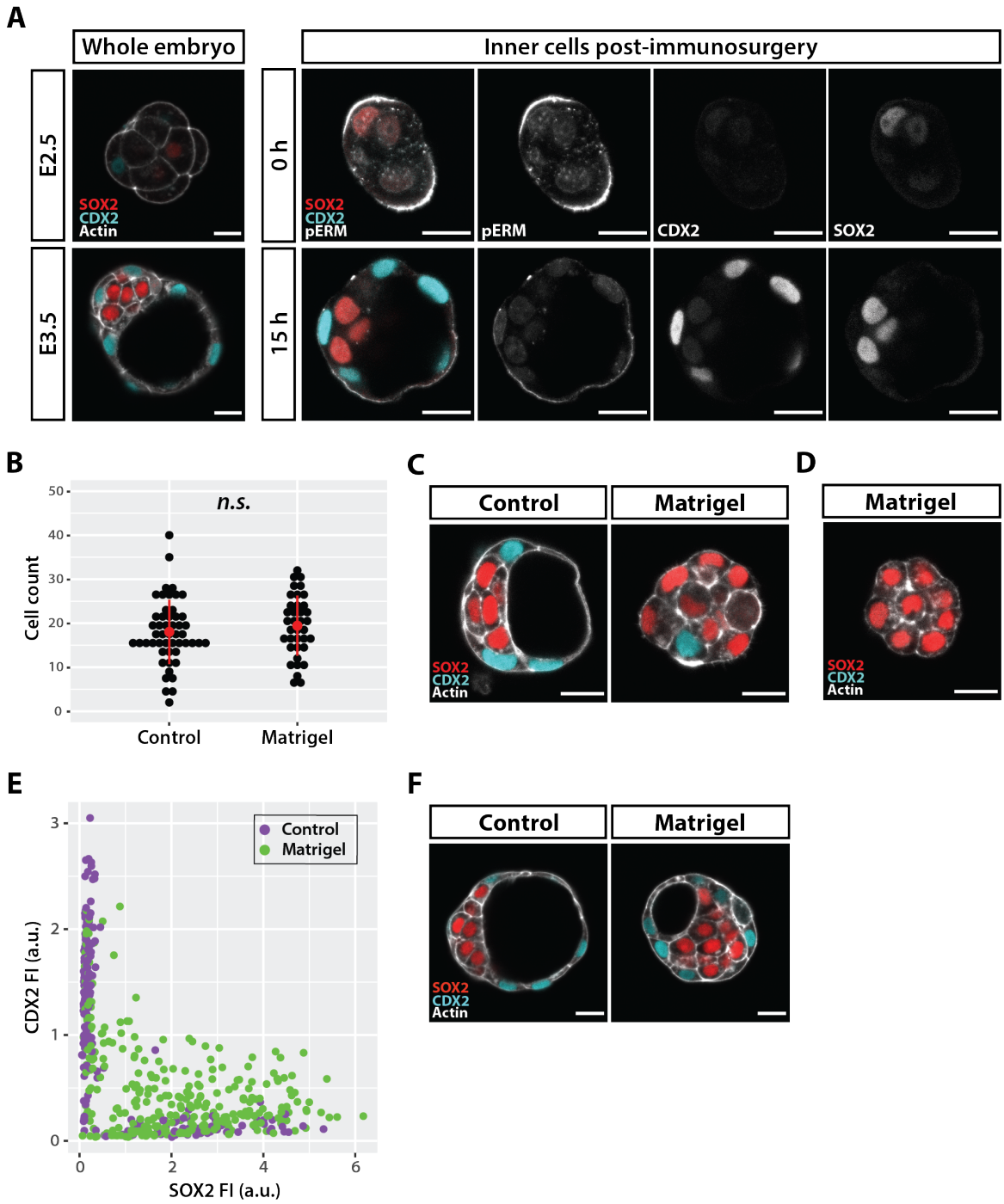


**Figure 13. Exogenous ECM induces ICM specification following immunosurgery.**

**A.** Immunosurgery is performed on 16-32-cell embryos on E2.5. Most inner cells are not yet ICM-specified at this stage, as indicted by low expression of fate markers in the whole morula compared to blastocysts at E3.5. Following immunosurgery, the outer surface of isolated inner cell clusters swiftly becomes polarised. Even upon immediate fixation after immunosurgery, cells may exhibit pERM enrichment on the outer surface. These newly outer cells upregulate CDX2. By 15 hours post-immunosurgery, patterned specification of TE/ICM is evident in these 'mini-blastocysts'.

**B.** Cell count 17-18 hours post-immunosurgery shows no significant difference between culture in Matrigel and in standard KSOM medium. Graph indicates mean ± S.D. Cell count: *p*-value = 0.36, independent student's *t*-test. N=5, 88 embryos.
**C.** While inner cells cultured in standard medium (control) exhibit patterned inside-outside specification of TE/ICM, this patterning is lost in Matrigel culture. Matrigel-embedded clusters exhibit SOX2-positive cells on the periphery. In some cases, all cells, located both inside and outside, are SOX2-positive, as in **D.**
**E.** Analysis of CDX2/SOX2 fluorescence intensities of individual nuclei 16-18 hours post-immunosurgery reveals a significant shift towards ICM specification in Matrigel culture. Matrigel culture induces increased incidence and intensity of SOX2 expression, and a considerable portion of nuclei co-express SOX2 and CDX2. SOX2 intensity: *p*-value = 2.2e-16; CDX2 intensity: *p*-value = 7.16e-8, Mann-Whitney U test. N=3, 43 embryos.
**F.** TE/ICM specification and patterning is unaffected in whole 16-32-cell stage embryos embedded and cultured in Matrigel for 20 hours. Scale bars, 20 μm.

***Immunosurgery disrupts spatial coordinates by isolating inner cells***

TE specification requires polarisation of outer cells. Despite reduced cell number, successful cavitation and initiation of implantation implies that a functional TE layer forms in *Itgb1* KO embryos, suggesting that outer positional signalling remains intact in mutants (Stephens et al., 1995). In contrast, the subtle yet ambiguous defects in the ICM prompted closer examination of the inner cell environment. In order to identify prominent cues received by inner cells from their immediate surrounding, a top-down approach was chosen to mimic the embryonic interior *in vitro*.

As a first step, the physical barrier posed by the outer TE layer was removed by immunosurgery to access inner cells. Through selective complement-mediated lysis of outer cells of an embryo, immunosurgery allows isolation of inner cells for direct experimental manipulation (Handyside and Barton, 1977; Solter and Knowles, 1975). Immunosurgery was performed on 16-32 cell stage embryos prior to lineage commitment of inner cells, as indicated by low or undetectable levels of SOX2 (Figure 13A). Upon immunosurgery, the newly exposed surface of the inner cell cluster undergoes rapid polarisation and eventually a new TE layer is generated *de novo* (Stephenson et al., 2010; Wigger et al., 2017). Prolonged culture of these inner cell clusters yields 'mini-blastocysts' replete with outer TE cells surrounding ICM cells and usually a small fluid-filled cavity (Figure 13A).

The way in which the system adapts to immunosurgery demonstrates how robustly blastomeres can sense changes to their microenvironment and adjust lineage commitment according to their new spatial context. The duration of the immunosurgery protocol is

approximately 80 minutes, and upon immediate fixation of isolated cells at the end of the procedure, surface accumulation of apical pERM was already apparent (Figure 13A). As in earlier stages, the apical domain thus marks outer surfaces and promotes TE lineage commitment over the next 15-18 hours (Figure 13A).

***Induction of cell-ECM contact drives position-independent ICM specification***

Earlier observations in whole embryos showed that laminin is present at the cell-cell interface, whose signals are most likely relayed by the receptor integrin α6β1. To test whether this inner microenvironment could be mimicked *in vitro* by provision of ECM components, cells were embedded in Matrigel after immunosurgery. Matrigel, a gelatinous secretion from Engelbreth-Holm-Swarm mouse sarcoma cells, consists of a rich mixture of ECM components including laminin (Orkin 1977). If Matrigel could sufficiently mimic the embryonic interior, inner cells embedded within it are expected to become ICM-specified and proliferate into a mass of SOX2-positive cells without a surrounding TE layer.

At 16-18 hours post-immunosurgery of morulae, survival and proliferation of inner cells were comparable between Matrigel and standard culture conditions in KSOM medium (Figure 13B). Strikingly, however, inner cells cultured in Matrigel formed a compact mass of cells where the majority of nuclei was SOX2-positive (Figure 13C). Fluid-filled cavities were noticeably absent. Clusters entirely composed of SOX2-positive cells were also consistently observed across independent experiments, albeit at low frequency (Figure 13D). Quantitative analysis of each nucleus for fluorescence intensity of SOX2 and CDX2 levels pointed to significant increase in ICM-specification induced by Matrigel (Figure 13E). There was also an increase in cells expressing both SOX2 and CDX2 at intermediate levels, which may indicate cells in the midst of fate transition. CDX2-positive cells in Matrigel cultured samples were either clustered or scattered at the periphery, lacking coherent epithelial structure. Furthermore, in virtually every Matrigel-cultured sample, SOX2-positive cells were observed on the outer surface of the cluster. These findings demonstrate that exogenously supplied ECM can mimic 'inner' positional cues to an extent sufficient to induce ICM specification while suppressing TE formation.

In contrast, however, when whole 16-32-cell stage embryos were embedded in Matrigel, TE/ICM lineages were appropriately specified and segregated despite the frequent absence or reduction of a blastocyst cavity (Figure 13F). These findings suggest that inner and outer cells of the morula may be differentially sensitive to signals provided by the ECM.

***Mechanical constraints of gel culture only partially contribute to ICM specification***

The absence of fluid-filled cavities in Matrigel culture suggested that mechanical constraints may be exerted by the gel-like substrate to prevent blastocyst expansion. Moreover, mechanical factors may subsequently modulate cell fate. To discern whether Matrigel-induced effects stem from its biochemically active ECM constituents or the mechanical constraints of gel culture, inner cells were embedded in either PEG (polyethylene glycol)-based inert hydrogel or decreasing concentrations of Matrigel. Hydrogel exerts mechanical constraints without providing biologically active cues (Gjorevski et al., 2016). Conversely, diluting Matrigel attenuates mechanical constraints while biologically active ECM components are still present, albeit at lower concentrations.

Inner cells that were cultured in hydrogel were able to divide, but fluid-filled cavities were either reduced in size or absent altogether (Figure 14A). In terms of TE/ICM patterning, SOX2-positive cells were occasionally observed on the surface of hydrogel cultured clusters (arrow, Figure 14A). However, inner-outer patterning was largely preserved, and TE and ICM lineages were clearly distinguishable based on CDX2/SOX2 levels (Figure 14B). The prevalence of CDX2/SOX2 double positive cells seen in Matrigel culture was not reproduced with hydrogel.

When the Matrigel concentration was reduced from the standard value of 4.5 mg/ml to as little as 0.56 mg/ml, inner cells were no longer embedded in a gel-like matrix but practically suspended in an aqueous environment. Despite reduced mechanical constraints, however, the distribution of TE/ICM cells were comparable to those cultured in higher concentrations of Matrigel (Figure 14C). Even in the absence of jelled support, an increase in SOX2-expressing cells was observed, many of which were located on the outer surface. In addition, cavity formation was impaired at all concentrations of Matrigel. This suggests that impaired fluid accumulation is not only due to mechanical inhibition of expansion, but also the absence of a TE-mediated permeability seal to prevent leakage. Although observations in hydrogel suggest that mechanical factors may play a modest part in patterning inner cells, it is the ECM components that provide potent biochemical cues to promote ICM specification.

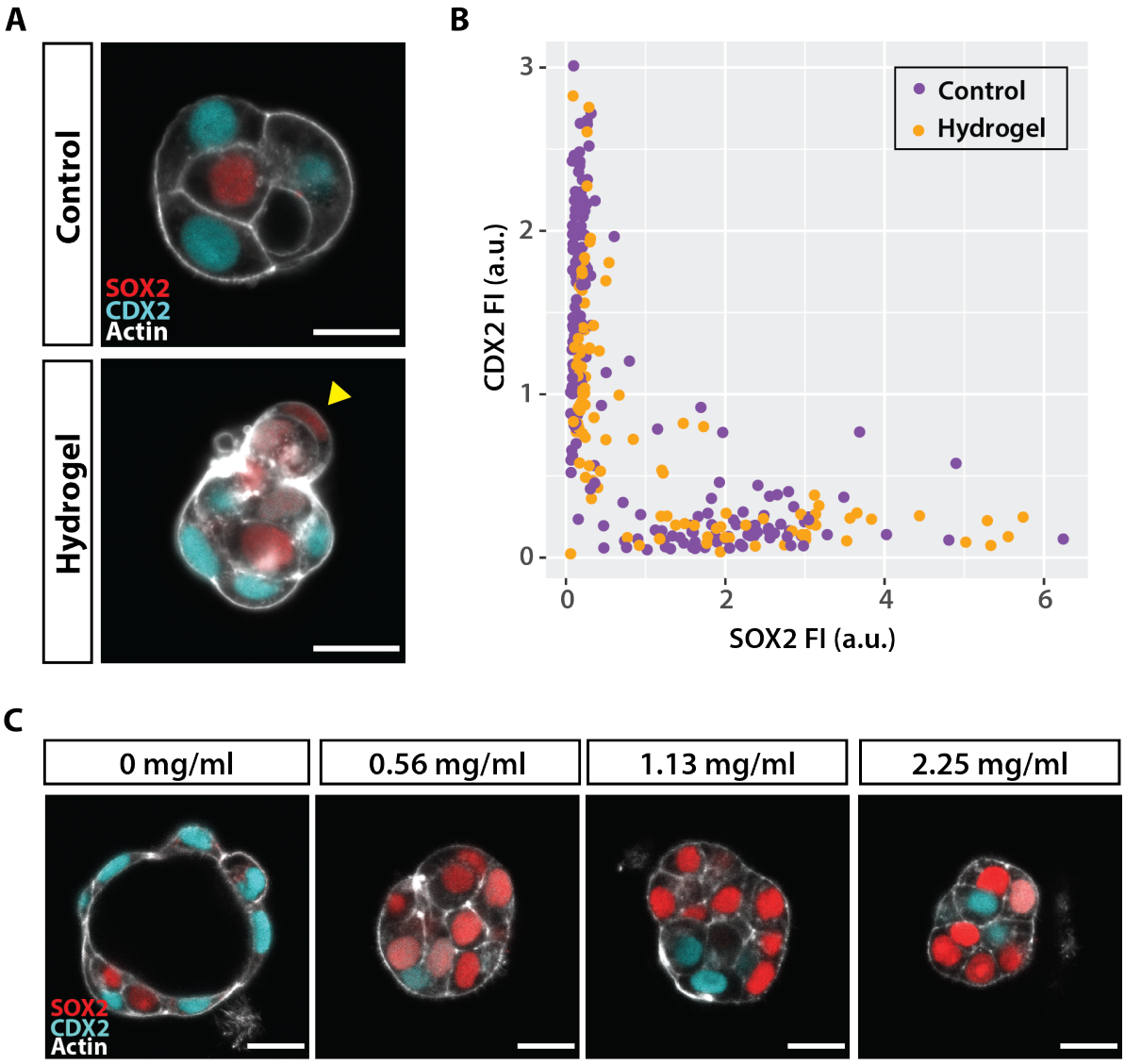


**Figure 14. Mechanical constraint alone cannot induce ICM specification following immunosurgery.**

**A.** Cells are embedded in hydrogel following immunosurgery, and fate is assessed after 16-18 hours of culture. Hydrogel-embedded cells generally exhibit patterned inside-outside specification of TE/ICM, but an occasional SOX2-positive outer cell can be observed (marked by arrow).
**B.** Analysis of CDX2/SOX2 fluorescence intensities in individual nuclei 16-18 hours post-immunosurgery reveals that, despite slight increase in the distribution of SOX2-positive cells, hydrogel culture is insufficient to drive strong ICM specification as seen with Matrigel. SOX2 intensity: *p*-value = 0.002381; CDX2 intensity: *p*-value = 0.07824, Mann-Whitney U test. N=3, 28 embryos.
**C.** Cells are embedded in low concentrations of Matrigel following immunosurgery, and fate is assessed after 16-18 hours. Despite attenuation of mechanical constraints, low concentrations of Matrigel are capable of inducing ICM specification, and SOX2-positive cells are observed on the outer surface of clusters. N=1, 14 embryos. Scale bars, 20 μm.

### *Apico-basal polarity is disrupted in Matrigel culture*

As described previously, the outer surface of isolated cells polarises rapidly following immunosurgery, and subsequently become TE-specified. In many epithelial cell systems, integrin β1 marks the basal surface in a manner spatially complementary to the apical domain (Rodriguez-Boulan and Macara, 2014). Indeed, when isolated and cultured inner cells were co-stained for integrin β1 and apical domain marker pERM to assess apicobasal polarity, these two proteins displayed non-overlapping localisation (Figure 15A). In cell clusters cultured in standard medium, pERM labelled the outer surface of the polarised TE layer, while integrin β1 was enriched at cell-cell interfaces. In marked contrast, integrin β1 was enriched at both the outer surface as well as cell-cell interfaces in Matrigel-cultured clusters (Figure 15A). Meanwhile, peripheral pERM signal was visibly diminished. Discontinuous patches of pERM were sometimes present on the outer surface to varying degrees, and these generally coincided with CDX2-positive nuclei. The disruption of polarity was further confirmed with another apical marker Pard6b, which showed similar localisation patterns as pERM (Figure 15B).

### *Integrin activity is required for ICM specification*

Although Matrigel is heterogenous in composition, given the upregulation of laminin and integrin α6β1 in whole embryos around the time of inner cell emergence, we deduced that laminin may be the main component underlying Matrigel-induced effects following immunosurgery. In support of this notion, integrin α6 subunit showed a similar pattern of localisation as the β1 subunit (Figure 15C), suggesting that the laminin present in Matrigel leads to the recruitment of integrin α6β1 to the cell-ECM interface. This negatively correlates with cortical accumulation of apical proteins on the outer surface, ultimately disrupting apicobasal polarity.

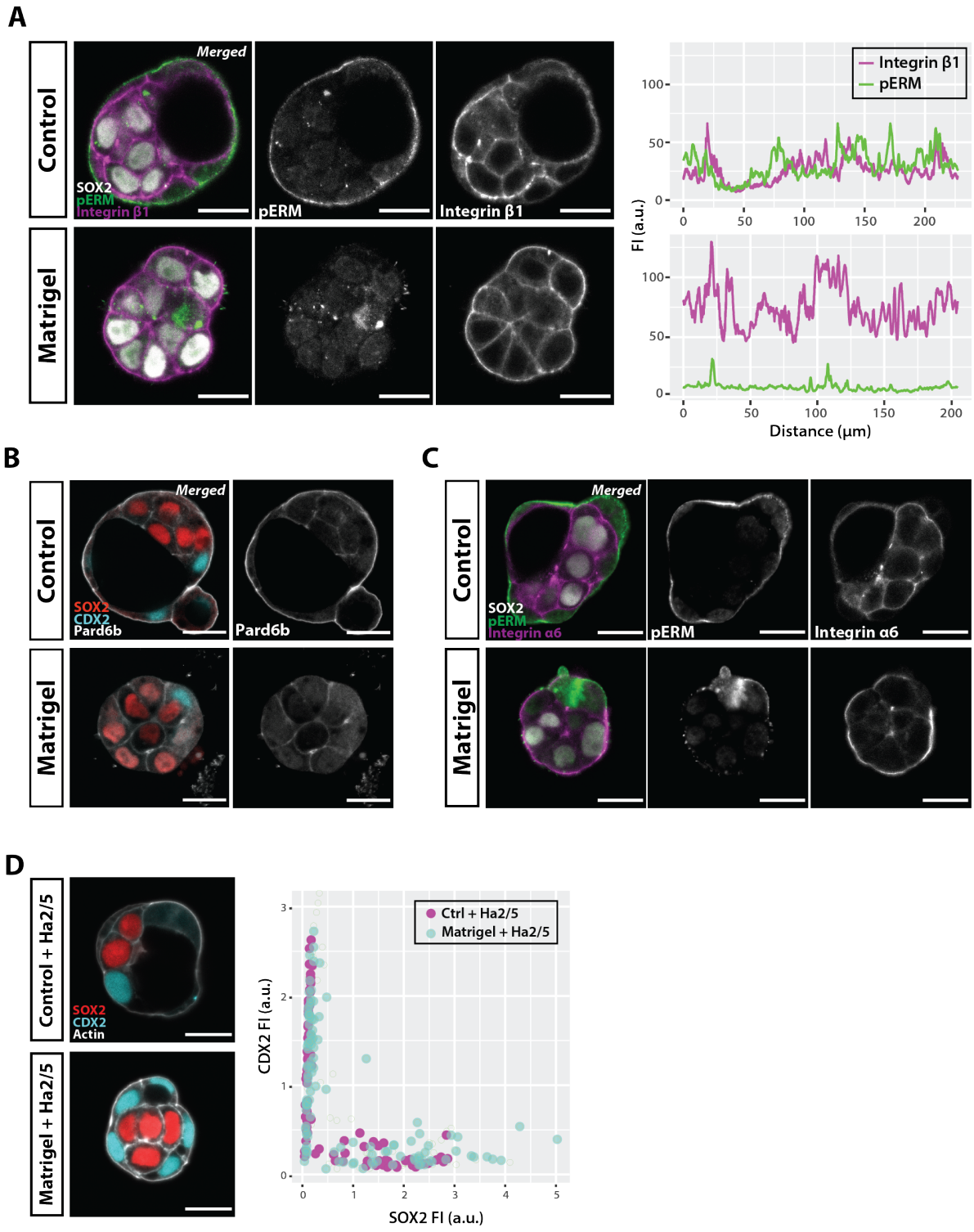


**Figure 15. Surface recruitment and activity of integrin β1 is required for ICM induction following immunosurgery.**

**A.** Apical polarisation of the outer surface post-immunosurgery is disrupted in Matrigel culture. Where control samples peripherally accumulate pERM, enrichment of integrin β1 is instead observed in Matrigel culture. These observations are quantitatively confirmed by comparing

fluorescence intensities of pERM and integrin β1 around the circumference of representative samples whose images are shown. N = 3, 32 embryos.
**B.** Diminished peripheral accumulation of apical marker Pard6b further confirms Matrigel-induced disruption of polarity. N = 1, 9 embryos.
**C.** Following immunosurgery and Matrigel embedding, integrin α6 exhibits a similar pattern of localisation as integrin β1, being enriched at the cell-gel interface. N = 1, 6 embryos.
**D.** Administration of integrin β1-blocking antibody, Ha2/5, attenuates Matrigel-induced effects on TE/ICM patterning post-immunosurgery. Assessment of SOX2/CDX2 fluorescence intensities of individual nuclei quantitatively confirm this. SOX2 intensity: *p*-value = 0.031; CDX2 intensity: *p*-value = 0.973, Mann-Whitney U test. N=1, 14 embryos. Scale bars, 20 μm.

To subsequently test whether integrin α6β1 is functionally required for ICM-induction at the cell-gel interface, Ha2/5, a function-blocking antibody that inhibits integrin β1, was added to the Matrigel culture. Administration of Ha2/5 almost completely attenuated the effects of Matrigel on isolated inner cells (Figure 15D). Outer cells were TE specified with high levels of CDX2, whereas ICM specification was confined to the interior. Although fluid-filled cavities were less frequently observed, cell clusters embedded in Matrigel in the presence of Ha2/5 were indistinguishable from control samples. This indicates that while Matrigel, particularly its constituent laminin, provides 'inner' positional information, interpretation of these cues for ICM specification depends on integrin β1 activity.

***Matrigel disrupts spatial sorting of EPI and PrE within the ICM***

Having substantiated the significance of ECM-integrin interactions in patterned TE/ICM specification, we further examined whether this influence persists in the blastocyst. During the latter part of preimplantation development, cells of the ICM further diverge into two lineages: EPI and PrE. Unlike TE/ICM specification where cell position predicts and directs differential CDX2/SOX2 regulation, EPI and PrE lineages initally emerge without spatial distinction. Nanog and GATA6, respective markers for EPI and PrE, are co-expressed by cells of the ICM at first, but their expression becomes mutually exclusive in a salt-and-pepper pattern (Chazaud et al., 2006; Plusa et al., 2008). Differential lineage marker expression hence precedes spatial sorting of EPI and PrE cells. PrE cells line the blastocoel cavity while EPI cells are sandwiched between the PrE and the overlying TE. Given the aberrant organisation of the ICM within *Itgb1* KO blastocysts, we predicted that exogenous ECM would similarly alter the spatial arrangement between EPI/PrE cells.

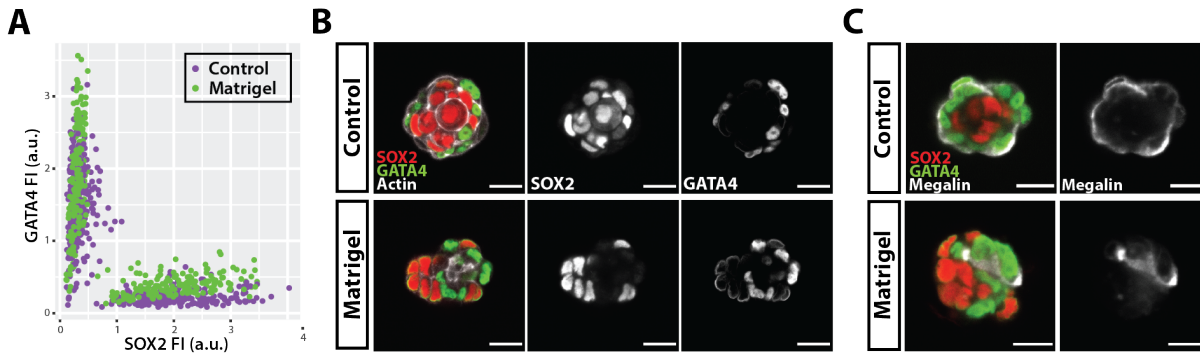


**Figure 16. Exogenous ECM disrupts patterned PrE/EPI arrangement in the isolated ICM.**

**A.** ICMs were isolated from E3.5 blastocysts by immunosurgery and cultured for 20 hours. Analysis of GATA4/SOX2 fluorescence intensities, respective markers for PrE/EPI, reveals a slight negative shift in the distribution of GATA4 expression in Matrigel. However, the two lineages remain clearly distinct based on marker expression. SOX2 intensity: *p*-value = 0.1664; GATA4 intensity: *p*-value = $3.705e^{-6}$, Mann-Whitney U test. N=2, 29 embryos.

**B.** Spatial arrangement of PrE/EPI cells is altered in Matrigel culture. SOX2-positive EPI cells are not limited to the interior but found on the outer surface of the ICM.

**C.** Polarity of the ICM is disrupted in Matrigel culture, as assessed by localisation of PrE apical marker megalin. In control conditions, megalin lines the surface of outer PrE cells in a continuous fashion. In contrast, irregular pockets of accumulation is observed in Matrigel-cultured ICMs. Scale bars, 20 μm.

Wildtype ICMs were immunosurgically isolated from blastocysts at E3.5 and embedded in Matrigel. Patterning and specification of EPI and PrE lineages were examined by staining for SOX2 and GATA4 expression, respectively. Although a statistically significant shift in GATA4 expression was observed in Matrigel, the two lineages were clearly separable by their marker expression (Figure 16A). More evident, however, was the disruption in the arrangement of PrE and EPI cells in Matrigel culture. An isolated E3.5 ICM suspended in standard culture medium typically forms a mass of cells where a single layer of PrE cells surrounds an inner core of EPI cells. In contrast, PrE and EPI cells are either intermingled or segregated into separate hemispheres in Matrigel (Figure 16B).

In whole blastocysts, PrE cells mature into a polarised epithelium once sorted to the ICM surface. Polarisation becomes apparent as apical proteins such as aPKC and megalin accumulate on the cell cortex facing the blastocoel cavity (Plusa et al., 2008; Saiz et al., 2013). Although immunosurgery removes the blastocoel cavity by lysing the TE layer, PrE cells nevertheless sort towards the external environment and polarise on the outer surface of

the ICM, similar to embryoid bodies (Figure 17C) (Moore et al., 2014). While megalin is observed near GATA4-positive nuclei, overall polarity of the ICM is disrupted in Matrigel culture since PrE cells fail to sort to the outer surface.

These observations show that for Matrigel-embedded ICMs, the shift in fate is not as dramatic as that described for inner cells isolated during the 16-32 cell stage. Nevertheless, the disruption of patterning persists, suggesting that ECM components remain critical positional cues for ICM patterning and polarisation of the PrE epithelium. Whether this sorting defect is also driven by laminin and integrin α6β1 activity remains to be examined.

***Polarisation during the 8-cell stage is unaffected by exogenous ECM***

Immunosurgery followed by Matrigel culture thus far resulted in clear disruption of polarity (Figure 15A-B, Figure 16C). Therefore, we examined whether the very first polarisation event that occurs during the 8-cell stage is similarly affected by exogenously provided ECM. It is worth noting that when Cooper and MacQueen described the timing of laminin expression in preimplantation embryos, they remarked that the presence of laminin β1 and γ1 chains during the 8 cell stage may serve not only as an adhesive to hold the embryo together, but also as a directional cue for polarisation (Cooper and MacQueen, 1983). Although the fact that laminin-deficient embryos polarise normally suggests otherwise, this may be attributed to maternally deposited laminin (Miner et al., 2004; Smyth et al., 1999).

In order the test this hypothesis first put forth by Cooper and MacQueen, the reduced system was employed to minimise possible influences by variable cell contact and asynchronous divisions within the whole embryo. Blastomeres dissociated from 4-cell stage embryos (‘1/4’) were embedded in Matrigel and let to divide to form doublets equivalent to the 8-cell stage (‘2/8’). In contrast to observations in isolated inner cells and ICMs, polarisation in 8-cell stage blastomeres was not affected by Matrigel culture. Apical domain formation in 2/8 doublets, as assessed by pERM localisation, was comparable between control and Matrigel conditions, suggesting that polarity establishment during the 8-cell stage is refractory to exogenous ECM (Figure 17A).

Comparable polarisation in Matrigel-embedded and control doublets indicate that ECM-independent positional signals direct symmetry-breaking during the 8-cell stage. Importantly, this stage of mouse development coincides with two crucial morphogenetic events: compaction and polarisation. Contractile activity of the cortical actomyosin network and E-cadherin-mediated interactions bring cells closer together, while the outer surface

undergoes apical polarisation for the first time (Figure 17B) (Ducibella et al., 1977; Larue et al., 1994; Maître et al., 2015). Spatial asymmetry is thus established within each blastomere along the radial axis, and persists through subsequent rounds of division as inner and outer cell identities emerge.

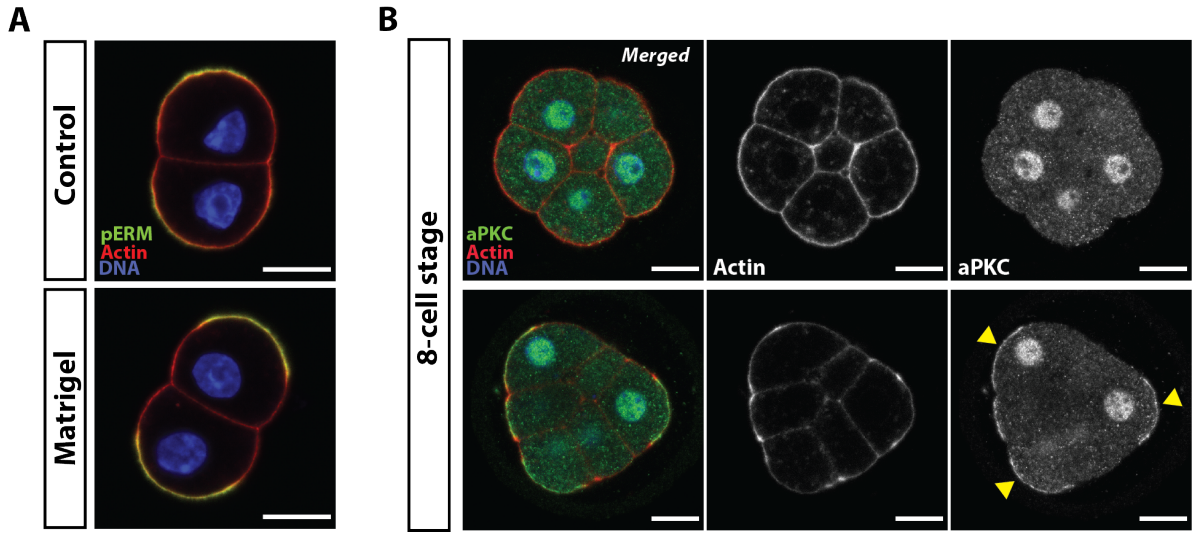


**Figure 17. ECM-independent cues polarise the 8-cell stage embryo.**

**A.** Apical domain assembly in 2/8-doublets is comparable between cells in standard medium (control) and those embedded in Matrigel, as assessed by localisation of pERM. N = 2, 43 doublets.

**B.** Polarisation and compaction during the 8-cell stage mark symmetry-breaking. Top panels represent the early 8-cell stage, and bottom panels represent the late 8-cell stage. In the latter, polarisation is evident by accumulation of atypical protein kinase C (aPKC) on the outer cortex of the embryo (marked by arrows). Compaction is evident based on increased cell-cell interface and reduced embryonic surface area. Scale bars, 20 μm.

### *Polarisation of the 8-cell embryo persists does not require myosin activity*

While polarisation during the 8-cell stage signifies conversion of some form of upstream positional information, the source of this spatial cue is poorly understood. One possible candidate is the propagation pattern of cortical actomyosin waves that emerge during the 8-cell stage (Maître et al., 2016). Earlier work from our group demonstrated that these periodic waves are locally suppressed at cell-cell interfaces, evoking the phase shift model proposed by Goodwin and Cohen (Goodwin and Cohen, 1969; Maître et al., 2016). In this model, wave-like propagation of local pacemaker activity synchronises a group of cells, while

a delayed second wave provides positional information based on the phase difference between the two events. As a result, both temporal and spatial information is conveyed among a group of cells to coordinate cell differentiation and patterning during morphogenesis. In the context of the 8-cell stage embryo, contact asymmetry experienced by each blastomere may modulate cortical wave patterns to identify the cell-free surface suited for apical domain assembly.

To examine whether cortical contractility has an instructive role for patterning, TE/ICM specification was examined in embryos completely lacking Myosin heavy chain -9 (hereafter referred to as 'myosin') encoded by *Myh9*. Previous reports have demonstrated that absence of zygotic *Myh9* results in embryonic lethality by E7.5, but an earlier role of myosin in preimplantation development had been obscured by compensation by maternally deposited reserves (Conti et al., 2004). Therefore, the maternal copy of *Myh9* was deleted by *Cre*-lox recombination in female mice carrying oocyte-specific *Zp3-Cre* (de Vries et al., 2000). Upon crossing them to *Myh9*+/- males, maternal zygotic (mz) *Myh9* knockout (KO) embryos were obtained. Since contractile actomyosin activity is required in several cellular processes including cell division and cytokinesis, mz *Myh9* mutants displayed multinucleate blastomeres, and consisted of fewer cells compared to age-matched wildtype control embryos (Figure 18A).

Nevertheless, mutant embryos polarised in the correct orientation by forming an apical domain on the outer surface, as judged by pERM accumulation (Figure 18A). To observe whether polarisation in these mz *Myh9* KO embryos leads to subsequent TE specification as in wildtype embryos, these were cultured until the blastocyst stage. Despite the presence of CDX2-positive nuclei, however, the morphology of mutant embryos was severely perturbed (Figure 18B). Instead of a single coalesced blastocoel cavity, enlarged intracellular pockets of fluid were observed throughout the embryo. The embryo consisted of fluid-filled cells that were often binucleate, held together by the surrounding zona pellucida. Its CDX2-positive cells did not form an epithelial monolayer around the embryo, and such harsh disruption of patterning indicates lethality occurs considerably earlier than the post-implantation period reported in zygotic *Myh9* KO embryos.

Given the diverse functions of myosin and the severe phenotype mz *Myh9* KO embryos, a pharmaceutical inhibitor of myosin, blebbistatin, was used to examine its requirement for patterning in a temporally controllable manner. Consistent with the involvement of cortical myosin activity in compaction, all treated embryos displayed

decompacted morphology where individual blastomeres appeared more rounded compared to control conditions. Embryos were treated both pre- and post-polarisation, but regardless of the timing of drug administration, apical domain formation persisted on the outer surface of the embryos (Figure 19C), as previously shown (Zhu et al., 2017). Consistent with findings in *Myh9* mutants, these observations suggest that both initiation and maintenance of the proper polarity during the 8-cell stage does not require cortical actomyosin activity.

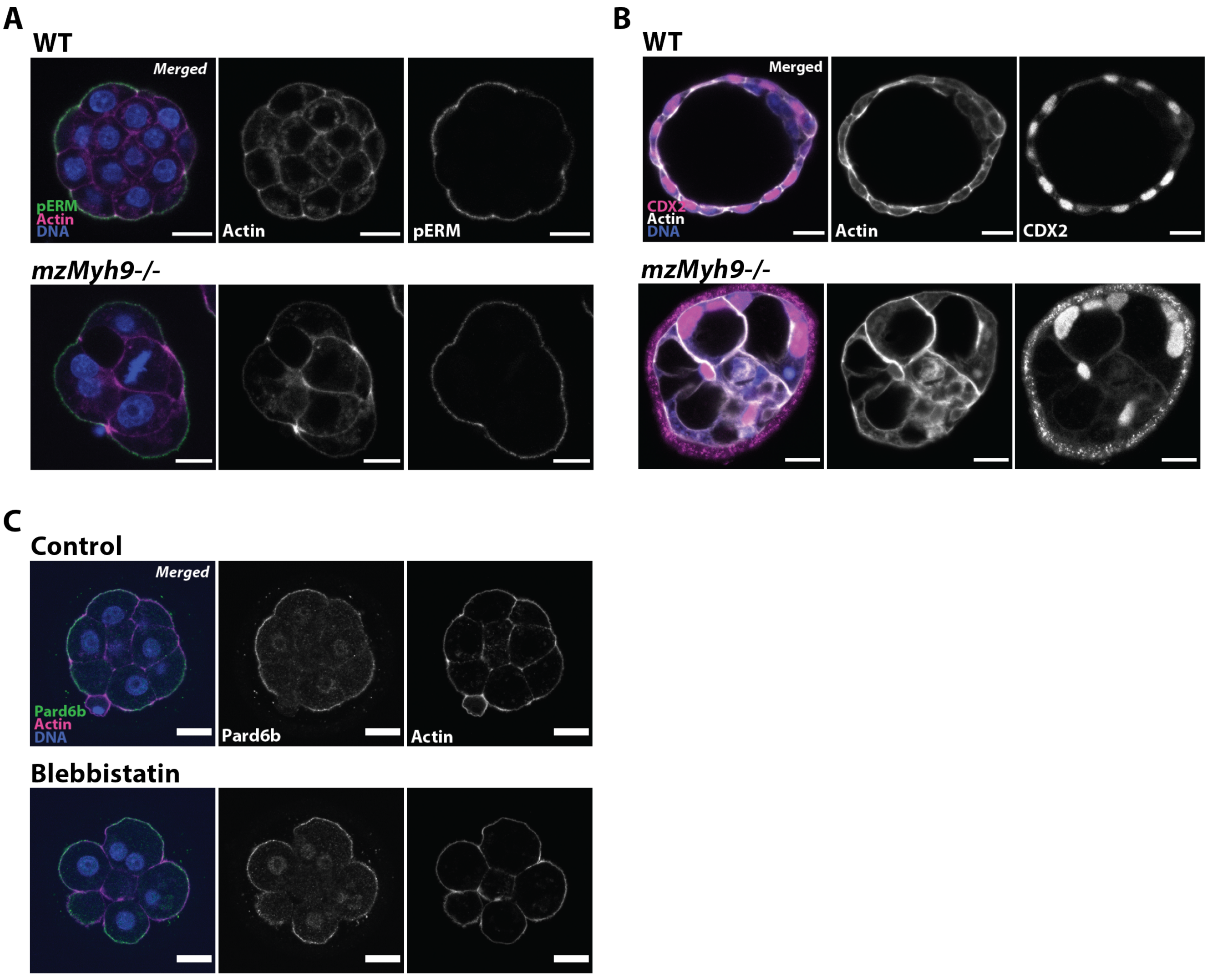


**Figure 18. Polarisation of 8-cell stage embryos does not require myosin activity.**

**A.** Maternal zygotic (mz) *Myh9* KO embryos recovered at E2.5 are polarised despite reduced cell number, as judged by cortical pERM accumulation. N = 2, 25 embryos.
**B.** Mz *Myh9* KO embryos exhibit severely disrupted morphology at E3.5. Cell division, formation of functional TE layer, and blastocoel fluid accumulation are impaired. N = 1, 9 embryos.
**C.** Early 8-cell stage WT embryos are treated with myosin inhibitor blebbistatin (25μM) for 12 hours. Polarisation is comparable between drug-treated embryos and control embryos cultured in DMSO. Scale bars, 20 μm.

***Patterned specification of TE/ICM persists upon myosin inhibition***

Next, to examine fate specification in the absence of myosin activity, blebbistatin was administered to 16-32-cell embryos. Despite impaired compaction, outer cells became TE-specified. In both drug-treated and control embryos, outer cells were polarised, CDX2-positive with high levels of nuclear YAP, while inner cells were apolar, CDX2-negative with cytoplasmic YAP accumulation (Figure 19A).

Asymmetric inheritance of polarity during the 8-cell stage drives differential Hippo signalling and *Cdx2* expression (Anani et al., 2014). Moreover, asymmetric polarity affects relative cortical tension between daughter cells to subsequently establish the inside-outside configuration through sorting (Maître et al., 2016; Samarage et al., 2017). Therefore, the apical domain drives TE-specification and underlies positional differences within the embryo.

In order to examine how polarisation contributes to patterning, we decoupled the TE-inducing and mechanical sorting functions of the apical domain by again utilising the reduced system. Blastomeres singled from 8-cell stage embryos were left to divide to 2/16 doublets. The majority of divisions at this stage are asymmetric, such that one daughter cell inherits the apical domain but not the other (Johnson and Ziomek, 1981; Korotkevich et al., 2017). Under these circumstances, local inhibition of actomyosin contractility at the apical domain results in mechanical asymmetry between the daughter cells, such that the polarised cell becomes stretched around the internalising apolar cell (Figure 19B). In this way, inner-outer configuration of the whole embryo is recapitulated in in 2/16 doublets, and TE markers are positively regulated in the outer cell.

In the presence of blebbistatin, however, differential cortical tension between daughter cells is abolished despite asymmetric inheritance of the apical domain. As a result, inner-outer spatial arrangement is lost and the two daughter cells remain geometrically equivalent. In spite of this, nuclear YAP and CDX2 were prominent in the daughter cell that inherited the apical domain (Figure 19B). These findings suggest that though myosin is involved in several cellular processes, it is not strictly required for asymmetric TE specification while polarity is preserved. Furthermore, even in the absence of positional differences, asymmetric inheritance of polarity can drive differential fate specification among 16-cell stage blastomeres.

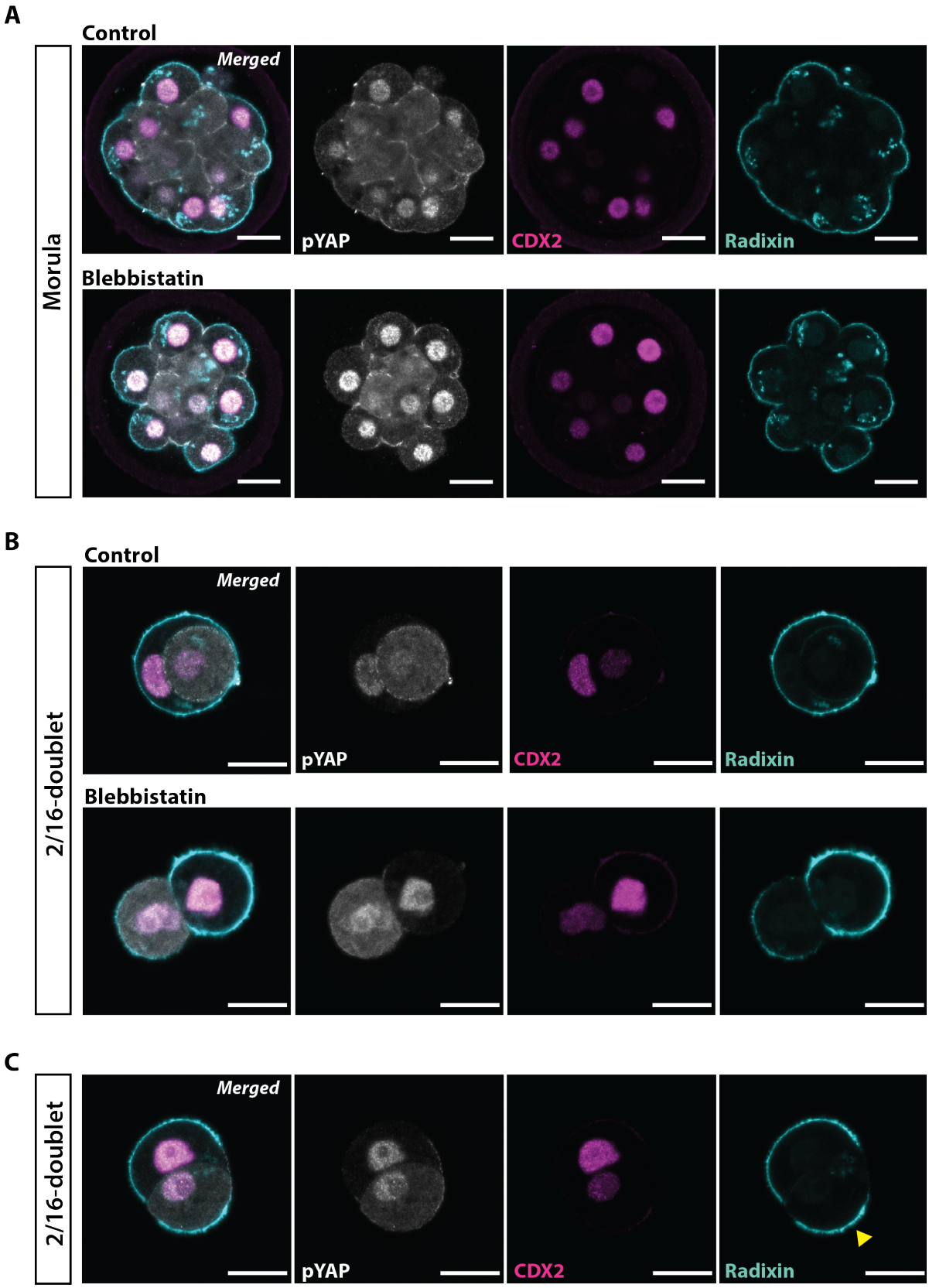


**Figure 19. Patterned specification of TE/ICM persists despite myosin inhibition.**

**A.** WT embryos are treated with blebbistatin (25μM) for 3 hours during the 16-32-cell stage to assess inside-outside patterning in the absence of myosin activity. Radixin marks the apical

domain. As fate assessment was made too early for appreciable SOX2 expression, CDX2 expression and YAP localisation were used to examine patterning. Despite impaired compaction, both drug-treated and control embryos in DMSO exhibit polarised, CDX2-positive cells with nuclear YAP on the outside, while apolar, CDX2-negative cells with cytoplasmic YAP reside inside. N = 2, 27 embryos.
**B.** 2/16-doublets were obtained by dissociating 8-cell stage embryos and letting blastomeres divide and develop in the presence of blebbistatin (25μM) or DMSO (control) for 3 h. Upon asymmetric inheritance of the apical domain, differences in cortical tension drive internalisation of the apolar daughter cell, as shown in the representative control doublet. However, myosin inhibition prevents such positional sorting. Despite lack of positional differences, however, TE marker asymmetry is observed. The daughter cell that inherited the apical domain (right side) upregulates CDX2 and YAP signal is prominent in the nucleus. N = 3, 51 doublets.
**C.** In cases where the apolar daughter is not internalised in a timely manner, *de novo* apical domain assembly is observed, as judged by radixin enrichment (yellow arrow). Similar *de novo* apical domain assembly was also observed with blebbistatin in **B.** Scale bars, 20 μm.

***Outer cells retain ability to polarise without an inherited apical domain***

Is it important to note however, that formation of an apical domain is not strictly limited to the 8-cell stage. Despite asymmetric Hippo signalling and CDX2 expression, some control and blebbistatin-treated 2/16-doublets exhibited apical domains on both cells. Polarised cells exhibiting low levels of CDX2 and nuclear YAP were observed in 2/16 doublets where full internalisation had not taken place (arrow, Figure 19C). Studies tracking live cell movements and polarisation in whole embryos previously showed that apolar cells can in fact polarise *de novo* if they acquire a cell-free surface by occupying an outer position (Korotkevich et al., 2017). This is also consistent with the robust polarisation that was described earlier following immunosurgery of 16-32-cell stage embryos.

Therefore, it appears that while asymmetric inheritance of the apical domain leads to differential TE specification, if the apolar daughter cell is exposed to the external environment for an extended duration, its cell-free surface can be "sensed" and become polarised. As for the eventual fate of these *de novo* polarised cells, they most likely become TE-specified. This assumption is based on observations made by others that the frequency of trophoblastic vesicle formation from 1/8 blastomeres is higher than the number of asymmetric divisions, indicating that not all asymmetric divisions lead to ICM specification of the apolar daughter cell (Johnson and Ziomek, 1981; Tarkowski and Wróblewska, 1967).

The retention of the ability to polarise beyond the 8-cell stage signifies that position-sensing remains active during the early preimplantation period to robustly ensure patterned

TE/ICM specification. As for the axis of polarity, the apical domain is consistently assembled on the exposed surface through a yet unidentified mechanism, away from the cell-cell interface.

***Reduced cell-cell contact combined with myosin inhibition disrupts polarity***

Despite cell-autonomous ability of blastomeres to polarise during the 8-cell stage, the incidence of polarisation is low when cells are in isolation without a cell-cell interface. To examine the importance of cellular contact in driving and orienting apical domain formation, 4-cell stage embryos were dissociated and their blastomeres (1/4) were let to divide to 2/8-doublets that have a single cell-cell interface. As seen from earlier experiments, blebbistatin inhibits compaction but not polarisation, and thus the drug was used to reduce the degree of contact between daughter cells. The adhesive contact surface, as approximated by the diameter of the cell-cell interface, was significantly reduced in drug-treated doublets compared to untreated samples (Figure 20A).

In the presence of blebbistatin, incidence of polarisation was lower and accumulation of the apical marker pERM was often weak compared to control doublets. Furthermore, among drug treated cells that did show cortical pERM accumulation, the position of the apical domain was often aberrant (Figure 20B). Enrichment of pERM in blebbistatin-treated cells often occurred close to the cell-cell interface. In contrast, the apical domain generally formed diametrically opposite the cell-cell interface under control conditions, despite increase in the exposed surface area in reduced systems. For quantification of apical domain positioning, a line was drawn perpendicular to the cell-cell interface and another through the geometric centre of the cell and the apical domain. The angle at the intersection of these two lines was measured, with lower values indicating better 'centred' apical domains. Measured angles were significantly higher in blebbistatin treated 2/8 doublets, indicating more 'off-centredness' (Figure 20C). Similar irregularities in apical domain positioning was also observed in 2/8 doublets derived from *Myh9* heterozygous embryos lacking maternally contributed myosin (Figure 20D). Although these embryos are zygotically heterozygous for *Myh9*, the reduction in myosin was sufficient to mimic blebbistatin treatment in doublets.

Notably, in both blebbistatin-treated and control doublets, the centring of the apical domain did not necessarily correlate with size of the contact interface (Figure 20E). This suggests that although myosin activity is not required for assembly of the apical domain *per se*, it guides its positioning. While a cell-cell interface is important for efficient polarisation

and proper positioning of the apical domain, its perception by the cell appears to require myosin activity during the 8-cell stage.

There is a considerably smaller margin for apical domain mispositioning in whole embryos where the cell-free surface area is physically limited. In comparison, centring the apical domain relative to the cell-cell interface is more challenging in doublets given the increased free surface area. As a result, the requirement for myosin in sensing the cell-cell interface may become more stringent in 2/8-doublets, thus reconciling the discrepancies in apical domain formation between experiments in whole embryos and the reduced system. We speculate that myosin activity provides one form of positional information during the 8-cell stage, but the high degree of intercellular contact can compensate for its loss in whole embryos. Moreover, as cell proliferation continues, increased intercellular contact can correct for mispositioned polarity, such that inside-outside patterning of TE/ICM specification is robustly achieved.

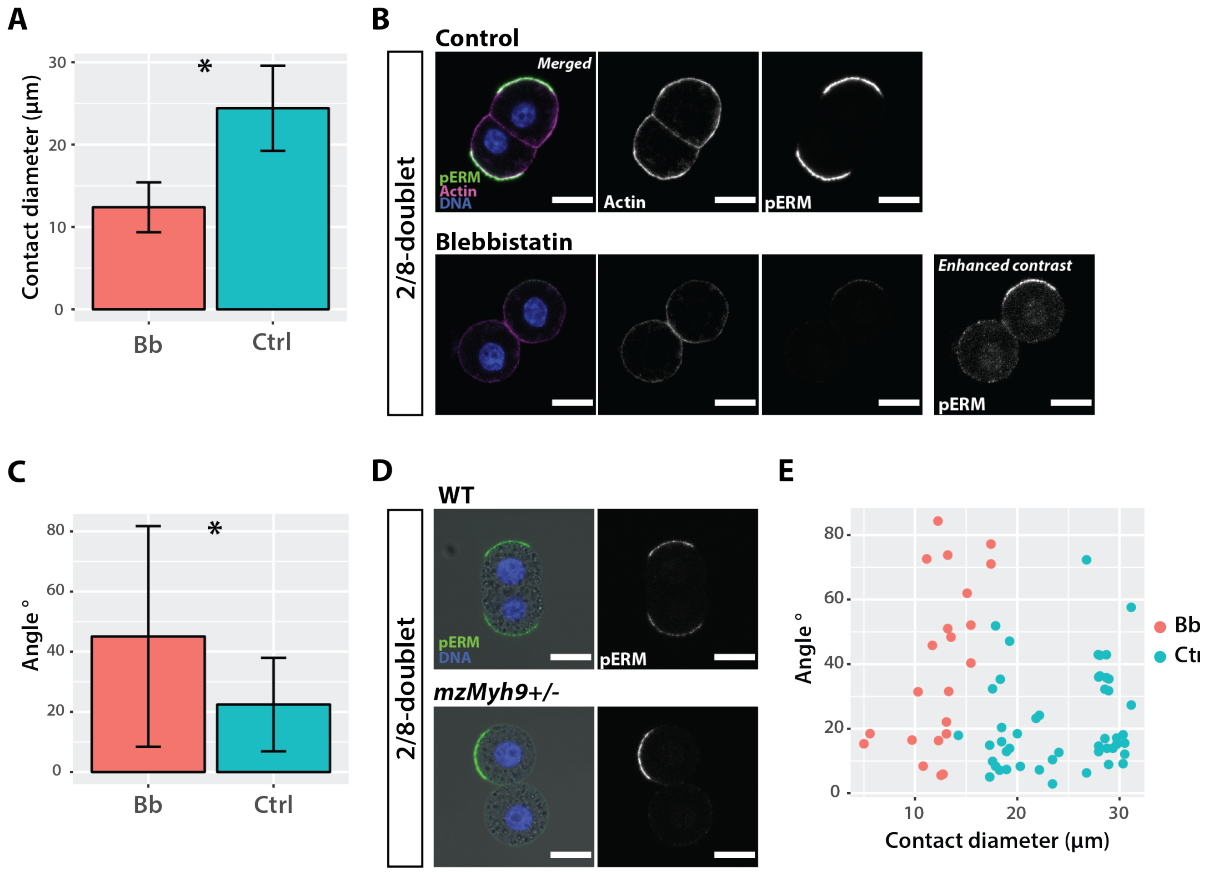


**Figure 20. Patterned specification of TE/ICM persists despite myosin inhibition.**

**A.** 2/8-doublets were obtained by dissociating 4-cell stage embryos and letting individual blastomeres divide and develop in the presence of blebbistatin (25µM) or DMSO (control) for 12 hours. The contact surface, as measured by diameter of the cell-cell interface, is significantly reduced with blebbistatin treatment. Graph shows mean± S.D. p-value = $5.289e^{-18}$, independent student's *t*-test. N = 3, 70 doublets.

**B.** pERM enrichment indicates apical domain assembly. In drug-treated 2/8-doublets, the apical domain is typically 'off-centre' relative to the cell-cell interface, and the pERM signal is often weak. Therefore, representative apical domain in treated sample is shown with enhanced contrast.

**C.** Positioning of the apical domain relative to the cell-cell interface is significantly altered with blebbistatin treatment. For quantification of apical domain positioning, a line was drawn perpendicular to the cell-cell interface and another through the geometric centre of the cell and the apical domain. The angle at the intersection of these two lines was measured, with lower values indicating better 'centred' apical domains. The mean angle is significantly higher with blebbistatin treatment, indicating that the apical domain is less 'centred'. Graph shows mean± S.D. p-value = 0.0074, independent student's *t*-test. N = 3, 70 doublets.

**D.** Similar to blebbistatin-treated doublets, those derived from genetic mutants lacking maternal contribution of *Myh9* exhibit off-centred apical domain assembly. N = 1, 23 doublets.

**E.** Although blebbistatin treatment impairs compaction and apical domain positioning, the size of the cell-cell interface does not strongly correlate with apical domain centring. For drug-treated group, r = 0.252. For control group, r = 0.206. N = 3, 70 doublets, Pearson correlation. Scale bars, 20 µm.

.

# Discussions

The present study examined which positional cues contribute to embryonic patterning during preimplantation development of the mouse. Guided by contact asymmetry, the apical domain, either passed down through cell division or assembled *de novo*, consistently marks the embryonic outer surface from the 8-cell stage onwards. Soon thereafter, laminin-integrin adhesive interactions in the embryonic interior distinguish inner cells from polarised outer cells. By transducing position-specific cues from the microenvironment, polarised outer cells and adhesion-rich inner cells become TE and ICM-specified, respectively. Moreover, mimicking the inner microenvironment through combining immunosurgery with Matrigel culture potently drives ICM specification in an integrin β1-dependent manner.

***Integrin-ECM interactions promote ICM specification***

Earlier studies of ICM specification placed heavy emphasis on transcriptional changes that occur in individual cells of the early embryo. While these provide valuable insight into gene expression changes and the regulatory factors involved in lineage divergence, they lack spatial resolution as dissociation of the embryo disrupts cell-cell/ECM adhesions. The significance of events that occur at the cell-cell interface was thus overlooked with these approaches. In addressing this vacuum, the most striking outcome from Matrigel-induced changes following immunosurgery is the increase in ICM specification. The effects of Matrigel are dependent on integrin β1 activity, which likely functions in a heterodimer with integrin α6. A major question prompted by this finding is how interactions at the cell surface can result in transcriptional changes that dictate cell fate.

Differentiation of various types of stem cells is governed the mechanical properties and adhesive interactions fostered by the culture substrate (Chowdhury et al., 2009; Engler et al., 2006; Hazenbiller et al., 2017). Even the upregulation of pluripotency genes, including *Sox2*, is sensitive to the physical surrounding during reprogramming of somatic cells to induced pluripotent stem cells (Downing et al., 2013). It is well-established that integrins not only sense the mechanical microenvironment, but are mechanically linked to the nucleus via the cytoskeleton and a host of interacting partners (Huveneers and Danen, 2009; Lammerding, 2011; Maniotis et al., 1997). Therefore, it is plausible that tensional forces applied to integrin may be transferred to discrete regions of the nuclear envelope via cytoskeletal filaments to affect transcription of lineage markers in the early embryo. Although our experiments with hydrogel and diluted Matrigel suggest that substrate stiffness

plays a relatively minor role in promoting ICM specification, this is far from conclusive as quantitative measures of mechanical parameters are lacking.

To understand which processes bridge integrin activity at the cell surface to transcriptional changes, one may also identify its downstream effectors. While intracellular signalling is mainly mediated by the cytoplasmic tail of the integrin β1 subunit, how these affect the epigenetic landscape to upregulate ICM-specific genes is unknown. Complications lie in the fact that ICM specification is poorly understood even in the context of unperturbed embryos, let alone in experimentally manipulated systems. To gain clearer understanding of the events leading to ICM specification, future endeavours should aim to correlate how transcriptional dynamics spatially evolve with the changing microenvironment. In addition, the role of individual ECM components that emerge with the ICM should be re-assessed with advanced imaging and analysis tools available today.

***Itgb1 is required for patterning the embryonic interior***

If transduction of ECM signals from the cortex is necessary and sufficient as the inner positional cue to direct ICM fate, absence of ECM receptors would be expected impair ICM specification. However, *Itgb1* KO embryos develop to expanded blastocysts, albeit with slightly reduced cell number, indicating that patterned TE/ICM specification persists in the absence of zygotic integrin β1. Although polarisation during the 8-cell stage was not examined in *Itgb1* KO embryos, we can surmise from their blastocyst formation that compaction and polarisation are most likely intact. As preimplantation development proceeds, expression of integrin α6β1 and laminin chains becomes prominent in the ICM region of the blastocyst. Accordingly, the effect of *Itgb1* deficiency is more discernible at this stage. In mutant blastocysts, the PrE fails to sort into a monolayer around the EPI. Instead, cells of each lineage are segregated in clusters and thus a multilayered PrE is observed. Matrigel culture of ICMs isolated from E3.5 blastocysts recapitulates this sorting defect. These findings suggest that EPI/PrE patterning within in the ICM relies on ECM-integrin interactions.

As for the mild phenotype of *Itgb1* KO morulae with respect to TE/ICM patterning, preservation of the polarity in outer cells, combined with contact mediated by other adhesive proteins such as E-cadherin, may compensate for *Itgb1* deficiency. Alternatively, rescue by

maternally deposited integrin β1 may mask defects from zygotic deficiency. For this reason, future experiments should examine TE/ICM patterning in maternal zygotic *Itgb1* mutants.

***The influence of the ECM is developmental stage-dependent***

Although Matrigel was chiefly used to mimic the inner microenvironment of the embryo to affect lineage segregation, it also provides clues to how the ECM affects apicobasal polarity. Immunosurgery allowed manipulation of the existing contact microenvironment within preimplantation embryos. Inner cells that became newly exposed underwent polarisation and adjusted their fate to generate a TE layer. In contrast, apical polarisation and TE specification was visibly suppressed in cells embedded in Matrigel.

Despite such pronounced effects on inner cells of the morula, however, Matrigel had little visible impact on polarity establishment in 8 cell stage blastomeres. Both the assembly and positioning of the apical domain in 2/8-doublets were unaffected by Matrigel culture. Since neither laminin nor integrin subunits are appreciably expressed at cell-cell interfaces until the 16-32 cell stage, it is perhaps not surprising that polarisation in 8-cell stage blastomeres is refractory to Matrigel. Studies in ESCs have demonstrated that adhesion and thus response to Matrigel is mainly mediated by a β1 subunit-containing integrin heterodimer (Moore et al., 2014). Therefore, positional information that instructs polarisation may be spatiotemporally controlled by regulating the cell's interpretation of the cell-cell interface as well as its receptivity to the ECM.

Yet another speculation is that differences in material properties between 4-8 cell stage blastomeres and isolated inner cells dictate how they respond to external ECM cues. Parameters such as baseline stress, stiffness, cytoskeletal structure, and endogenous contractility are known to contribute to the material properties or mechanical wiring of the cell (Humphrey et al., 2014). In support of this notion, cell spreading response is much more sensitive to stress applied through integrins in soft embryonic stem cells compared to their stiffer differentiated counterparts (Chowdhury et al., 2009). Whether inner cells of the morula are softer than outer cells or early blastomeres and hence more sensitive to exogenously provided ECM, remains to be examined.

The difference in sensitivity to Matrigel between 8-cell stage blastomeres and inner cells of the E2.5 morula indicates that the mechanism of initial polarity establishment for symmetry-breaking may differ from *de novo* polarisation that occurs at later stages. During the 8-cell stage, all blastomeres share the same overall geometry. Each blastomere has a cell-

free portion of the cortex and an adhesive interface shared with its neighbours. The polarisation programme is turned on in every cell for apical domain assembly. However, as divisions continue and the contact environment becomes varied between blastomeres, the polarisation programme must be selectively engaged in outer cells during the 16-32 cell stage. As a means of achieving spatial distinction, we propose that inner cells depend on the evolving ECM microenvironment, particularly interactions between laminin and its receptor integrin α6β1. Our findings show that polarisation is suppressed where there is enrichment of laminin-integrin α6β1.

***Polarisation in the 8-cell embryo does not require myosin activity***

Although embryos were refractory to exogenous ECM cues prior to the 16-32-cell stage, some form of asymmetry must be present in earlier stages to initiate patterning. During mouse development, polarisation breaks symmetry along the radial axis of the 8-cell stage embryo. This feat is twofold. In addition to the assembly of the apical domain, each cell must appropriately orient the polarity axis to ensure coherent patterning of the embryo. In the wildtype embryo, the apical domain is positioned on the cell-free outer surface. Similarly, apical domain assembly persists on the outer surface of myosin-inhibited whole embryos. Despite decompacted morphology, apical proteins accumulate on the outer cortex of blebbistatin-treated embryos as well as mz*Myh9* mutants. As expected from the various functions of myosin, the morphology of mz*Myh9* mutants is severely impaired during the latter half of preimplantation development. However, our observations at the 8-16-cell stage suggest that apical polarisation of the outer surface is independent cortical contractility. Furthermore, polarisation occurs in a temporally controlled manner regardless of cell number or size, as reported previously (Korotkevich et al., 2017).

***Myosin activity orients the apical domain upon reduced cell-cell contact***

Only upon combination with drastic removal of cell-cell contact does myosin inhibition lead to aberrant polarisation. As studies with embryos that lack E-cadherin have previously shown, intercellular contacts are critical for proper positioning of the apical domain, but not for its cortical assembly *per se* (Larue et al., 1994; Stephenson et al., 2010). Through unknown mechanisms, adhesive interfaces locally suppress apical domain formation and thereby spatially restrict it to the cell-free surface. In our reduced system where the

embryo is quartered at the 4-cell stage, intercellular interactions are reduced to a single cell-cell interface and the cell-free surface area is increased. With little variation in positioning, however, apical domain formation in these 2/8-doublets is mostly restricted to the cell hemisphere further from the cell-cell interface. This implies that the influence of the cell-cell interface in guiding polarisation is not limited to the immediate vicinity of cell contact but spans across the whole blastomere.

Cortical waves of contractile actomyosin activity may be one way to sense a contact interface across the cell (Goodwin & Cohen, 1969; Maître et al., 2016). These waves periodically travel through the cortex of 8-cell stage blastomeres. Since the propagation of these waves is locally suppressed at intercellular junctions, their pattern may convey relative distance between a cell-free surface and the cell-cell interface. Where contact cues are scarce, as in the reduced experimental system, there may be an increased dependence on these contractile waves to perceive contact asymmetry and designate the outermost surface for polarisation. This would explain why the apical domain generally forms furthest from the cell-cell interface in 2/8-doublets under control conditions, but in an 'off-centred' manner upon myosin inhibition.

Although blebbistatin prevented compaction of 2/8 doublets, the degree of 'off-centred'-ness did not inversely correlate with contact area between cells within the treatment group. Under normal conditions, provision of a contact interface is known to potentiate polarisation, as polarisation is considerably more efficient in doublets compared to isolated 1/8 blastomeres. Therefore, the comparatively weak polarisation with blebbistatin treatment further suggests that rather than simply a decrease in the physical contact area, the perception of contact itself is impaired when actomyosin waves are inhibited. The discrepancy in polarisation observed between blebbistatin-treated whole embryos and 2/8-doublets indicate that, although myosin activity is one means to detect contact, its absence can be robustly overcome if sufficient cell contact is present. Thus, contact cues may direct apical domain assembly through more than one mechanism.

Once assembled, the functional capacity of the apical domain to direct TE specification is preserved under myosin inhibition. Although these embryos exhibit decompacted morphology, their outer cells are marked by increased nuclear intensity of YAP and CDX2. Likewise, cells with strongly labelled apical domain in drug treated 2/16 doublets express TE markers. Therefore, as much as myosin activity is important for cell division,

compaction, and mechanical sorting among cells, polarisation can robustly overcome myosin deficiency, especially where TE specification is concerned.

***Polarised domains are critical positional hallmarks in the embryo***

Observations described here and by others indicate that the apical domain robustly marks cell-free surfaces during preimplantation development. In whole embryos, blastomeres with exposed surfaces exhibit an apical domain, either inherited or assembled *de novo*, such that the outer surface of the embryo remains polarised from the 8-cell stage until implantation. In reduced systems, both cells of a 2/16-doublet may exhibit polarity despite asymmetric inheritance of the apical domain if the apolar surface is sufficiently exposed to the external environment. For this reason, apical proteins can be found on the outer surface of CDX2-low cells in both blebbistatin-treated and untreated 2/16-doublets where neither cell is completely internalised. Although live-imaging data is not available, such *de novo* polarisation presumably promotes TE specification despite initially low levels of CDX2 and nuclear YAP. This would reconcile earlier observations that culture of 1/8 blastomeres more often gives rise to ICM-free trophoblastic vesicles despite the majority of 1/8 to 2/16 divisions being asymmetric (Johnson and Ziomek, 1981; Tarkowski and Wróblewska, 1967). Similarly, inner cells that become exposed to the external environment by immunosurgery at E2.5 or E3.5 also undergo robust surface polarisation (Stephenson et al., 2010; Wigger et al., 2017).

It must be noted for the latter, however, that polarisation seen after immunosurgery at different stages may not necessarily be achieved through the same mechanism. *In vivo*, emergence of TE and PrE polarities are spatiotemporally dissimilar. Despite shared markers of the apicobasal membrane domains, their orientation is reversed with respect to the blastocoel cavity. Moreover, while polarisation *precedes* TE fate specification in outer cells, it *follows* PrE specification and sorting within the ICM (Chazaud et al., 2006; Korotkevich et al., 2017; Ralston and Rossant, 2008; Saiz et al., 2013). Since the central fluid-filled cavity is removed by immunosurgery at E3.5, PrE cells that sort to the periphery of the isolated ICM are polarised towards the external environment in lieu of the blastocoel fluid. Future comparative analyses between TE and PrE would inform how positional information is differentially provided and interpreted to direct polarity during preimplantation development.

***The ECM at the cell-cell interface is a critical source of positional information***

In multicellular systems, the pattern of cell-cell/ECM interactions critically underlies spatial arrangement amongst different populations of cells. However, despite dynamic bidirectional signalling between cells and their surrounding ECM, there is an implicit tendency to regard the ECM as a separate structural entity. As a result, while numerous developmental studies have revealed its function as adhesive substrates, physical boundary between tissues, and guidance cues for growth and migration, the ECM has been mostly overlooked at the cell-cell interface in favour of cadherin-mediated interactions. Although contact geometry was long recognised as an important determinant of patterned TE/ICM specification, earlier studies in mouse development were inclined to focus on cadherin-mediated adhesions rather than the ECM.

While the outer surface is marked by a polarised domain across different stages and experimental manipulations, events at the cell-cell interface are subtler. The present work has demonstrated that the ECM and its receptor integrins are present alongside E-cadherin at the cell-cell interface of the preimplantation embryo. Moreover, these molecules are not merely glue to hold cells together, but critically direct cell differentiation and affect embryo morphology. In particular, laminin-integrin $\alpha 6\beta 1$ ligation potently drives ICM specification during the morula stage. As the embryonic geometry evolves, cells are able to sense and distinguish signals from the cell-free and adhesive surfaces. Just as the apical domain identifies outer surfaces, we propose that ECM components at the cell-cell interface provide positional information imperative to patterning of the embryonic interior.

# Perspectives

## Outstanding questions

***How is information from adhesive contacts recognised and integrated by the cell?***

Our observations indicate that direct cell-cell adhesions and cell-ECM adhesions can share the same contact interface. Both types of adhesions can serve as sensors of the biochemical and physical environment to convey positional information. Nevertheless, little is known about the relationship between these two types of adhesions, and how their activities may influence one another to drive cell behaviour.

Both integrins and cadherins are intracellularly linked to the actin cytoskeleton, which they dynamically remodel by regulating of the Rho family of GTPases. They also share several downstream effectors, among them vinculin, an anchor protein that binds to actin filaments as well as other junctional proteins including talin, actinin and paxillin (Kanchanawong et al., 2010; Sehgal et al., 2018). Engagement of cadherin or integrin leads to phosphorylation of distinct tyrosine residues in vinculin, and submembrane 'plaques' form to stabilise adhesive interactions. In mouse, vinculin is detected around the cell cortex in pre-compacted embryos, and becomes selectively enriched at cell-cell interfaces between flattened outer cells and adjacent inner cells during the morula stage (Lehtonen and Reima, 1986). Detailed characterisation of vinculin localisation alongside integrin β1 and E-cadherin, as well as how its distribution changes in Matrigel culture and in *Itgb1* and *Cdh1* mutant embryos, may reveal distinct and shared functions of these two types of adhesions. Feedback interaction between cell-cell and cell-ECM adhesions may be in place to ensure robust maintenance of the inner cell identity during preimplantation development.

Studies in other systems indeed point to reciprocal regulation between cadherin and integrin-mediated adhesions, where strengthening of one opposes formation of the other (Mui et al., 2016). Induction of integrin-mediated adhesion in monolayers of endothelial cells results in weakening of VE-cadherin-mediated junctions (Wang et al., 2006). From a mechanical standpoint, such balancing of forces transmitted from cadherin and integrin-mediated adhesions may be important for tensional homeostasis and subsequent regulation of downstream mechanosensitive processes. Conversely, in ESCs, controlled force application by ferromagnetic beads revealed that although both integrin and cadherin are mechanosensitive, only integrin-mediated force transduction lead to transcriptional changes that affect differentiation state (Uda et al., 2011).

Both cadherins and ECM components are highly conserved among metazoans and critically required for tissue integrity and function. Therefore, spatial overlap between these

adhesions may be found in a myriad of cell-cell interfaces. To what degree their contributions are shared or distinct, and how their activities at the cell cortex are integrated to affect transcriptional changes are important questions for future work.

***What are the biomechanical features of the embryonic ECM microenvironment?***

From a mechanical standpoint, the ECM can simultaneously function as a source of mechanical force as well as a stress sensor. Both roles converge on integrin-mediated signalling to guide cellular behaviour, and the cell can in turn remodel its ECM microenvironment. However, mechanical characterisation of the ECM in the embryonic interior and its effect on lineage decisions are yet to be come. Parameters such as traction force generated at cell-ECM adhesions, matrix stiffness, elasticity, as well as its precise structural composition could provide significant insight into morphogenesis of the early embryo (Humphrey et al., 2014; Mammoto and Ingber, 2010). Although the present study emphasises the biochemical role of laminin, Matrigel is a heterogeneous mixture of ECM components and therefore it is difficult to pinpoint its effect to a single molecule.

Furthermore, other ECM components such as collagen IV, nidogen, and fibronectin are also secreted during preimplantation development. Each confers distinct mechanical properties to the matrix, and specific cross-linking interactions add further complexity to the extracellular microenvironment. The combined effect of ECM-mediated force may deform the nucleus and bring about changes in nuclear stiffness, nucleoplasm rheology, as well as chromatin state. Future experiments should prioritise replacing Matrigel with a biochemically and mechanically defined combination of ECM components, and better characterise how mechanosensitive processes in blastomeres affect cell fate specification.

***What mechanisms underlie apical domain formation at different stages?***

While the literature and the evidence presented thus far clearly illustrate that surface polarisation conveys outer positional information, the molecular mechanism underlying apical domain assembly on the cell-free surface is largely unknown. Although disruption of the actin cytoskeleton is known to suppress polarisation in the mouse embryo, it is difficult to untangle which of its myriad of cellular roles is specifically involved in apical domain assembly (Ducibella and Anderson, 1975; Fleming et al., 1986; Zhu et al., 2017).

Studies in other polarised cell systems indicate that assembly of a specialised membrane domain requires directed intracellular trafficking and activity of small GTPases of the Rho and Rab families (Kreitzer and Myat, 2017). The apical domain does not form in mouse embryos deficient in Rho family member Cdc42, which is heavily involved in actin remodelling, trafficking of vesicles, as well as cell cycle progression (Korotkevich et al., 2017). In order to understand how the outer surface polarises during preimplantation development, it would be necessary to dissect how intercellular adhesions spatiotemporally modulate Cdc42 activity and intracellular trafficking, with or without influence by myosin (Kim et al., 2000; Osmani et al., 2010). These are no trivial tasks as perturbation of either would interfere with not only polarisation, but a slew of other cellular processes including cytoskeletal remodelling and cell division. Reduced systems coupled to optogenetic control of small GTPases may be necessary to understand how blastomeres execute apical domain assembly in future studies (Tischer and Weiner, 2014). Moreover, given the differences observed between polarisation in 8-cell stage blastomeres, isolated inner cells from the morula, and sorted PrE cells, it would be necessary to examine how the mechanism of apical domain formation evolves during development.

## Concluding remarks

Embryonic development entails specification and patterned arrangement of diverse lineages of cells. This requires that cells sense and transduce cues from their microenvironment to spatiotemporally coordinate their behaviour. In understanding these processes, the distinction between positional information and the interpretation of positional information is significant. While adhesive interactions are highly conserved, being both ubiquitous and indispensable for multicellular organisation, there are a myriad of variations in the type of receptors and ligands available. Additionally, the ability of cells to sense and respond to geometric cues are varied. In this way, conserved mechanisms of cell-cell and cell-ECM interactions give rise to diverse outcomes.

In the early mouse embryo, contact, polarisation, and cell-ECM asymmetry are spatiotemporally controlled to achieve patterning. In particular, the emergence of an ECM-rich microenvironment within the embryonic interior facilitates laminin-integrin $\alpha 6\beta 1$ interactions that potently induce ICM specification. Therefore, the present study joins the increasing body of work uncovering an active role of ECM in embryonic patterning.

A recent study highlights how the complex interplay of adhesive interactions brings about neural tube closure and body elongation in zebrafish. The major ECM component fibronectin functions as a 'glue' that attaches the folding tube to the surrounding tissue (Guillon et al., 2020). The strength of this attachment must be finely controlled. If it is too adhesive, it is difficult for the neural tube to curl up and converge, if too weak, bilateral symmetry of the tissue is impaired. In fact, the authors found that cells locally remodel fibronectin deposition to concentrate it where mechanical stress is high. This remodelling is dependent on integrin activity, which is in fact modulated by N(neural)-cadherin (Jülich et al., 2015; Lele et al., 2002). Therefore, cooperative and dynamic regulation of cell-cell and cell-ECM activity critically underlies neural tube morphogenesis and body elongation at the tissue level. Subsequently, a different set of positional information dorsoventrally patterns cellular differentiation in the neural tube upon its closure, as described briefly in the introduction of this thesis

While many questions remain as to the mechanism of position-sensing and the transduction of cell surface events – both biochemical and mechanical – to behavioural or transcriptional responses within individual cells, these are undoubtedly pertinent to understanding spatial patterning in biology. Moreover, improved comprehension of adhesive interactions at the tissue level will aid identification of specific questions relevant to intracellular regulatory phenomena. Principles of positional information and patterning uncovered here may carry broad implications for appreciating morphogenesis in other model systems and disease processes in the adult.

# References

Aceto, D., Beers, M., and Kemphues, K.J. (2006). Interaction of PAR-6 with CDC-42 is required for maintenance but not establishment of PAR asymmetry in C. elegans. Developmental Biology *299*, 386–397.

Adamo, J.E., Moskow, J.J., Gladfelter, A.S., Viterbo, D., Lew, D.J., and Brennwald, P.J. (2001). Yeast Cdc42 functions at a late step in exocytosis, specifically during polarized growth of the emerging bud. J Cell Biol *155*, 581–592.

Alarcon, V.B. (2010). Cell Polarity Regulator PARD6B Is Essential for Trophectoderm Formation in the Preimplantation Mouse Embryo1. Biology of Reproduction *83*, 347–358.

Alarcon, V.B., and Marikawa, Y. (2005). Unbiased contribution of the first two blastomeres to mouse blastocyst development. Mol. Reprod. Dev. *72*, 354–361.

Anani, S., Bhat, S., Honma-Yamanaka, N., Krawchuk, D., and Yamanaka, Y. (2014). Initiation of Hippo signaling is linked to polarity rather than to cell position in the pre-implantation mouse embryo. Development *141*, 2813–2824.

Arjonen, A., Alanko, J., Veltel, S., and Ivaska, J. (2012). Distinct recycling of active and inactive β1 integrins. Traffic *13*, 610–625.

Aulehla, A., Wiegraebe, W., Baubet, V., Wahl, M.B., Deng, C., Taketo, M., Lewandoski, M., and Pourquié, O. (2008). A beta-catenin gradient links the clock and wavefront systems in mouse embryo segmentation. Nat Cell Biol *10*, 186–193.

Aumailley, M., Pesch, M., Tunggal, L., Gaill, F., and Fässler, R. (2000). Altered synthesis of laminin 1 and absence of basement membrane component deposition in (beta)1 integrin-deficient embryoid bodies. J Cell Sci *113 Pt 2*, 259–268.

Aumailley, M., Timpl, R., and Sonnenberg, A. (1990). Antibody to integrin alpha 6 subunit specifically inhibits cell-binding to laminin fragment 8. Exp. Cell Res. *188*, 55–60.

Austin, J., and Kimble, J. (1987). glp-1 is required in the germ line for regulation of the decision between mitosis and meiosis in C. elegans. Cell *51*, 589–599.

Barbier, F.F., Dun, E.A., and Beveridge, C.A. (2017). Apical dominance. Curr. Biol. *27*, R864–R865.

Bazzoni, G., Ma, L., Blue, M.L., and Hemler, M.E. (1998). Divalent cations and ligands induce conformational changes that are highly divergent among beta1 integrins. J. Biol. Chem. *273*, 6670–6678.

Belkin, A.M., and Stepp, M.A. (2000). Integrins as receptors for laminins. Microsc. Res. Tech. *51*, 280–301.

Biggers, J.D., McGinnis, L.K., and Raffin, M. (2000). Amino acids and preimplantation development of the mouse in protein-free potassium simplex optimized medium. Biology of Reproduction *63*, 281–293.

Briscoe, J., Sussel, L., Serup, P., Hartigan-O'Connor, D., Jessell, T.M., Rubenstein, J.L., and Ericson, J. (1999). Homeobox gene Nkx2.2 and specification of neuronal identity by graded Sonic hedgehog signalling. Nature *398*, 622–627.

Bun, P., Liu, J., Turlier, H., Liu, Z., Uriot, K., Joanny, J.-F., and Coppey-Moisan, M. (2014). Mechanical checkpoint for persistent cell polarization in adhesion-naive fibroblasts. Biophys. J. *107*, 324–335.

Calderwood, D.A., Zent, R., Grant, R., Rees, D.J., Hynes, R.O., and Ginsberg, M.H. (1999). The Talin head domain binds to integrin beta subunit cytoplasmic tails and regulates integrin activation. J. Biol. Chem. *274*, 28071–28074.

Caswell, P.T., Vadrevu, S., and Norman, J.C. (2009). Integrins: masters and slaves of endocytic transport. Nature Reviews Molecular Cell Biology *10*, 843–853.

Cattavarayane, S., Palovuori, R., Tanjore Ramanathan, J., and Manninen, A. (2015). α6β1- and αV-integrins are required for long-term self-renewal of murine embryonic stem cells in the absence of LIF. BMC Cell Biol. *16*, 3.

Cetera, M., Ramirez-San Juan, G.R., Oakes, P.W., Lewellyn, L., Fairchild, M.J., Tanentzapf, G., Gardel, M.L., and Horne-Badovinac, S. (2014). Epithelial rotation promotes the global alignment of contractile actin bundles during Drosophila egg chamber elongation. Nat Commun *5*, 5511.

Chazaud, C., Yamanaka, Y., Pawson, T., and Rossant, J. (2006). Early lineage segregation between epiblast and primitive endoderm in mouse blastocysts through the Grb2-MAPK pathway. Devcel *10*, 615–624.

Cheeks, R.J., Canman, J.C., Gabriel, W.N., Meyer, N., Strome, S., and Goldstein, B. (2004). C. elegans PAR proteins function by mobilizing and stabilizing asymmetrically localized protein complexes. Current Biology *14*, 851–862.

Chowdhury, F., Na, S., Li, D., Poh, Y.-C., Tanaka, T.S., Wang, F., and Wang, N. (2009). Material properties of the cell dictate stress-induced spreading and differentiation in embryonic stem cells. 1–7.

Cinquin, O., Crittenden, S.L., Morgan, D.E., and Kimble, J. (2010). Progression from a stem cell-like state to early differentiation in the C. elegans germ line. Proc. Natl. Acad. Sci. U.S.a. *107*, 2048–2053.

Clark, E.A., King, W.G., Brugge, J.S., Symons, M., and Hynes, R.O. (1998). Integrin-mediated signals regulated by members of the rho family of GTPases. J Cell Biol *142*, 573–586.

Clark, G.L., and Schaad, J.A. (1936). X-ray Diffraction Studies of Tendon and Intestinal Wall Collagen. Radiology *27*, 339–356.

Clyde, D.E., Corado, M.S.G., Wu, X., Paré, A., Papatsenko, D., and Small, S. (2003). A self-organizing system of repressor gradients establishes segmental complexity in Drosophila. Nature *426*, 849–853.

Cockburn, K., Biechele, S., Garner, J., and Rossant, J. (2013). The Hippo pathway member Nf2 is required for inner cell mass specification. Curr. Biol. *23*, 1195–1201.

Coles, E.G., Gammill, L.S., Miner, J.H., and Bronner-Fraser, M. (2006). Abnormalities in neural crest cell migration in laminin alpha5 mutant mice. Developmental Biology *289*, 218–228.

Collins, J.E., and Fleming, T.P. (1995). Epithelial differentiation in the mouse preimplantation embryo: making adhesive cell contacts for the first time. Trends Biochem. Sci. *20*, 307–312.

Conti, M.A., Even-Ram, S., Liu, C., Yamada, K.M., and Adelstein, R.S. (2004). Defects in cell adhesion and the visceral endoderm following ablation of nonmuscle myosin heavy chain II-A in mice. J. Biol. Chem. *279*, 41263–41266.

Cooper, A.R., and MacQueen, H.A. (1983). Subunits of laminin are differentially synthesized in mouse eggs and early embryos. Developmental Biology *96*, 467–471.

Cooper, H.M., Tamura, R.N., and Quaranta, V. (1991). The major laminin receptor of mouse embryonic stem cells is a novel isoform of the alpha 6 beta 1 integrin. J Cell Biol *115*, 843–850.

Crittenden, S.L., Leonhard, K.A., Byrd, D.T., and Kimble, J. (2006). Cellular analyses of the mitotic region in the Caenorhabditis elegans adult germ line. Mol Biol Cell *17*, 3051–3061.

Dard, N., Louvet, S., Santa-Maria, A., Aghion, J., Martin, M., Mangeat, P., and Maro, B. (2001). In vivo functional analysis of ezrin during mouse blastocyst formation. Developmental Biology *233*, 161–173.

Dard, N., Le, T., Maro, B., and Louvet-Vallée, S. (2009a). Inactivation of aPKClambda reveals a context dependent allocation of cell lineages in preimplantation mouse embryos. PLoS ONE *4*, e7117.

Dard, N., Louvet-Vallée, S., and Maro, B. (2009b). Orientation of mitotic spindles during the 8- to 16-cell stage transition in mouse embryos. PLoS ONE *4*, e8171.

de Vries, W.N., Binns, L.T., Fancher, K.S., Dean, J., Moore, R., Kemler, R., and Knowles, B.B. (2000). Expression of Cre recombinase in mouse oocytes: A means to study maternal effect genes. Genesis *26*, 110–112.

Dessaud, E., Yang, L.L., Hill, K., Cox, B., Ulloa, F., Ribeiro, A., Mynett, A., Novitch, B.G., and Briscoe, J. (2007). Interpretation of the sonic hedgehog morphogen gradient by a temporal adaptation mechanism. Nature *450*, 717–720.

Dietrich, J.-E., and Hiiragi, T. (2007). Stochastic patterning in the mouse pre-implantation embryo. Development *134*, 4219–4231.

Downing, T.L., Soto, J., Morez, C., Houssin, T., Fritz, A., Yuan, F., Chu, J., Patel, S., Schaffer, D.V., and Li, S. (2013). Biophysical regulation of epigenetic state and cell reprogramming. Nat Mater *12*, 1154–1162.

Duband, J.L., and Thiery, J.P. (1987). Distribution of laminin and collagens during avian neural crest development. Development *101*, 461–478.

Duband, J.L., Monier, F., Delannet, M., and Newgreen, D. (1995). Epithelium-mesenchyme transition during neural crest development. Acta Anat (Basel) *154*, 63–78.

Ducibella, T., and Anderson, E. (1975). Cell shape and membrane changes in the eight-cell mouse embryo: prerequisites for morphogenesis of the blastocyst. Developmental Biology *47*, 45–58.

Ducibella, T., Ukena, T., Karnovsky, M., and Anderson, E. (1977). Changes in cell surface and cortical cytoplasmic organization during early embryogenesis in the preimplantation mouse embryo. J Cell Biol *74*, 153–167.

Dziadek, M., and Timpl, R. (1985). Expression of nidogen and laminin in basement membranes during mouse embryogenesis and in teratocarcinoma cells. Developmental Biology *111*, 372–382.

Engler, A.J., Sen, S., Sweeney, H.L., and Discher, D.E. (2006). Matrix Elasticity Directs Stem Cell Lineage Specification. Cell *126*, 677–689.

Erickson, C.A., and Weston, J.A. (1983). An SEM analysis of neural crest migration in the mouse. J Embryol Exp Morphol *74*, 97–118.

Ericson, J., Rashbass, P., Schedl, A., Brenner-Morton, S., Kawakami, A., van Heyningen, V., Jessell, T.M., and Briscoe, J. (1997). Pax6 controls progenitor cell identity and neuronal fate in response to graded Shh signaling. Cell *90*, 169–180.

Etienne-Manneville, S. (2004). Cdc42--the centre of polarity. J Cell Sci *117*, 1291–1300.

Evans, M.J., and Kaufman, M.H. (1981). Establishment in culture of pluripotential cells from mouse embryos. Nature *292*, 154–156.

Fässler, R., and Meyer, M. (1995). Consequences of lack of beta 1 integrin gene expression in mice. Genes & Development *9*, 1896–1908.

Fleming, T.P., Pickering, S.J., Qasim, F., and Maro, B. (1986). The generation of cell surface polarity in mouse 8-cell blastomeres: the role of cortical microfilaments analysed using cytochalasin D. J Embryol Exp Morphol *95*, 169–191.

Futaki, S., Nakano, I., Kawasaki, M., Sanzen, N., and Sekiguchi, K. (2019). Molecular profiling of the basement membrane of pluripotent epiblast cells in post-implantation stage mouse embryos. Regen Ther *12*, 55–65.

Gavis, E.R., and Lehmann, R. (1994). Translational regulation of nanos by RNA localization. Nature *369*, 315–318.

Georges-Labouesse, E.N., George, E.L., Rayburn, H., and Hynes, R.O. (1996). Mesodermal development in mouse embryos mutant for fibronectin. Dev. Dyn. *207*, 145–156.

Gjorevski, N., and Lutolf, M.P. (2017). Synthesis and characterization of well-defined hydrogel matrices and their application to intestinal stem cell and organoid culture. Nat Protoc *12*, 2263–2274.

Gjorevski, N., Sachs, N., Manfrin, A., Giger, S., Bragina, M.E., Ordóñez-Morán, P., Clevers, H., and Lutolf, M.P. (2016). Designer matrices for intestinal stem cell and organoid culture. Nature *539*, 560–564.

Goodwin, B.C., and Cohen, M.H. (1969). A phase-shift model for the spatial and temporal organization of developing systems. J. Theor. Biol. *25*, 49–107.

Green, J.B.A., and Sharpe, J. (2015). Positional information and reaction-diffusion: two big ideas in developmental biology combine. Development *142*, 1203–1211.

Guillon, E., Das, D., Jülich, D., Hassan, A.-R., Geller, H., and Holley, S. (2020). Fibronectin is a smart adhesive that both influences and responds to the mechanics of early spinal column development. eLife *9*, 69.

Haas, T.A., and Plow, E.F. (1996). The cytoplasmic domain of alphaIIb beta3. A ternary complex of the integrin alpha and beta subunits and a divalent cation. J. Biol. Chem. *271*, 6017–6026.

Haigo, S.L., and Bilder, D. (2011). Global tissue revolutions in a morphogenetic movement controlling elongation. Science *331*, 1071–1074.

Handyside, A.H., and Barton, S.C. (1977). Evaluation of the technique of immunosurgery for the isolation of inner cell masses from mouse blastocysts. J Embryol Exp Morphol *37*, 217–226.

Hannigan, G.E., Leung-Hagesteijn, C., Fitz-Gibbon, L., Coppolino, M.G., Radeva, G., Filmus, J., Bell, J.C., and Dedhar, S. (1996). Regulation of cell adhesion and anchorage-dependent growth by a new beta 1-integrin-linked protein kinase. Nature *379*, 91–96.

Harfe, B.D., Scherz, P.J., Nissim, S., Tian, H., McMahon, A.P., and Tabin, C.J. (2004). Evidence for an expansion-based temporal Shh gradient in specifying vertebrate digit identities. Cell *118*, 517–528.

Hazenbiller, O., Duncan, N.A., and Krawetz, R.J. (2017). Reduction of pluripotent gene expression in murine embryonic stem cells exposed to mechanical loading or Cyclo RGD peptide. BMC Cell Biol. *18*, 32–15.

Henderson, D.J., and Copp, A.J. (1997). Role of the extracellular matrix in neural crest cell migration. J. Anat. *191 ( Pt 4)*, 507–515.

Hiiragi, T., and Solter, D. (2004). First cleavage plane of the mouse egg is not predetermined but defined by the topology of the two apposing pronuclei. Nature *430*, 360–364.

Hirate, Y., and Sasaki, H. (2014). The role of angiomotin phosphorylation in the Hippo pathway during preimplantation mouse development. Tissue Barriers *2*, e28127–e28127.

Hirate, Y., Hirahara, S., Inoue, K.-I., Suzuki, A., Alarcon, V.B., Akimoto, K., Hirai, T., Hara, T., Adachi, M., Chida, K., et al. (2013). Polarity-Dependent Distribution of Angiomotin Localizes Hippo Signaling in Preimplantation Embryos. Current Biology *23*, 1181–1194.

Hird, S.N., Paulsen, J.E., and Strome, S. (1996). Segregation of germ granules in living Caenorhabditis elegans embryos: cell-type-specific mechanisms for cytoplasmic localisation. Development *122*, 1303–1312.

Holland, J.J., Roberts, D., and Liscum, E. (2009). Understanding phototropism: from Darwin to today.

Hughes, P.E., Diaz-Gonzalez, F., Leong, L., Wu, C., McDonald, J.A., Shattil, S.J., and Ginsberg, M.H. (1996). Breaking the integrin hinge. A defined structural constraint regulates integrin signaling. J. Biol. Chem. *271*, 6571–6574.

Humphrey, J.D., Dufresne, E.R., and Schwartz, M.A. (2014). Mechanotransduction and extracellular matrix homeostasis. Nature Reviews Molecular Cell Biology *15*, 802–812.

Humphries, J.D., Byron, A., and Humphries, M.J. (2006). Integrin ligands at a glance. J Cell Sci *119*, 3901–3903.

Humphries, J.D., Wang, P., Streuli, C., Geiger, B., Humphries, M.J., and Ballestrem, C. (2007). Vinculin controls focal adhesion formation by direct interactions with talin and actin. J Cell Biol *179*, 1043–1057.

Huveneers, S., and Danen, E.H.J. (2009). Adhesion signaling - crosstalk between integrins, Src and Rho. J Cell Sci *122*, 1059–1069.

Hynes, R.O. (1987). Integrins: a family of cell surface receptors. Cell *48*, 549–554.

Hynes, R.O. (2004). The emergence of integrins: a personal and historical perspective. Matrix Biol. *23*, 333–340.

Jacobelli, J., Friedman, R.S., Conti, M.A., Lennon-Dumenil, A.-M., Piel, M., Sorensen, C.M., Adelstein, R.S., and Krummel, M.F. (2010). Confinement-optimized three-dimensional T cell amoeboid motility is modulated via myosin IIA-regulated adhesions. Nat. Immunol. *11*, 953–961.

Johnson, M.H., and Ziomek, C.A. (1981). The foundation of two distinct cell lineages within the mouse morula. Cell *24*, 71–80.

Jülich, D., Cobb, G., Melo, A.M., McMillen, P., Lawton, A.K., Mochrie, S.G.J., Rhoades, E., and Holley, S.A. (2015). Cross-Scale Integrin Regulation Organizes ECM and Tissue Topology. Devcel *34*, 33–44.

Kanchanawong, P., Shtengel, G., Pasapera, A.M., Ramko, E.B., Davidson, M.W., Hess, H.F., and Waterman, C.M. (2010). Nanoscale architecture of integrin-based cell adhesions. Nature *468*, 580–584.

Kawagishi, R., Tahara, M., Sawada, K., Morishige, K., Sakata, M., Tasaka, K., and Murata, Y. (2004). Na+ / H+ exchanger-3 is involved in mouse blastocyst formation. J. Exp. Zoolog. Part a Comp. Exp. Biol. *301*, 767–775.

Kemphues, K. (2000). PARsing embryonic polarity. Cell *101*, 345–348.

Kemphues, K.J., Priess, J.R., Morton, D.G., and Cheng, N.S. (1988). Identification of genes required for cytoplasmic localization in early C. elegans embryos. Cell *52*, 311–320.

Kim, S.H., Li, Z., and Sacks, D.B. (2000). E-cadherin-mediated cell-cell attachment activates Cdc42. J. Biol. Chem. *275*, 36999–37005.

Kimble, J.E., and White, J.G. (1981). On the control of germ cell development in Caenorhabditis elegans. Developmental Biology *81*, 208–219.

Klaffky, E.J., Gonzáles, I.M., and Sutherland, A.E. (2006). Trophoblast cells exhibit differential responses to laminin isoforms. Developmental Biology *292*, 277–289.

Klein, G., Langegger, M., Timpl, R., and Ekblom, P. (1988). Role of laminin A chain in the development of epithelial cell polarity. Cell *55*, 331–341.

Kondo, S., and Miura, T. (2010). Reaction-Diffusion Model as a Framework for Understanding Biological Pattern Formation. Science *329*, 1616–1620.

Korotkevich, E., Niwayama, R., Courtois, A., Friese, S., Berger, N., Buchholz, F., and Hiiragi, T. (2017). The Apical Domain Is Required and Sufficient for the First Lineage Segregation in the Mouse Embryo. Devcel *40*, 235–247.e237.

Kreitzer, G., and Myat, M.M. (2017). Microtubule Motors in Establishment of Epithelial Cell Polarity. Cold Spring Harbor Perspectives in Biology a027896–16.

Lallier, T., Leblanc, G., Artinger, K.B., and Bronner-Fraser, M. (1992). Cranial and trunk neural crest cells use different mechanisms for attachment to extracellular matrices. Development *116*, 531–541.

Lammerding, J. (2011). Mechanics of the nucleus. Compr Physiol *1*, 783–807.

Lander, A.D., Kimble, J., Clevers, H., Fuchs, E., Montarras, D., Buckingham, M., Calof, A.L., Trumpp, A., and Oskarsson, T. (2012). What does the concept of the stem cell niche really mean today? BMC Biol. *10*, 19–15.

Larue, L., Ohsugi, M., Hirchenhain, J., and Kemler, R. (1994). E-cadherin null mutant embryos fail to form a trophectoderm epithelium. Proceedings of the National Academy of Sciences *91*, 8263–8267.

Lawitts, J.A., and Biggers, J.D. (1991). Optimization of mouse embryo culture media using simplex methods. J. Reprod. Fertil. *91*, 543–556.

Lehtonen, E. (1980). Changes in cell dimensions and intercellular contacts during cleavage-stage cell cycles in mouse embryonic cells. J Embryol Exp Morphol *58*, 231–249.

Lehtonen, E., and Reima, I. (1986). Changes in the distribution of vinculin during preimplantation mouse development. Differentiation *32*, 125–134.

Leivo, I., Vaheri, A., Timpl, R., and Wartiovaara, J. (1980). Appearance and distribution of collagens and laminin in the early mouse embryo. Developmental Biology *76*, 100–114.

Lele, Z., Folchert, A., Concha, M., Rauch, G.-J., Geisler, R., Rosa, F., Wilson, S.W., Hammerschmidt, M., and Bally-Cuif, L. (2002). parachute/n-cadherin is required for morphogenesis and maintained integrity of the zebrafish neural tube. Development *129*, 3281–3294.

Li, L., and Xie, T. (2005). Stem cell niche: structure and function. Annual Review of Cell and Developmental Biology *21*, 605–631.

Li, R., and Bowerman, B. (2010). Symmetry Breaking in Biology. Cold Spring Harbor Perspectives in Biology *2*, a003475–a003475.

Li, R., Mitra, N., Gratkowski, H., Vilaire, G., Litvinov, R., Nagasami, C., Weisel, J.W., Lear, J.D., DeGrado, W.F., and Bennett, J.S. (2003). Activation of integrin alphaIIbbeta3 by modulation of transmembrane helix associations. Science *300*, 795–798.

Li, S., Harrison, D., Carbonetto, S., Fässler, R., Smyth, N., Edgar, D., and Yurchenco, P.D. (2002). Matrix assembly, regulation, and survival functions of laminin and its receptors in embryonic stem cell differentiation. J Cell Biol *157*, 1279–1290.

Lorthongpanich, C., Doris, T.P.Y., Limviphuvadh, V., Knowles, B.B., and Solter, D. (2012). Developmental fate and lineage commitment of singled mouse blastomeres. Development *139*, 3722–3731.

Louvet-Vallée, S., Vinot, S., and Maro, B. (2005). Mitotic spindles and cleavage planes are oriented randomly in the two-cell mouse embryo. Current Biology *15*, 464–469.

Maître, J.-L., Niwayama, R., Turlier, H., Nédélec, F., and Hiiragi, T. (2015). Pulsatile cell-autonomous contractility drives compaction in the mouse embryo. Nat Cell Biol *17*, 849–855.

Maître, J.-L., Turlier, H., Illukkumbura, R., Eismann, B., Niwayama, R., Nédélec, F., and Hiiragi, T. (2016). Asymmetric division of contractile domains couples cell positioning and fate specification. Nature 1–14.

Mammoto, T., and Ingber, D.E. (2010). Mechanical control of tissue and organ development. Development *137*, 1407–1420.

Manejwala, F.M., Cragoe, E.J., and Schultz, R.M. (1989). Blastocoel expansion in the preimplantation mouse embryo: role of extracellular sodium and chloride and possible apical routes of their entry. Developmental Biology *133*, 210–220.

Maniotis, A.J., Chen, C.S., and Ingber, D.E. (1997). Demonstration of mechanical connections between integrins, cytoskeletal filaments, and nucleoplasm that stabilize nuclear structure. Proceedings of the National Academy of Sciences *94*, 849–854.

Marikawa, Y., and Alarcon, V.B. (2009). Establishment of trophectoderm and inner cell mass lineages in the mouse embryo. Mol. Reprod. Dev. *76*, 1019–1032.

Maro, B., Gueth-Hallonet, C., Aghion, J., and Antony, C. (1991). Cell polarity and microtubule organisation during mouse early embryogenesis. Dev. Suppl. *1*, 17–25.

Martin, G.R. (1981). Isolation of a pluripotent cell line from early mouse embryos cultured in medium conditioned by teratocarcinoma stem cells. Proceedings of the National Academy of Sciences *78*, 7634–7638.

Martí, E., Takada, R., Bumcrot, D.A., Sasaki, H., and McMahon, A.P. (1995). Distribution of Sonic hedgehog peptides in the developing chick and mouse embryo. Development *121*, 2537–2547.

Meyer, K., and Palmer, J.W. (1934). THE POLYSACCHARIDE OF THE VITREOUS HUMOR. J. Biol. Chem. *107*, 629–634.

Meyer, K., Davidson, E., Linker, A., and Hoffman, P. (1956). The acid mucopolysaccharides of connective tissue. Biochimica Et Biophysica Acta *21*, 506–518.

Miner, J.H., Li, C., Mudd, J.L., Go, G., and Sutherland, A.E. (2004). Compositional and structural requirements for laminin and basement membranes during mouse embryo implantation and gastrulation. Development *131*, 2247–2256.

Miyamoto, S., Akiyama, S.K., and Yamada, K.M. (1995). Synergistic roles for receptor occupancy and aggregation in integrin transmembrane function. Science *267*, 883–885.

Moore, R., Tao, W., Smith, E.R., and Xu, X.-X. (2014). The primitive endoderm segregates from the epiblast in β1 integrin-deficient early mouse embryos. Mol. Cell. Biol. *34*, 560–572.

Moscona, A., and Moscona, H. (1952). The dissociation and aggregation of cells from organ rudiments of the early chick embryo. J. Anat. *86*, 287–301.

Mui, K.L., Chen, C.S., and Assoian, R.K. (2016). The mechanical regulation of integrin-cadherin crosstalk organizes cells, signaling and forces. J Cell Sci *129*, 1093–1100.

Munro, E., Nance, J., and Priess, J.R. (2004). Cortical flows powered by asymmetrical contraction transport PAR proteins to establish and maintain anterior-posterior polarity in the early C. elegans embryo. Devcel *7*, 413–424.

Nance, J., Munro, E.M., and Priess, J.R. (2003). C. elegans PAR-3 and PAR-6 are required for apicobasal asymmetries associated with cell adhesion and gastrulation. Development *130*, 5339–5350.

Nishioka, N., Inoue, K.-I., Adachi, K., Kiyonari, H., Ota, M., Ralston, A., Yabuta, N., Hirahara, S., Stephenson, R.O., Ogonuki, N., et al. (2009). The Hippo signaling pathway components Lats and Yap pattern Tead4 activity to distinguish mouse trophectoderm from inner cell mass. Developmental Cell *16*, 398–410.

Nusslein-Volhard, C., Frohnhöfer, H.G., and Lehmann, R. (1987). Determination of anteroposterior polarity in Drosophila. Science *238*, 1675–1681.

O'Toole, T.E., Mandelman, D., Forsyth, J., Shattil, S.J., Plow, E.F., and Ginsberg, M.H. (1991). Modulation of the affinity of integrin alpha IIb beta 3 (GPIIb-IIIa) by the cytoplasmic domain of alpha IIb. Science *254*, 845–847.

Ohashi, T., Kiehart, D.P., and Erickson, H.P. (1999). Dynamics and elasticity of the fibronectin matrix in living cell culture visualized by fibronectin–green fluorescent protein. Proceedings of the National Academy of Sciences *96*, 2153–2158.

Osmani, N., Peglion, F., Chavrier, P., and Etienne-Manneville, S. (2010). Cdc42 localization and cell polarity depend on membrane traffic. J Cell Biol *191*, 1261–1269.

Ozbek, S., Balasubramanian, P.G., Chiquet-Ehrismann, R., Tucker, R.P., and Adams, J.C. (2010). The evolution of extracellular matrix. Mol Biol Cell *21*, 4300–4305.

Palecek, S.P., Loftus, J.C., Ginsberg, M.H., Lauffenburger, D.A., and Horwitz, A.F. (1997). Integrin-ligand binding properties govern cell migration speed through cell-substratum adhesiveness. Nature *385*, 537–540.

Pauken, C.M., and Capco, D.G. (2000). The expression and stage-specific localization of protein kinase C isotypes during mouse preimplantation development. Developmental Biology *223*, 411–421.

Pfaff, M., Liu, S., Erle, D.J., and Ginsberg, M.H. (1998). Integrin beta cytoplasmic domains differentially bind to cytoskeletal proteins. J. Biol. Chem. *273*, 6104–6109.

Pietri, T., Eder, O., Breau, M.A., Topilko, P., Blanche, M., Brakebusch, C., Fässler, R., Thiery, J.-P., and Dufour, S. (2004). Conditional beta1-integrin gene deletion in neural crest cells causes severe developmental alterations of the peripheral nervous system. Development *131*, 3871–3883.

Pinzón-Duarte, G., Daly, G., Li, Y.N., Koch, M., and Brunken, W.J. (2010). Defective formation of the inner limiting membrane in laminin beta2- and gamma3-null mice produces retinal dysplasia. Invest. Ophthalmol. Vis. Sci. *51*, 1773–1782.

Plusa, B., Piliszek, A., Frankenberg, S., Artus, J., and Hadjantonakis, A.-K. (2008). Distinct sequential cell behaviours direct primitive endoderm formation in the mouse blastocyst. Development *135*, 3081–3091.

Raghavan, S., Bauer, C., Mundschau, G., Li, Q., and Fuchs, E. (2000). Conditional ablation of beta1 integrin in skin. Severe defects in epidermal proliferation, basement membrane formation, and hair follicle invagination. J Cell Biol *150*, 1149–1160.

Rahman, S., Patel, Y., Murray, J., Patel, K.V., Sumathipala, R., Sobel, M., and Wijelath, E.S. (2005). Novel hepatocyte growth factor (HGF) binding domains on fibronectin and vitronectin coordinate a distinct and amplified Met-integrin induced signalling pathway in endothelial cells. BMC Cell Biol. *6*, 1–17.

Ralston, A., and Rossant, J. (2008). Cdx2 acts downstream of cell polarization to cell-autonomously promote trophectoderm fate in the early mouse embryo. Developmental Biology *313*, 614–629.

Riechmann, V., and Ephrussi, A. (2001). Axis formation during Drosophila oogenesis. Current Opinion in Genetics & Development *11*, 374–383.

Rodriguez-Boulan, E., and Macara, I.G. (2014). Organization and execution of the epithelial polarity programme. Nature Reviews Molecular Cell Biology *15*, 225–242.

Roelink, H., Porter, J.A., Chiang, C., Tanabe, Y., Chang, D.T., Beachy, P.A., and Jessell, T.M. (1995). Floor plate and motor neuron induction by different concentrations of the amino-terminal cleavage product of sonic hedgehog autoproteolysis. Cell *81*, 445–455.

Roignot, J., Peng, X., and Mostov, K. (2013). Polarity in Mammalian Epithelial Morphogenesis. Cold Spring Harbor Perspectives in Biology *5*, a013789–a013789.

Rongo, C., Gavis, E.R., and Lehmann, R. (1995). Localization of oskar RNA regulates oskar translation and requires Oskar protein. Development *121*, 2737–2746.

Roth, S., and Lynch, J.A. (2009). Symmetry breaking during Drosophila oogenesis. Cold Spring Harbor Perspectives in Biology *1*, a001891–a001891.

Ruoslahti, E., and Vaheri, A. (1975). Interaction of soluble fibroblast surface antigen with fribrinogen and fibrin. The Journal of Experimental Medicine *141*, 497–501.

Sagner, A., and Briscoe, J. (2017). Morphogen interpretation: concentration, time, competence, and signaling dynamics. Wiley Interdiscip Rev Dev Biol *6*, e271.

Saiz, N., Grabarek, J.B., Sabherwal, N., Papalopulu, N., and Plusa, B. (2013). Atypical protein kinase C couples cell sorting with primitive endoderm maturation in the mouse blastocyst. Development *140*, 4311–4322.

Samarage, C.R., White, M.D., Álvarez, Y.D., Fierro-González, J.C., Henon, Y., Jesudason, E.C., Bissiere, S., Fouras, A., and Plachta, N. (2017). Cortical Tension Allocates the First Inner Cells of the Mammalian Embryo. 1–14.

Schmitt, F.O., Hall, C.E., and Jakus, M.A. (1942). Electron microscope investigations of the structure of collagen. Journal of Cellular and Comparative Physiology *20*, 11–33.

Schofield, R. (1978). The relationship between the spleen colony-forming cell and the haemopoietic stem cell. Blood Cells *4*, 7–25.

Sehgal, P., Kong, X., Wu, J., Sunyer, R., Trepat, X., and Leckband, D. (2018). Epidermal growth factor receptor and integrins control force-dependent vinculin recruitment to E-cadherin junctions. J Cell Sci *131*, jcs206656.

Shimizu, T., Yabe, T., Muraoka, O., Yonemura, S., Aramaki, S., Hatta, K., Bae, Y.-K., Nojima, H., and Hibi, M. (2005). E-cadherin is required for gastrulation cell movements in zebrafish. Mechanisms of Development *122*, 747–763.

Shirayoshi, Y., Okada, T.S., and Takeichi, M. (1983). The calcium-dependent cell-cell adhesion system regulates inner cell mass formation and cell surface polarization in early mouse development. Cell *35*, 631–638.

Smyth, N., Vatansever, H.S., Murray, P., Meyer, M., Frie, C., Paulsson, M., and Edgar, D. (1999). Absence of Basement Membranes after Targeting the LAMC1Gene Results in Embryonic Lethality Due to Failure of Endoderm Differentiation. J Cell Biol *144*, 151–160.

Solter, D., and Knowles, B.B. (1975). Immunosurgery of mouse blastocyst. Proceedings of the National Academy of Sciences *72*, 5099–5102.

Sorokin, L., Sonnenberg, A., Aumailley, M., Timpl, R., and Ekblom, P. (1990). Recognition of the laminin E8 cell-binding site by an integrin possessing the alpha 6 subunit is essential for epithelial polarization in developing kidney tubules. J Cell Biol *111*, 1265–1273.

Stainier, D.Y., Lee, R.K., and Fishman, M.C. (1993). Cardiovascular development in the zebrafish. I. Myocardial fate map and heart tube formation. Development *119*, 31–40.

Steinberg, M. S. (1963). Reconstruction of tissues by dissociated cells. Science *141*, 401–408.

Stephens, L.E., Sutherland, A.E., Klimanskaya, I.V., Andrieux, A., Meneses, J., Pedersen, R.A., and Damsky, C.H. (1995). Deletion of beta 1 integrins in mice results in inner cell mass failure and peri-implantation lethality. Genes & Development *9*, 1883–1895.

Stephenson, R.O., Yamanaka, Y., and Rossant, J. (2010). Disorganized epithelial polarity and excess trophectoderm cell fate in preimplantation embryos lacking E-cadherin. Development *137*, 3383–3391.

Strachan, L.R., and Condic, M.L. (2003). Neural crest motility and integrin regulation are distinct in cranial and trunk populations. Developmental Biology *259*, 288–302.

Strachan, L.R., and Condic, M.L. (2008). Neural crest motility on fibronectin is regulated by integrin activation. Exp. Cell Res. *314*, 441–452.

Strome, S., and Wood, W.B. (1982). Immunofluorescence visualization of germ-line-specific cytoplasmic granules in embryos, larvae, and adults of Caenorhabditis elegans. Proceedings of the National Academy of Sciences *79*, 1558–1562.

Strumpf, D., Mao, C.-A., Yamanaka, Y., Ralston, A., Chawengsaksophak, K., Beck, F., and Rossant, J. (2005). Cdx2 is required for correct cell fate specification and differentiation of trophectoderm in the mouse blastocyst. Development *132*, 2093–2102.

Tadokoro, S., Shattil, S.J., Eto, K., Tai, V., Liddington, R.C., de Pereda, J.M., Ginsberg, M.H., and Calderwood, D.A. (2003). Talin binding to integrin beta tails: a final common step in integrin activation. Science *302*, 103–106.

Takagi, J., Petre, B.M., Walz, T., and Springer, T.A. (2002). Global conformational rearrangements in integrin extracellular domains in outside-in and inside-out signaling. Cell *110*, 599–511.

Takeichi, M. (1977). Functional correlation between cell adhesive properties and some cell surface proteins. J Cell Biol *75*, 464–474.

Tamkun, J.W., DeSimone, D.W., Fonda, D., Patel, R.S., Buck, C., Horwitz, A.F., and Hynes, R.O. (1986). Structure of integrin, a glycoprotein involved in the transmembrane linkage between fibronectin and actin. Cell *46*, 271–282.

Tarkowski, A.K., and Wróblewska, J. (1967). Development of blastomeres of mouse eggs isolated at the 4- and 8-cell stage. J Embryol Exp Morphol *18*, 155–180.

Timpl, R., Rohde, H., Robey, P.G., Rennard, S.I., Foidart, J.M., and Martin, G.R. (1979). Laminin--a glycoprotein from basement membranes. J. Biol. Chem. *254*, 9933–9937.

Tischer, D., and Weiner, O.D. (2014). Illuminating cell signalling with optogenetic tools. Nature Reviews Molecular Cell Biology *15*, 551–558.

Townes, P.L., and Holtfreter, J. (1955). Directed movements and selective adhesion of embryonic amphibian cells. Journal of Experimental Zoology *128*, 53–120.

Trinh, L.A., and Stainier, D.Y.R. (2004). Fibronectin regulates epithelial organization during myocardial migration in zebrafish. Devcel *6*, 371–382.

Turing, A.M. (1952). The Chemical Basis of Morphogenesis. Philosophical Transactions of the Royal Society B: Biological Sciences *237*, 37–72.

Tzu, J., and Marinkovich, M.P. (2008). Bridging structure with function: structural, regulatory, and developmental role of laminins. Int. J. Biochem. Cell Biol. *40*, 199–214.

Uda, Y., Poh, Y.-C., Chowdhury, F., Wu, D.C., Tanaka, T.S., Sato, M., and Wang, N. (2011). Force via integrins but not E-cadherin decreases Oct3/4 expression in embryonic stem cells. Biochemical and Biophysical Research Communications *415*, 396–400.

Villa-Diaz, L.G., Kim, J.K., Laperle, A., Palecek, S.P., and Krebsbach, P.H. (2016). Inhibition of Focal Adhesion Kinase Signaling by Integrin α6β1 Supports Human Pluripotent Stem Cell Self-Renewal. Stem Cells *34*, 1753–1764.

Vinot, S., Le, T., Ohno, S., Pawson, T., Maro, B., and Louvet-Vallée, S. (2005). Asymmetric distribution of PAR proteins in the mouse embryo begins at the 8-cell stage during compaction. Developmental Biology *282*, 307–319.

Wang, Y., Jin, G., Miao, H., Li, J.Y.-S., Usami, S., and Chien, S. (2006). Integrins regulate VE-cadherin and catenins: dependence of this regulation on Src, but not on Ras. Proceedings of the National Academy of Sciences *103*, 1774–1779.

Watanabe, T., Biggins, J.S., Tannan, N.B., and Srinivas, S. (2014). Limited predictive value of blastomere angle of division in trophectoderm and inner cell mass specification. Development *141*, 2279–2288.

Wedlich-Soldner, R., Altschuler, S., Wu, L., and Li, R. (2003). Spontaneous cell polarization through actomyosin-based delivery of the Cdc42 GTPase. Science *299*, 1231–1235.

Went, D.F. (1978). Oocyte maturation without follicular epithelium alters egg shape in a dipteran insect. Journal of Experimental Zoology *205*, 149–155.

Whittaker, C.A., Bergeron, K.-F., Whittle, J., Brandhorst, B.P., Burke, R.D., and Hynes, R.O. (2006). The echinoderm adhesome. Developmental Biology *300*, 252–266.

Wicklow, E., Blij, S., Frum, T., Hirate, Y., Lang, R.A., Sasaki, H., and Ralston, A. (2014). HIPPO pathway members restrict SOX2 to the inner cell mass where it promotes ICM fates in the mouse blastocyst. PLoS Genet. *10*, e1004618.

Wigger, M., Kisielewska, K., Filimonow, K., Plusa, B., Maleszewski, M., and Suwińska, A. (2017). Plasticity of the inner cell mass in mouse blastocyst is restricted by the activity of FGF/MAPK pathway. Nature Publishing Group *7*, 15136.

Wiley, L.M. (1984). Cavitation in the mouse preimplantation embryo: Na/K-ATPase and the origin of nascent blastocoele fluid. Developmental Biology *105*, 330–342.

Williamson, R.A., Henry, M.D., Daniels, K.J., Hrstka, R.F., Lee, J.C., Sunada, Y., Ibraghimov-Beskrovnaya, O., and Campbell, K.P. (1997). Dystroglycan is essential for early embryonic development: disruption of Reichert's membrane in Dag1-null mice. Hum. Mol. Genet. *6*, 831–841.

Willingham, M.C., Yamada, K.M., Yamada, S.S., Pouysségur, J., and Pastan, I. (1977). Microfilament bundles and cell shape are related to adhesiveness to substratum and are dissociable from growth control in cultured fibroblasts. Cell *10*, 375–380.

Wilson, H.V. (1907). A NEW METHOD BY WHICH SPONGES MAY BE ARTIFICIALLY REARED. Science *25*, 912–915.

Wolpert, L. (1969). Positional information and the spatial pattern of cellular differentiation. J. Theor. Biol. *25*, 1–47.

Wu, T.-C., Wan, Y.-J., Chung, A.E., and Damjanov, I. (1983). Immunohistochemical localization of entactin and laminin in mouse embryos and fetuses. Developmental Biology *100*, 496–505.

Xiong, F., Tentner, A.R., Huang, P., Gelas, A., Mosaliganti, K.R., Souhait, L., Rannou, N., Swinburne, I.A., Obholzer, N.D., Cowgill, P.D., et al. (2013). Specified neural progenitors sort to form sharp domains after noisy Shh signaling. Cell *153*, 550–561.

Xiong, J.-P., Stehle, T., Zhang, R., Joachimiak, A., Frech, M., Goodman, S.L., and Arnaout, M.A. (2002). Crystal structure of the extracellular segment of integrin alpha Vbeta3 in complex with an Arg-Gly-Asp ligand. Science *296*, 151–155.

Yamada, K.M., Yamada, S.S., and Pastan, I. (1976). Cell surface protein partially restores morphology, adhesiveness, and contact inhibition of movement to transformed fibroblasts. Proceedings of the National Academy of Sciences *73*, 1217–1221.

Yamada, T., Pfaff, S.L., Edlund, T., and Jessell, T.M. (1993). Control of cell pattern in the neural tube: motor neuron induction by diffusible factors from notochord and floor plate. Cell *73*, 673–686.

Yauch, R.L., Felsenfeld, D.P., Kraeft, S.K., Chen, L.B., Sheetz, M.P., and Hemler, M.E. (1997). Mutational evidence for control of cell adhesion through integrin diffusion/clustering, independent of ligand binding. The Journal of Experimental Medicine *186*, 1347–1355.

Yayon, A., Klagsbrun, M., Esko, J.D., Leder, P., and Ornitz, D.M. (1991). Cell surface, heparin-like molecules are required for binding of basic fibroblast growth factor to its high affinity receptor. Cell *64*, 841–848.

Yoshida, C., and Takeichi, M. (1982). Teratocarcinoma cell adhesion: Identification of a cell-surface protein involved in calcium-dependent cell aggregation. Cell *28*, 217–224.

Zhu, M., Leung, C.Y., Shahbazi, M.N., and Zernicka-Goetz, M. (2017). Actomyosin polarisation through PLC-PKC triggers symmetry breaking of the mouse embryo. Nat Commun *8*, 921–16.

Ziomek, C.A., and Johnson, M.H. (1980). Cell surface interaction induces polarization of mouse 8-cell blastomeres at compaction. Cell *21*, 935–942.

# Acknowledgements

I was mindlessly munching away on sandwich cookies on a hostel bunk bed in Fukuoka when my phone alerted me to an email - an invitation to interview for an EMBL PhD position. I spewed a few cookie crumbs and even cried a little. Months later, I received an offer from Takashi to join his lab, and since then the past four years have been an immensely enriching journey.

The lab provided a fair share of bitter frustration and disappointments, but it has also been a period of incredible privilege and stimulation. While the science at EMBL is great, the most integral part of my PhD experience has been the people that I met, without whom my time in Heidelberg would have been several shades duller.

First and foremost, I am most sincerely grateful to Takashi for giving me the opportunity to work in his group, and providing constant and patient support. I hope I can emulate even a fraction of his work ethic and scientific curiosity in the years to come. Meanwhile, out of the lab, playing tennis with Takashi was immensely helpful for overcoming my PhD blues. (Every PhD student gets stressed out by his/her supervisor, but unlike most I had legitimate means to take my stress out on my boss!)

I have spent more time with my lab mates than anyone else during these past four years, and I adore our group to bits. I would like to thank Katya, Laura, Steffi, Ramona, Ritsuya, Allyson, Joe, Dimitri, Takafumi, Hui Ting, Vlad and Prachiti for their scientific and non-scientific contributions in making lab life so colourful and full of warmth. Their company, mingled with humour, chocolate, tea and coffee provided all the cushioning and more necessary to take on the knocks from my project. I probably annoyed them more frequently than I realised, but thankfully I received bountiful kindness in return. I especially thank Steffi and Ramona for all their lab support and generous German aid, and Katya for teaching me much of the lab techniques indispensable for my project.

I would also like to thank Laboratory Animal Resources (LAR) for their phenomenal support. None of the experiments I performed at EMBL would have been possible without the maintenance, breeding, tailing and injections of mice performed by LAR caretakers. Many caretakers have looked after our mice, but I would particularly like to thank Sandro, Kerstin, George, Yvonne and Isabel for their kindness and support.

I thank my TAC members, Alexander Aulehla, Nicholas Foulkes, and Darren Gilmour for providing not only scientific guidance but also encouragement to keep my motivation

afloat through the four years. Although we gathered only once a year, the discussions were valuable both as affirmation of the project and for warding off complacency.

I would also like to thank members of the Developmental Biology Unit – we may be the smallest unit in EMBL but what we lack in number we make up in comradery. In particular, I thank members of the Aulehla and Ikmi groups for shared discussions during our joint meetings.

I am grateful to our Matthias Lutolf and Lydia Sorokin for kindly providing of reagents necessary for my experiments. I also thank members of the Graduate Office for driving such a wonderful PhD programme – acceptance into this programme has been the most valuable privilege so far in my education.

Through the best and worst of these last four years, I had generous friends by my side. It is my fervent wish that these friendships last for many years to come, and I thank them for all the great times we shared, both in sobriety and inebriety.

Last but definitely not least, I would not be standing on both feet at the end of my PhD without the love and support from my family. The countless Skype calls were sustenance to my sanity and they kept me grounded through the most difficult times in Heidelberg. The pandemic has kept us apart for longer than expected, and I cannot to wait until I give them huge suffocating hugs.

As such, the work presented in the present thesis represents direct and indirect contributions from numerous wonderful people over the past four years. I hope my work does their generosity justice.

Thank you everyone from the bottom of my heart!